haematologica
Journal of the Ferrata Storti Foundation

HES6 knockdown in human hematopoietic precursor cells reduces their *in vivo* engraftment potential and their capacity to differentiate into erythroid cells, B cells, T cells and plasmacytoid dendritic cells

by Tamara De Vos, Nicole Oatman, Lena Boehme, Tom Putteman, Imke Velghe, Yana Van Droogenbroeck, Stijn De Munter, Michaela Cesneková, Filip Van Nieuwerburgh, Bart Vandekerckhove, Jan Philippé, and Tom Taghon

Received: April 27, 2023.
Accepted: March 21, 2024.

Citation: Tamara De Vos, Nicole Oatman, Lena Boehme, Tom Putteman, Imke Velghe, Yana Van Droogenbroeck, Stijn De Munter, Michaela Cesneková, Filip Van Nieuwerburgh, Bart Vandekerckhove, Jan Philippé, and Tom Taghon. HES6 knockdown in human hematopoietic precursor cells reduces their in vivo engraftment potential and their capacity to differentiate into erythroid cells, B cells, T cells and plasmacytoid dendritic cells.
Haematologica. 2024 Apr 4. doi: 10.3324/haematol.2023.283432 [Epub ahead of print]

HES6 knockdown in human hematopoietic precursor cells reduces their *in vivo* engraftment potential and their capacity to differentiate into erythroid cells, B cells, T cells and plasmacytoid dendritic cells.

Tamara De Vos[1,2], Nicole Oatman[1,2], Lena Boehme[1], Tom Putteman[1], Imke Velghe[1,2], Yana Van Droogenbroeck[1,2], Stijn De Munter[1,2], Michaela Cesneková[1,2], Filip Van Nieuwerburgh[2,3], Bart Vandekerckhove[1,2], Jan Philippé[1], Tom Taghon[1,2]

[1]Department of Diagnostic Sciences, Ghent University, Ghent, Belgium.

[2]Cancer Research Institute Ghent, Ghent, Belgium.

[3]Laboratory of Pharmaceutical Biotechnology, Ghent University, Ghent, Belgium

Short title: The role of *HES6* during human hematopoiesis

Corresponding author:

Tom Taghon

Department of Diagnostic Sciences

Ghent University

C. Heymanslaan 10

MRB2, Entrance 38

9000 Ghent, Belgium

+32 (0) 9 332 01 33

tom.taghon@ugent.be

Data sharing statement: The RNA-seq data are available through GEO Series accession number GSE229196.

Authorship: Conceptualization, T.D.V., J.P., T.T.; methodology, T.D.V., F.V.N., T.T.; investigation, T.D.V., L.B., T.P., N.O., Y.V.D., S.D.M., I.V., M.C.; resources, B.V., J.P., T.T.; supervision, T.T.; writing T.D.V., T.T..

All authors have read and agreed to the submitted version of the manuscript.

Conflict-of-interest disclosure: The authors declare no competing financial interests.

Text word count: 3963

Abstract word count: 202

Number of figures: 8

Number of tables: 0

Number of references: 49

Number of supplemental figures: 11

Number of supplemental tables: 13

Acknowledgments: The computational resources and services used in this work were provided by the VSC (Flemish Supercomputer Center), funded by the Research Foundation—Flanders (FWO) and the Flemish Government—department EWI. Research reported in this publication was performed at the CORE Flow Cytometry and NXTGNT sequencing facilities of Ghent University, Belgium. Figure 6A, Figure S2A, Figure S8A and Figure S10A and were created using BioRender.com. Vendiagram in Figure S10 was created using https://bioinformatics.psb.ugent.be/webtools/Venn.

Funding: This work was supported by grants of the Fund for Scientific Research Flanders (project grant G038618N and fellowships for TDV:1155821N, LB:12D9523N, SDM:12AP724N), the Concerted Research Action of Ghent University (GOA), a BOF postdoctoral fellowship for NO and the Foundation against Cancer (STK: F/2020/1413).

Abstract

Hematopoiesis is driven by molecular mechanisms that induce differentiation and proliferation of hematopoietic stem cells and their progeny. This involves the activity of various transcription factors, such as members of the Hairy/Enhancer of Split (HES) family, and important roles for both HES1 and HES4 have been shown in normal and malignant hematopoiesis. Here, we investigated the role of HES6 in human hematopoiesis using *in vitro* and *in vivo* models. Using bulk and scRNA-seq data, we show that *HES6* is expressed during erythroid/megakaryocyte and pDC development, as well as in multipotent precursors and at specific stages of T- and B-cell development following preBCR and preTCR signalling, respectively. Consistently, knockdown of *HES6* in cord blood-derived hematopoietic precursors in well-defined *in vitro* differentiation assays resulted in reduced differentiation of human hematopoietic precursors towards megakaryocytes, erythrocytes, pDCs, B- and T-cells. In addition, *HES6* knockdown HSPCs displayed reduced colony forming unit capacity *in vitro* and impaired potential to reconstitute hematopoiesis *in vivo* in a competitive transplantation assay. We demonstrate that loss of *HES6* expression impacts cell cycle progression during erythroid differentiation and provide evidence for potential downstream target genes that impact these perturbations. Thus, our study uncovers new insights for a role of HES6 in human hematopoiesis.

Introduction

The vast majority of hematopoietic cells in the human body arise from multipotent hematopoietic stem and progenitor cells (HSPCs) that reside in the bone marrow and their differentiation into mature blood cells is the result of successful integration of external stimuli and cell-intrinsic mechanisms that lead to chromatin remodeling and changes in gene expression, thereby activating and repressing specific molecular pathways[1,2]. Research on normal hematopoiesis is important to increase knowledge on stem cell function and differentiation. This will facilitate blood cell regeneration and serve as a reference to uncover mechanisms that induce hematological malignancies. While animal models are instrumental to advance this field, human studies provide a more direct translational perspective and the opportunity to reveal human-specific mechanisms.

The Notch signaling pathway is an important regulator of normal hematopoiesis and often involved in leukemia[3–6]. Notch activation induces expression of downstream target genes, including members of the HES family of transcription factors that contains seven members in human (*HES1-7*). While important roles for HES1, HES4 and HES5 have been described in hematopoiesis[7–9], the potential involvement of HES6 in hematopoietic stem cell differentiation has remained unclear. During embryonic development, HES6 is implicated in mesoderm specification and neurogenesis where it can inhibit the transcriptional repression activity of HES1[10–12]. HES6 also acts as an oncogene in different types of cancer including colorectal, prostate and gastric cancer, as well as melanoma and glioma[13–18]. In these malignancies, it mainly drives metastatic disease and proliferation[13,15,17]. In a hematological context, *HES6* appears overexpressed in blastic plasmacytoid dendritic cell neoplasm (BPDCN)[19,20]. And while HES6 had been proposed to mediate erythropoiesis[21,22], only recently it was shown to be a cofactor for GATA1 during erythroid development[23]. In this manuscript, we more broadly studied the functional role of HES6 in human hematopoiesis using both *in vitro* and *in vivo* models and these studies revealed, in addition to a role for HES6 in erythropoiesis, that this gene is

also important to support the *in vivo* reconstitution potential of human HSPCs, and the capacity of HSPCs to differentiate into erythrocytes, B cells, T-cells and pDCs.

Methods

Isolation of CD34$^+$ hematopoietic precursor cells and transduction

Human cord blood (CB) was obtained from the Hematopoietic cell Biobank UZ Gent with informed consent and according to the Medical Ethical Committee of Ghent University Hospital (EC protocol: EC-Bio/1-2018/sds, EC/2021-010/sds, EC/2021-020/sds, EC/2019/0826). CD34$^+$ HSPCs were processed as described[9] and cultured (density of 5*10^5 cells/ml) for two days in medium that depended on the further experimental set-up (Table S1). Subsequently, cells were transduced for two days with lentivirus using Retronectin (TAKARA; #T100B).

Other methods are available in the *Supplementary Material and Methods*.

Results

HES6 is required during early T-cell development

Notch signaling initiates T-cell development and induces expression of downstream target genes, including members of the HES family. Bulk RNA-seq data[24] confirmed that the Notch targets *HES1* and *HES4* are expressed during early T-cell development until the β-selection checkpoint. In contrast, *HES6* expression was only detected after β-selection (Figure S1A). Consistently, *HES6* did not show Notch-dependent transcriptional activation in hematopoietic progenitors, in contrast to *DTX1* and *HES1* (Figure S1B-C)[25,26]. We further explored *HES1* and *HES6* expression in a published single cell RNA-seq (scRNA-seq) dataset[27] (Figure S1D) and confirmed *HES1* expression in the immature stages of T-cell development (Figure S1E). Similar to in bulk RNA-seq, *HES6* expression peaked in the DP stages after β-selection, but we also observed expression in immature, proliferating CD4$^-$CD8$^-$ double-negative (DN) thymocytes (Figure 1A). Thus, scRNA-seq reveals that *HES6* is mainly expressed in proliferating thymocytes (Figure S1F-G).

To study HES6 function in human T-cell development, we used lentiviral-based shRNA-mediated knockdown and cultured transduced HSPCs in the *in vitro* OP9-DLL4 T-cell differentiation assay[28] (Figure S2A). All three shRNA constructs significantly decreased *HES6* expression compared to control shRNA transduced HSPCs, ranging from 55 – 75% knockdown (Figure 1B). While started the coculture with a sorting purity of > 95% transduced cells (BFP^+), the frequency of BFP^+ cells at day 21 was significantly lower in *HES6* knockdown cultures compared to the control (Figure S2B-C). *HES6* knockdown consistently reduced the absolute cell number of BFP^+ cells compared to in control transduced cultures (Figure S2D). After 14 days, the frequencies of HSPCs ($CD34^+CD7^-$) and T-cell precursors ($CD34^+CD7^+$) were increased following *HES6* knockdown but there was an inconsistent impact on the cell numbers of those populations (Figure 1C, Figure S2E-F). At this time point, the frequencies and total cell numbers of more differentiated T-cell precursor cells ($CD34^-CD7^+$) were significantly reduced (Figure 1C, Figure S2E-F). After 21 days of coculture, *HES6* knockdown decreased differentiation from $CD7^+CD5^-$ cells to T-cell specified precursor cells ($CD7^+CD5^+$), resulting in reduced total numbers of T-cell specified precursor cells (Figure 1D, Figure S2G-H). Furthermore, we observed reduced frequencies and absolute cell numbers for $CD4^+CD8b^-$ as well as $CD4^+CD8b^+$ cells after *HES6* knockdown compared to control (Figure 1E, Figure S2I-J). In conclusion, *HES6* knockdown inhibits the development of T-cell specified precursor cells as well as DP cells, in agreement with its expression in proliferating DN cells and β-selected developing thymocytes.

Stage-specific role for HES6 during human B-cell development

To further explore the role of HES6 in hematopoiesis, we analyzed published scRNA-seq data of human bone marrow (BM)[29] and observed *HES6* expression in NK cells, plasmacytoid dendritic cells (pDCs), immature B-cells and particularly erythroid cells (Figure 2A). Using a BM dataset[30], with distinct stages of human B-cell development annotated (Figure 2B), we discovered *HES6* expression in proliferating cells (Figure S3A) and particularly in large, cycling pre-B-cells as confirmed by expression of proliferation marker *MKI67* (Figure 2C). To study HES6 in B-cell development, we cultured shRNA transduced HSPCs in an *in vitro* B-cell differentiation assay[28]. The frequencies and

absolute cell numbers of BFP$^+$ cells were significantly reduced for *HES6* knockdown compared to the control, and the effect increased progressively from day 7 to day 21 (Figure 2D, Figure S3B). We used intracellular staining of CD179b (λ5 which is part of the preBCR) to investigate the effect of *HES6* knockdown on early B-cell development. Because of fixation and permeabilization that degrades BFP, we were unable to select BFP$^+$ cells for flow cytometric analysis, possibly diluting the effect of *HES6* knockdown because of including non-targeted BFP$^-$ cells in the analysis. At day 7, we observed no difference in the frequencies of pro-B-cells (CD34$^+$icCD179b$^+$) for *HES6* knockdown samples compared to control, although the absolute cell numbers were slightly reduced for two of the three knockdown constructs (Figure S3C-D). At day 21, no clear effect of *HES6* knockdown on the frequencies of pro-B-cells was observed (icCD179b$^+$CD19$^-$), but there was a significant reduction in the frequencies of pre-B-cells (icCD179b$^+$CD19$^+$) (Figure 2E, Figure S3E). For both stages, the absolute cell numbers were reduced after *HES6* knockdown (Figure S3F). Cell surface staining at day 21 revealed that, within the BFP$^+$ compartment, the frequencies and absolute cell numbers of B-cells (CD19$^+$) were strongly reduced upon *HES6* knockdown, while this was not the case in the BFP$^-$ compartment (Figure 2F, Figure S3G-H). Thus, *HES6* is specifically expressed in proliferating large pre-B-cells that received preBCR signaling following successful heavy chain rearrangement, and knockdown of *HES6* inhibits the *in vitro* development of B-cells beyond this stage.

Knockdown of *HES6* impairs pDC differentiation

We detected *HES6* expression in pDCs (Figure 2A) and high expression of this gene is associated with a hematological malignancy from this lineage (BPDCN)[19,20]. Using an *in vitro* differentiation protocol[31], we investigated if HES6 is essential for pDC development. After 14 days of culture, the frequency of BFP$^+$ cells was significantly reduced in *HES6* knockdown cultures compared to the control (Figure S4A). Total cell numbers of BFP$^+$ cells were also reduced for two of the three *HES6* knockdown conditions (Figure S4A). *HES6* knockdown resulted in a significant reduction in the frequency of pDCs (CD45RA$^+$CD123$^+$) (Figure 3A-B). For two of the shRNAs, this was accompanied with a significant reduction in the absolute number of pDCs (Figure 3B). Within the BFP$^-$ population, no differences in

pDC development were observed between the different conditions, indicating that the observed effect of *HES6* knockdown on pDC development is specific (Figure S4B). Also cDCs ($CD4^+HLA\text{-}DR^+$ non-pDCs), which express higher levels of HLA-DR compared to pDCs, developed in these cultures (Figure 3C and Figure S4C). Within the BFP^+ compartment, *HES6* knockdown had no influence on the frequencies of cDCs compared to the control, but the absolute cell numbers were reduced for two *HES6*-targeting shRNAs (Figure 3D). We also investigated the role of HES6 during NK, monocyte and granulocyte development in specific *in vitro* differentiation cultures[28] but knockdown of *HES6* had no consistent impact on the development of these lineages (Figure S5). Overall, these results suggest a functional role for HES6 in pDC development, consistent with its expression in BM pDCs.

HES6 is essential for the colony formation capacity of early hematopoietic precursors

Since our differentiation cultures consistently revealed reduced cellular output upon *HES6* knockdown, we investigated if this was correlated with a reduced proliferative capacity of these *HES6* knockdown precursors. Gene expression datasets[32] revealed *HES6* expression in MPPs, CMPs and MEP cells (Figure 4A). To study if HES6 is important for precursor expansion, we performed colony forming assays. After 10 days, a strong reduction in the number of colonies in *HES6* knockdown conditions was observed compared to the control (Figure 4B) for both myeloid and particularly erythroid colonies (Figure 4C). Furthermore, the average cell number per colony was reduced upon *HES6* knockdown compared to the control (Figure 4B). Flow cytometric analysis of these cultures showed large variation in the frequencies of BFP^+ cells and, combined with the cellular output of these assays, the total numbers of BFP^+ cells were reduced upon *HES6* knockdown (Figure S6A). Within this BFP^+ compartment, *HES6* knockdown did not consistently impact $CD15^+$ myeloid cell development but in contrast, a strong reduction in both the frequencies and absolute numbers of $CD235^+$ erythroblasts was observed (Figure S6B-D), which was confirmed by microscopic analysis (Figure 4D). While there were mainly cells with basophilic cytoplasm in the control samples, which matches the different differentiation stages along the erythroid lineage that are observed in the BM of healthy individuals, the cytoplasm of the *HES6* knockdown cells was less basophilic, indicating

reduced development along the erythroid lineage. Furthermore, we observed fewer mitoses in *HES6* knockdown conditions compared to control. No differences were observed in the BFP^- cells (Figure S6E). These findings suggest that HES6 is important for the proliferative potential of hematopoietic precursor cells, as well as for their differentiation towards erythroid cells.

HES6 is required for erythroid and megakaryocyte development

We further explored the role of HES6 during erythroid and megakaryocyte development by culturing shRNA transduced HSPCs in liquid culture conditions that induce differentiation towards both lineages. After five days, both the frequencies and absolute cell numbers of BFP^+ cells were reduced in the *HES6* knockdown conditions compared to the control (Figure S7A-B). Within the BFP^+ population, a significant reduction in the frequency of megakaryocytes ($CD41^+$) and differentiating erythroblasts (characterized by upregulation of CD71 and CD235a) was observed in all three *HES6* knockdown conditions, resulting in significantly reduced cell numbers of these populations (Figure 4E-F, Figure S7C-D). Erythroblasts from *HES6* shRNA transduced precursors also displayed reduced CD71 expression compared to the control transduced erythroid cells (Figure S7E). After 10 and 14 days of culture, reductions in the frequencies of BFP^+ cells occurred in the control due to loss of BFP expression in differentiating $CD235^+$ erythroblasts, presumably a result of enucleation (Figure S7F-G). Therefore, at day 10 and 14, we used the total population of viable cells for comparison. At day 10, frequencies and total numbers of $CD235^+$ erythroblasts were reduced upon *HES6* knockdown (Figure S7H-I). At day 14 however, no difference could be observed between *HES6* knockdown and control for the frequencies of $CD235^+$ erythroblasts which probably results from the inclusion of BFP^- cells that mask the effect of *HES6* knockdown in the BFP^+ cells, but the absolute cell numbers were still reduced for two of the three *HES6* knockdown constructs (Figure S7H-I). Overall, these results show that HES6 is essential for the *in vitro* development of erythrocytes and megakaryocytes from human HSPCs, in agreement with its expression in erythrocytes and MEPs.

HES6 is needed for *in vivo* precursor engraftment and differentiation towards pDCs, erythroblasts and B-cells

To validate our *in vitro* experiments and to study the role of HES6 on human precursor engraftment and differentiation *in vivo*, we injected bulk control and *HES6* shRNA transduced HSPCs, intrahepatically in non-obese diabetic–severe combined immunodeficiency Il2RG$^{-/-}$ (NSG) mice (Figure S8A), a well-established mouse model that supports the development of various human hematopoietic lineages[33]. Injected cells were comprised of non-transduced BFP^{-} and transduced BFP^{+} HSPCs to create a competitive setting. After 8-9 weeks, both bone marrow and liver were engrafted with similar total human cell numbers for all conditions (Figure 5A). Engraftment of the thymus was too low and inconsistent to allow analysis of *in vivo* T-cell development. The frequency of BFP^{+} cells before injection was similar and above 10% for both *HES6* knockdown and control transduced cells, and this remained stable in the CD45^{+} control shRNA transduced precursors in the bone marrow and liver (Figure 5B). In contrast, there was a clear reduction in BFP^{+} cells at both anatomical sites for both *HES6* knockdown conditions at the end of the experiment (Figure 5B), indicating that HSPCs with reduced *HES6* expression have lower repopulating potential in this competitive setting. A BFP^{+} population was detected in only six out of twelve *HES6* knockdown animals, thereby limiting the number of datapoints for analysis (Figure 5B). Within the bone marrow of the animals with detectable reconstitution, *HES6* knockdown increased the frequency of NK cells and had no consistent impact on myeloid cells, but both NK and myeloid cell numbers were not significantly altered compared to the control (Figure 5C-D). Although this mouse model is not optimal in supporting human erythroid and megakaryocytic development[34], we did observe, within the mice that showed reconstitution, a reduction in both megakaryocytes and erythroblasts upon *HES6* knockdown (Figure 5C-D). In addition, the frequency and total number of B cells were decreased in case of *HES6* knockdown (Figure 5C-D). Within the BFP^{+} population in the liver, both the frequencies and total cell numbers of pDCs were reduced for *HES6* knockdown compared to control, while the effect on cDCs was variable (Figure 5E-F). Overall, and consistent with the colony formation assay *in*

vitro, loss of *HES6* expression in human HSPCs restricts their *in vivo* repopulating potential. Furthermore, in the mice that showed reconstitution, the pDC, megakaryo-erythroid and B-cell development was reduced upon *HES6* knockdown, in agreement with the *in vitro* experiments.

HES6 knockdown impacts gene expression during erythroid and megakaryocyte development

To study the downstream changes following *HES6* knockdown, we performed RNA-seq on sorted subpopulations from control and *HES6* shRNA transduced HSPCs after four days in liquid cultures that induce erythroid and megakaryocyte differentiation (Figure 6A, Figure S9A). In control samples, megakaryocytic genes (*VWF*, *GP1BA*, *GP9*, *ITGA2B*) were specifically expressed in megakaryocytes ($CD41^+$) while erythroid specific genes (*EPOR*, *TFRC*, *E2F4*, *E2F8*) were induced in $CD71^+CD235^-$ early and $CD71^+CD235^+$ late erythroblasts, validating our sorting strategy (Figure 6B). *HES6* and *TCF3* expression was highest in erythroid cells, while *HES1* showed the opposite pattern with highest expression in megakaryocytes. While megakaryocytes express both *GATA1* and *GATA2*, late erythroblasts only express GATA1. Consistent with the highest expression of *HES6*, the impact of *HES6* knockdown on gene expression was most pronounced in erythroblasts, but also notable in megakaryocytes where we observed biological variation for one donor (Figure S9B). In $CD34^-$ cells, the biological variation between donors dominated over the effect of *HES6* knockdown (Figure S9B). Differential gene expression analysis (DGEA) revealed more differentially expressed genes (DEGs) following *HES6* knockdown in erythroblasts compared to in megakaryocytes or $CD34^-$ cells, with substantial overlap in erythroblast stages (Figure S9C). Within these, we observed significantly reduced expression of erythroid-associated genes (*TFRC* which encodes CD71, *HBB*, *EPCAM, E2F4*; Figure 6C-D) and, consistently, gene set enrichment analysis (GSEA) revealed enriched erythroblast-related gene sets in control transduced samples (Figure S9D). Compared to the control, *HES6* knockdown erythroid cells failed to downregulate *GATA2* and *ID2* expression (Figure 6B-D). No impact on *GATA1* expression was observed (data not shown). DGEA within megakaryocytes showed significantly reduced expression of genes important for megakaryocyte development (*CD36*, *DLK1*)

and proliferation (*MKI67*, *HEMGN*) (Figure 6E). Within the more heterogenous and more immature CD34$^-$ population, pDC associated genes (*IRF8*, *TCF4)* [35,36], B-lineage genes (*BLNK*, *IGLL1*, *IGHM*)[37,38], the E-protein encoding gene *TCF3* and *RUNX2*, important for hematopoietic precursor cells and pDCs[39–41] were all downregulated in *HES6* knockdown cells compared to the control (Figure 6F).

Given that the GATA2 to GATA1 switch is critical to permit erythroid development[42], we investigated if failure to downregulate GATA2 mediated the block in erythroid development upon *HES6* knockdown. Therefore, we cultured *HES6-GATA2* double knockdown HSPCs in erythroid culture conditions (Figure S10A). Both *GATA2* shRNAs reduced *GATA2* expression by 50% (Figure 7A) and this did not significantly change megakaryocyte development compared to *HES6* knockdown alone (Figure 7B, Figure S10B), although a trend towards an increased frequency of megakaryocytes could be observed. Erythroid development was further decreased upon knockdown of both genes compared to *HES6* alone, both in frequencies and in total cell numbers (Figure 7B, Figure S10B). Single *GATA2* knockdown had a similar effect on megakaryocyte and erythroid development (Figure 7C, Figure S10C). Analysis of ChIP-seq data[23] revealed binding of HES6 at genes associated with erythroid (*HBB*, *TFRC*) and megakaryocyte (*HEMGN*, *CD36*) differentiation and proliferation (*MKI67*) (Figure 8A, Figure S11A), which were downregulated upon *HES6* knockdown (Figure 6C-E). Furthermore, we found HES6 binding peaks in genes important for T- and B-cell development (*BLNK*, *IGHM*, *TCF3*, *TCF12*) and pDC development (*TCF4* and *RUNX2*) (Figure S11A). For all these HES6 bound target genes, only *HBB* and *IGHM* showed overlapping *GATA1* binding[23] (data not shown). These data indicate that HES6 has an essential role during erythroid development that is independent of *GATA2* expression and suggest that HES6 may directly regulate the expression of genes that are important for erythroid, megakaryocyte, pDC, B- and T-cell development.

HES6 facilitates proliferation by mediating the G1-to-S phase transition

Since *HES6* knockdown reduced cellular output and downregulated genes associated with proliferation, we investigated the effect of *HES6* knockdown on proliferation. GSEA for late erythroblast samples as well as megakaryocytes showed enrichment of cell cycle related gene sets in

the control, including MYC targets, genes related to G1-S specific transcription, G2M checkpoint genes and E2F targets (Figure 8B, Figure S11B). Interestingly, *TFRC*, *E2F4* and *E2F8* were shown to be important for cell proliferation[43–45] and expressed during erythroid development (Figure 6B) but downregulated upon *HES6* knockdown in late erythroblasts (Figure 6D). This was confirmed for *TFRC* at the protein level (Figure S7E). Furthermore, in late erythroblasts, genes with specific *E2F4* binding motifs were enriched in control samples (Figure S11C), although not statistically significant. To investigate if *HES6* knockdown had an effect on cell proliferation or survival during erythroid development, we performed an EdU incorporation and apoptosis assay. A significant decrease in the frequency of cells in the proliferating S phase (EdU^+) and a significant increase in cells in the resting G1 phase (EdU^- and 2N DNA content) was observed upon *HES6* knockdown compared to in control transduced cells (Figure 8C, Figure S11D). Given that we did not detect any consistent differences in the relative number of early or late apoptotic cells upon *HES6* knockdown compared to control (Figure S11E-F), these results indicate that HES6 is required for the proliferation of erythroid cells and that this might involve the regulation of genes that mediate cell cycle progression.

Discussion

While important functions for several HES gene family members had been revealed in both normal and malignant hematopoiesis[5,6,9], only very recently a first role for HES6 has been demonstrated as a GATA1 cofactor during erythropoiesis[23]. In this study, we explored *HES6* expression and function during human hematopoiesis *in vivo* and *in vitro* and provide insights into potential lineage- and stage-specific roles for this transcription factor in human hematopoiesis.

Using well-described *in vitro* differentiation culturing systems[28,31] we showed a clear impact of *HES6* knockdown on the development of megakaryocytes, erythrocytes, pDCs, B and T-cells, consistent with its expression in these lineages. While this study confirms the importance of HES6 in normal erythropoiesis that was recently reported[23], our work reveals also other mechanisms through which

HES6 mediates this developmental process. In contrast to Wang et al.[23], we did not observe GATA1 binding at most HES6 target genes that we identified in our RNAseq data, suggesting GATA1-independent functions for HES6. Consistently, *GATA1* expression was not reduced following *HES6* knockdown in erythroblasts. Our knockdown experiments resulted in significantly fewer differentially expressed genes compared to Wang et al.[23] which presumably results from different experimental approaches. Our DGEA is based on shared differences induced by two different *HES6* shRNAs, compared to a single shRNA in their study. Moreover, we sorted surface marker-defined subpopulations prior to sequencing, allowing a comparison of developmental stage-matched cells and excluding an impact of different differentiation stages on gene expression. We could not confirm a higher degree of apoptosis upon *HES6* knockdown[23], but instead show that HES6 regulates proliferation by mediating the G- to-S cell cycle phase transition. RNA-seq and ChIPseq[23] data suggest direct regulatory roles for HES6 in positively regulating *TFRC* (encoding the transferrin receptor CD71) and *MKI67* expression, two important mediators of proliferation that do not display GATA1 binding. We confirmed reduced *TFRC* expression following *HES6* knockdown at the protein (CD71) level. Interestingly, previous work from our lab showed that *TFRC* is specifically upregulated following preTCR signaling at the $CD4^{+}CD28^{+}CD3^{-}$ stage of human T-cell development[46], the stage where *HES6* expression and clonal expansion are induced. We suggest that the requirement for HES6 is based on its induction of *TFRC* expression and thus the promotion of proliferation after preBCR/TCR signalling, analogous to the observations in erythropoiesis. Consistently, proliferation and differentiation are tightly coupled during erythropoiesis[47] and T cell development[48]. Importantly, *GATA2* levels were higher in erythroblasts upon *HES6* knockdown and, consequently, this perturbed GATA2 to GATA1 switch could potentially impact erythroid development[42]. However, Ahmed et al.[49] showed that *GATA2* downregulation during erythroid development is a consequence of shortened cell cycle length and not the result of reduced expression. Therefore, we hypothesize that the increased *GATA2* expression in *HES6* knockdown erythroblasts results from their reduced proliferation, in agreement with all our experimental data that support such a role for HES6 in mediating proliferation.

Consistent with this, *GATA2* knockdown did not rescue erythroid development following *HES6* knockdown. The proliferative capacity of HES6 in hematopoietic cells is consistent with its oncogenic role in various types of cancer[13–17]. Although the precise molecular mechanisms are still unclear, a link between HES6 and MYC activity has been proposed[18], and MYC target genes were also depleted in *HES6* shRNA transduced erythroblasts. Therefore, our study may help to unravel the oncogenic role of HES6, also in BPDCN.

Our study also reveals an important functional role for HES6 in HSPC function, consistent with its high expression in MPPs, although the mechanism is presently unclear. *HES6* knockdown HSPCs displayed a strongly reduced colony-forming capacity *in vitro* and impaired engraftment potential in an *in vivo* competitive transplantation model. This decreased proliferative capacity of *HES6* knockdown HSPCs may have also caused the observed reduction in the absolute number of monocytes, granulocytes, cDCs and NK cells, despite the lack of impact on the frequencies of these cells. We therefore did not connect these findings with a direct role for HES6 in the differentiation of these lineages. In each case, given that the few mice that showed reconstitution with *HES6* shRNAs also displayed reduced erythroid, pDC and B cell development, consistent with our *in vitro* experiments, we believe that our study reveals novel functional roles for HES6 in the engraftment potential of human HSPCs and in their differentiation potential towards particular hematopoietic lineages.

References

1. Rodrigues CP, Shvedunova M, Akhtar A. Epigenetic Regulators as the Gatekeepers of Hematopoiesis. Trends Genet. 2021;37(2):125-142.

2. Wilson NK, Foster SD, Wang X, et al. Combinatorial transcriptional control in blood stem/progenitor cells: genome-wide analysis of ten major transcriptional regulators. Cell Stem Cell. 2010;7(4):532-544.

3. Weng AP, Ferrando AA, Lee W, et al. Activating Mutations of NOTCH1 in Human T Cell Acute Lymphoblastic Leukemia. Science. 2004;306(5694):269-271.

4. Klinakis A, Lobry C, Abdel-Wahab O, et al. A novel tumour-suppressor function for the Notch pathway in myeloid leukaemia. Nature. 2011;473(7346):230-233.

5. D'Altri T, Gonzalez J, Aifantis I, Espinosa L, Bigas A. Hes1 expression and CYLD repression are essential events downstream of Notch1 in T-cell leukemia. Cell Cycle. 2011;10(7):1031-1036.

6. Espinosa L, Cathelin S, D'Altri T, et al. The Notch/Hes1 Pathway Sustains NF-κB Activation through CYLD Repression in T Cell Leukemia. Cancer Cell. 2010;18(3):268-281.

7. Varnum-Finney B, Dallas MH, Kato K, Bernstein ID. Notch target Hes5 ensures appropriate Notch induced T- versus B-cell choices in the thymus. Blood. 2008;111(5):2615-2620.

8. Wendorff AA, Koch U, Wunderlich FT, et al. Hes1 Is a Critical but Context-Dependent Mediator of Canonical Notch Signaling in Lymphocyte Development and Transformation. Immunity. 2010;33(5):671-684.

9. De Decker M, Lavaert M, Roels J, et al. HES1 and HES4 have non-redundant roles downstream of Notch during early human T-cell development. Haematologica. 2021;106(1):130-141.

10. Murai K, Vernon AE, Philpott A, Jones P. Hes6 is required for MyoD induction during gastrulation. Dev Biol. 2007;312(1):61-76.

11. Gratton MO, Torban E, Jasmin SB, Theriault FM, German MS, Stifani S. Hes6 promotes cortical neurogenesis and inhibits Hes1 transcription repression activity by multiple mechanisms. Mol Cell Biol. 2003;23(19):6922-6935.

12. Jhas S, Ciura S, Belanger-Jasmin S, et al. Hes6 Inhibits Astrocyte Differentiation and Promotes Neurogenesis through Different Mechanisms. J Neurosci. 2006;26(43):11061-11071.

13. Haapa-Paananen S, Kiviluoto S, Waltari M, et al. HES6 gene is selectively overexpressed in glioma and represents an important transcriptional regulator of glioma proliferation. Oncogene. 2012;31(10):1299-1310.

14. Carvalho FLF, Marchionni L, Gupta A, et al. HES6 promotes prostate cancer aggressiveness independently of Notch signalling. J Cell Mol Med. 2015;19(7):1624-1636.

15. Xu Y, Liu X, Zhang H, et al. Overexpression of HES6 has prognostic value and promotes metastasis via the Wnt/ß-catenin signaling pathway in colorectal cancer. Oncol Rep. 2018;40(3):1261-1274.

16. Zhang P, Yang M, Zhang Y, et al. Dissecting the Single-Cell Transcriptome Network Underlying Gastric Premalignant Lesions and Early Gastric Cancer. Cell Rep. 2020;30(12):4317.

17. Pandiani C, Strub T, Nottet N, et al. Single-cell RNA sequencing reveals intratumoral heterogeneity in primary uveal melanomas and identifies HES6 as a driver of the metastatic disease. Cell Death Differ. 2021;28(6):1990-2000.

18. Krossa I, Strub T, Martel A, et al. Recent advances in understanding the role of HES6 in cancers. Theranostics. 2022;12(9):4374-4385.

19. Dijkman R, Van Doorn R, Szuhai K, Willemze R, Vermeer MH, Tensen CP. Gene-expression profiling and array-based CGH classify CD4 +CD56+ hematodermic neoplasm and cutaneous myelomonocytic leukemia as distinct disease entities. Blood. 2007;109(4):1720-1727.

20. Sapienza MR, Fuligni F, Agostinelli C, et al. Molecular profiling of blastic plasmacytoid dendritic cell neoplasm reveals a unique pattern and suggests selective sensitivity to NF-kB pathway inhibition. Leukemia. 2014;28(8):1606-1616.

21. Roy A, Wang G, Iskander D, et al. Transitions in lineage specification and gene regulatory networks in hematopoietic stem/progenitor cells over human development. Cell Rep. 2021;36(11):109698.

22. Da Cunha AF, Brugnerotto AF, Duarte AS, et al. Global gene expression reveals a set of new genes involved in the modification of cells during erythroid differentiation. Cell Prolif. 2010;43(3):297-309.

23. Wang Z, Wang P, Zhang J, et al. The novel GATA1-interacting protein HES6 is an essential transcriptional cofactor for human erythropoiesis. Nucleic Acids Res. 2023;51(10):4774-4790.

24. Roels J, Kuchmiy A, De Decker M, et al. Distinct and temporary-restricted epigenetic mechanisms regulate human αβ and γδ T cell development. Nat Immunol. 2020;21(10):1280-1292.

25. Durinck K, Wallaert A, Van de Walle I, et al. The notch driven long non-coding RNA repertoire in T-cell acute lymphoblastic leukemia. Haematologica. 2014;99(12):1808-1816.

26. Loontiens S, Dolens AC, Strubbe S, et al. PHF6 Expression Levels Impact Human Hematopoietic Stem Cell Differentiation. Front Cell Dev Biol. 2020;8:599472.

27. Roels J, Van Hulle J, Lavaert M, et al. Transcriptional dynamics and epigenetic regulation of E and ID protein encoding genes during human T cell development. Front Immunol. 2022;13:960918

28. Dolens AC, Van de Walle I, Taghon T. Approaches to Study Human T Cell Development. In: Bosselut R, S. Vacchio M, eds. T-Cell Development: Methods and Protocols. Springer New York. 2016:239-251.

29. Regev A, Teichmann SA, Lander ES, et al. The human cell atlas. Elife. 2017;6:1-30.

30. Suo C, Dann E, Goh I, et al. Mapping the developing human immune system across organs. Science. 2022;376(6597):eabo0510.

31. Kirkling ME, Cytlak U, Lau CM, et al. Notch Signaling Facilitates In Vitro Generation of Cross-Presenting Classical Dendritic Cells. Cell Rep. 2018;23(12):3658-3672.

32. Rapin N, Bagger FO, Jendholm J, et al. Comparing cancer vs normal gene expression profiles identifies new disease entities and common transcriptional programs in AML patients. Blood. 2014;123(6):894-904.

33. Shultz LD, Lyons BL, Burzenski LM, et al. Human Lymphoid and Myeloid Cell Development in NOD/LtSz-scid IL2Rγnull Mice Engrafted with Mobilized Human Hemopoietic Stem Cells 12. J Immunol. 2005;174(10):6477-6489.

34. Mende N, Rahmig S, Waskow C. Multilineage readout after HSC expansion – erythrocytes matter. Cell Cycle. 2016;15(8):1032-1033.

35. Kuo YH, Zaidi SK, Gornostaeva S, Komori T, Stein GS, Castilla LH. Runx2 induces acute myeloid leukemia in cooperation with Cbfβ-SMMHC in mice. Blood. 2009;113(14):3323-3332.

36. Sichien D, Scott CL, Martens L, et al. IRF8 Transcription Factor Controls Survival and Function of Terminally Differentiated Conventional and Plasmacytoid Dendritic Cells, Respectively. Immunity. 2016;45(3):626-640.

37. Kwon K, Hutter C, Sun Q, et al. Instructive Role of the Transcription Factor E2A in Early B Lymphopoiesis and Germinal Center B Cell Development. Immunity. 2008;28(6):751-762.

38. Minegishi Y, Rohrer J, Coustan-Smith E, et al. An Essential Role for BLNK in Human B Cell Development. Science. 1999;286(5446):1954-1957.

39. Cisse B, Caton ML, Lehner M, et al. Transcription Factor E2-2 Is an Essential and Specific Regulator of Plasmacytoid Dendritic Cell Development. Cell. 2008;135(1):37-48.

40. Ghosh HS, Cisse B, Bunin A, Lewis KL, Reizis B. Continuous Expression of the Transcription Factor E2-2 Maintains the Cell Fate of Mature Plasmacytoid Dendritic Cells. Immunity. 2010;33(6):905-916.

41. Sawai CM, Sisirak V, Ghosh HS, et al. Transcription factor Runx2 controls the development and migration of plasmacytoid dendritic cells. J Exp Med. 2013;210(11):2151-2159.

42. Bresnick EH, Lee HY, Fujiwara T, Johnson KD, Keles S. GATA switches as developmental drivers. J Biol Chem. 2010;285(41):31087-31093.

43. Kinross KM, Clark AJ, Iazzolino RM, Humbert PO. E2f4 regulates fetal erythropoiesis through the promotion of cellular proliferation. Blood. 2006;108(3):886-895.

44. Ye L, Guo L, He Z, et al. Upregulation of E2F8 promotes cell proliferation and tumorigenicity in breast cancer by modulating G1/S phase transition. Oncotarget. 2016;7(17):23757-23771.

45. Fouquet G, Thongsa-ad U, Lefevre C, et al. Iron-loaded transferrin potentiates erythropoietin effects on erythroblast proliferation and survival: a novel role through transferrin receptors. Exp Hematol. 2021;99:12-20.

46. Taghon T, Van de Walle I, De Smet G, et al. Notch signaling is required for proliferation but not for differentiation at a well-defined β-selection checkpoint during human T-cell development. Blood. 2009;113(14):3254-3263.

47. Kadri Z, Lefevre C, Goupille O, et al. Erythropoietin and IGF-1 signaling synchronize cell proliferation and maturation during erythropoiesis. Genes 2015;29(24):2603-2616.

48. Kreslavsky T, Gleimer M, Miyazaki M, et al. β-Selection-Induced Proliferation Is Required for αβ T Cell Differentiation. Immunity. 2012;37(5):840-853.

49. Ahmed N, Kull T, Loeffler D, Hoppe P, van den Akker E, Schroeder T. 3001 – LIVE SINGLE CELL QUANTIFICATION OF THE GATA SWITCH DYNAMICS DURING ADULT AND DEVELOPMENTAL ERYTHROPOIESIS. Exp Hematol. 2021;12(100):S44.

Figure legends

Figure 1. *HES6* is important for early *in vitro* T-cell development. (A) Boxplots derived from scRNA-seq data showing pseudo-bulk log-normalized imputed mRNA expression level of *HES6* across different stages of human postnatal T-cell development[27]. Boxplots show median and first and third quartile. DN: double negative (CD4-CD8-); DP: double positive (CD4+CD8+); SP: single positive. (B) qRT-PCR of *HES6* in CB $CD34^+Lin^-BFP^+$ cells transduced with a control shRNA or three different *HES6* shRNAs, normalized to housekeeping genes (*ACTB*, *B2M*, *SDHA*) and relative to the expression in the control shRNA condition (shRNA1: N=6; shRNA2: N=5; shRNA3: N=4). Data are presented as average of all replicates ± standard error of the mean (paired students t-test, **P<0.01.). (C-E) Flow cytometric analysis of control shRNA and *HES6* shRNA-transduced $CD34^+Lin^-BFP^+$ hematopoietic stem and progenitor cells (HSPC) cultured *in vitro* in T-lineage supporting conditions for a total of three weeks (N=5), showing gating of differentiation stages based on CD34 and CD7 expression within BFP^+ cells at day 14 (C), CD7 and CD5 within BFP^+ cells at day 21 (D) and CD4 and CD8b within BFP^+ $HLA\text{-}DR^-$ cells at day 21 (E), with frequencies of BFP^+ cells of populations of interest. Contour plots shown are representative for five replicates.

Figure 2. *HES6* is important for early *in vitro* B-cell development. (A-B) UMAP visualization of *HES6* mRNA expression in human bone marrow cells based on scRNA-seq data [29] (A) and annotation of stages of B-cell development within the human bone marrow following label transfer (B)[30]. HPC: hematopoietic precursor cell. (C) Dot plots showing pseudo-bulk log-normalized expression level (color of dots) and percentage of cells within a cluster expressing (size of dots) different genes in clusters of human bone marrow B-lineage cells, as annotated in B. (D-F) Bar graphs and flow cytometric analysis of control shRNA and *HES6* shRNA-transduced $CD34^+Lin^-BFP^+$ HSPC cultured *in vitro* in B-lineage differentiation conditions for a total of three weeks. (D) Bar graph showing frequencies of $CD45^+BFP^+$ cells within population of live cells at day 7 (N=11) and day 21 (N=12; shRNA2: N=11). Data are presented as average of all replicates ± standard error of the mean (Wilcoxon matched-pairs signed-rank test, *P<0.05, **P<0.01; ***P<0.001). Flow cytometric analysis

of CD19 and intracellular CD179b expression with frequencies of populations of interest within live cells at day 21 (E) (N=7; shRNA2: N=6) and expression of CD19 and CD20 with frequencies of population of interest within $CD45^+BFP^+$ cells at day 21 (F) (N=12; shRNA2: N=11). Contour plots with frequencies shown are from a representative replicate.

Figure 3. *HES6* knockdown impairs *in vitro* pDC development. Flow cytometric analysis (A, C) and bar graphs (B, D) of control shRNA and *HES6* shRNA-transduced $CD34^+Lin^-BFP^+$ HSPC cultured in DC-lineage supporting conditions for a total of two weeks (N=6). Contour plots shown are representative for six replicates. Flow cytometric analysis showing pDC ($CD45RA^+CD123^+$) development, gated on BFP^+ cells (A) and cDC ($CD4^+$HLA-DR^+) development, gated on BFP^+ $[CD45RA^+CD123^+]^-$ cells (C) at day 14. Bar graphs showing frequencies and absolute cell numbers of pDC (B) and cDC cells (D) within BFP^+ population at day 14. (B, D) Data are presented as average of all replicates ± standard error of the mean (Wilcoxon matched-pairs signed-rank test, *P<0.05; ns: not significant).

Figure 4. *HES6* knockdown impairs colony forming capacity of HSPCs and *in vitro* erythroid development. (A) Graph derived from published micro-array data[32] show $\log_2$ normalized probe intensities for *HES6* in sorted subsets of HPSCs from human bone marrow, mean is shown with error bars representing standard error of the mean (HSC: N=4; MPP: N=2; CMP: N=3; GMP: N=5; MEP: N=2). HSC: hematopoietic stem cell; MPP: multipotent progenitor; CMP: common myeloid progenitor; GMP: Granulocyte-monocyte progenitors, MEP: megakaryocyte-erythroid progenitor. (B-D) Analysis of control shRNA and *HES6* shRNA-transduced $CD34^+Lin^-BFP^+$ HSPC cultured in semi-solid colony-forming assay, Methocult, for a total of 10 days. Bar graphs showing number of total colonies (B, left; N=8), absolute cell numbers per colony (B, right; N=6) and number of erythroid (BFU-E/CFU-E) or myeloid (CFU-GM) colonies (C) (N=8). (B-C) Data are presented as average of all replicates ± standard error of the mean (Wilcoxon matched-pairs signed-rank test, *P<0.05, **P<0.01; ns: not significant). (D) Representative microscopic images of cytospin slides using Leica DM 3000 LED microscope (original magnification of 500x). (E-F) Flow cytometric analysis of control shRNA and

HES6 shRNA-transduced $CD34^+Lin^-BFP^+$ HSPC cultured in megakaryocyte/erythroid-lineage supporting conditions for a total of two weeks, showing gating and frequencies of megakaryocytes ($CD41^+$) and erythroblasts ($CD71^+$ erythroblasts and late-stage $CD235^+$ erythroblasts) in $CD45^+BFP^+$ population at day 5 (N=14, shRNA3: N=11). Contour plots (E) and histograms (F) shown are representative for all replicates.

Figure 5. Knockdown of *HES6* reduces the *in vivo* engraftment potential of HSPCs and their *in vivo* capacity to differentiate into megakaryocytes, erythroid, B and pDC cells. (A-F) Bar graphs showing the *in vivo* engraftment of $hCD45^+$ cells (A-B, control N=6, shRNA1 N=8, shRNA2 N=4) and the specific lineage differentiation within the BFP^+ population of engrafted mice (C-F, control N=6, shRNA1 N=5, shRNA2 N=1). (A) Bar graph showing absolute $hCD45^+$ cell numbers in the bone marrow and liver for control or *HES6* knockdown conditions. (B) Bar graphs showing frequencies of BFP^+ cells within the $hCD45^+$ population at the start of the experiment after 24 hours of transduction (left), at the end of the experiment in the bone marrow (center) and liver (right) and the cut-off for BFP engraftment, resulting in fewer datapoints in subsequent analysis of BFP^+ population within engrafted mice (of which results are shown in panels C-F). (C-D) Bar graphs showing frequencies (C) and absolute cell numbers (D) of subpopulations within BFP^+ populations in the bone marrow. NK: $CD56^+CD3^-$, myeloid: $CD33^+$, mgk: $CD41^+$, ery: $CD71^+CD41^-$, B: $CD19^+$. (E-F) Bar graphs showing frequencies (E) and absolute cell numbers (F) of subpopulations within BFP^+ populations in the liver. pDC: $CD123^+CD45RA^+$, cDC: not pDC $CD4^+$HLA-DR^+. Data are presented as average of all replicates ± standard error of the mean (Mann Whitney U test on control versus *HES6* knockdown (pooled shRNA1 and shRNA2), *P<0.05, ***P<0.001; ns: not significant, ND: not detected).

Figure 6. RNA-seq analysis reveals molecular pathways downstream of *HES6* knockdown during erythroid development. (A) Overview of development of control shRNA and *HES6* shRNA-transduced (shRNA1 and shRNA2 were used) $CD34^+Lin^-BFP^+$ HSPC cultured for four days in megakaryocyte/erythroid-lineage supporting conditions. Bulk RNA-seq was performed on the four

indicated subpopulations. (B-C) Results from bulk RNA-seq data from three donors on the four subpopulations as shown in Figure 6A and Figure S9A. (B) Heatmap showing expression of genes in different cell populations in control samples. (C-F) Volcano plots showing differentially up- and downregulated genes (blue and red respectively) in different cell populations. (E-F) In volcano plots of megakaryocytes and $CD34^-$ precursors *HES6* is indicated in grey because its expression was not significantly downregulated. (F) In the volcano plot of $CD34^-$ precursors *TCF3* is indicated in grey considering downregulation was significant (padj <0.05) but log2FC values were just below cut-off.

Figure 7. *GATA2* knockdown fails to rescue impaired *in vitro* megakaryo-erythroid development upon *HES6* knockdown. Bar graphs (A, C) and line graphs (B) showing results of *in vitro* experiments to study the impact of double *GATA2-HES6* knockdown (GFP^+BFP^+) (B) or single *GATA2* knockdown (GFP^+BFP^-) (A, C) on human megakaryo-erythrocyte development (N=6) as described in Figure S10A. (A) qRT-PCR showing *GATA2* expression in CB $CD34^+$ Lin^- GFP^+BFP^- cells transduced with a control shRNA or two different *GATA2* shRNAs, normalized to expression of the housekeeping gene *SDHA* and relative to the expression in the control shRNA condition. Data are presented as average of five replicates ± standard error of the mean (SEM) (paired students t-test). (B-C) Line graphs (B) and bar graphs (C) showing megakaryocyte ($CD41^+$) and erythroblast ($CD71^+$) percentages within double *GATA2-HES6* knockdown (B) or single *GATA2* knockdown (C) cultures (N=6) with populations gated similar as shown in Figure 4E-F. (B-C) Data are presented as average of six replicates and error bars indicate SEM (Wilcoxon matched-pairs signed-rank test, *P<0.05, **P<0.01, ns: not significant).

Figure 8. *HES6* knockdown impacts cell cycle progression. (A) Analysis of recently published ChIP-seq data of *HES6* in erythroid cells[23], significant *HES6* binding peaks for *TFRC* gene are shown in red. (B) Results from data analysis of bulk RNA-seq of sorted cell populations as discussed in Figure 6. Preranked GSEA results showing enrichment of cell-cycle related gene sets in control sample within late erythroblasts. NES: Normalized enrichment score; FDR: false detection rate. (C) Results of control shRNA and *HES6* shRNA-transduced $CD34^+Lin^-BFP^+$ HSPC cultured in megakaryocyte/erythroid-

lineage supporting conditions for three days (N=5), showing gating and frequencies of cell-cycle stages within viable cells for a representative replicate (G1: EdU^- DAPI low (DNA 2N); S: EdU^+; G2M: EdU^- DAPI high (DNA 4N)).

FIGURE1

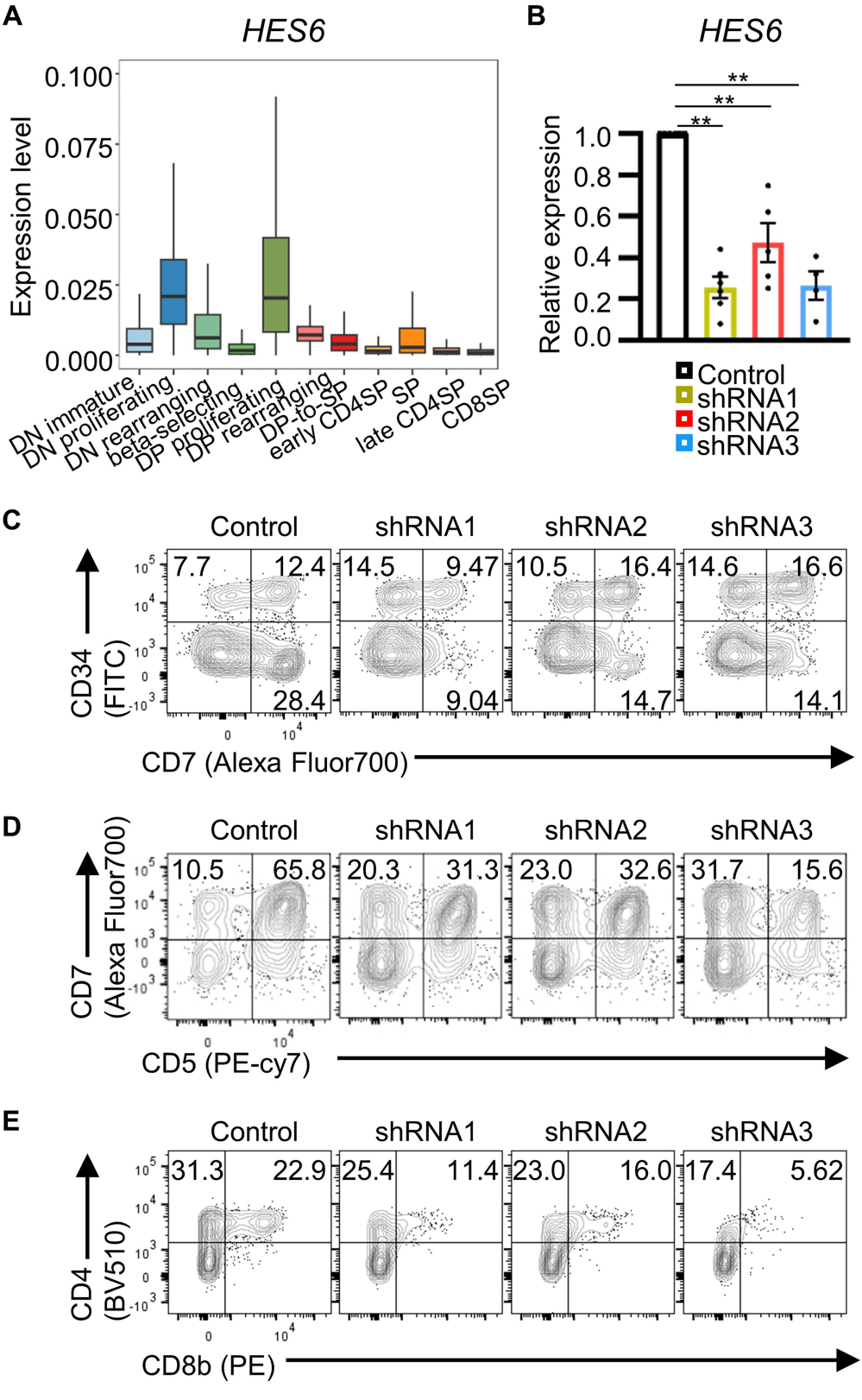
A
HES6
Expression level
0.100
0.075
0.050
0.025
0.000
DN immature
DN proliferating
DN rearranging
beta-selecting
DP proliferating
DP rearranging
DP-to-SP
early CD4SP
SP
late CD4SP
CD8SP
B
HES6
Relative expression
1.0
0.8
0.6
0.4
0.2
0.0
**
**
**
Control
shRNA1
shRNA2
shRNA3
C
Control
shRNA1
shRNA2
shRNA3
CD34 (FITC)
CD7 (Alexa Fluor700)
7.7
12.4
28.4
14.5
9.47
9.04
10.5
16.4
14.7
14.6
16.6
14.1
D
Control
shRNA1
shRNA2
shRNA3
CD7 (Alexa Fluor700)
CD5 (PE-cy7)
10.5
65.8
20.3
31.3
23.0
32.6
31.7
15.6
E
Control
shRNA1
shRNA2
shRNA3
CD4 (BV510)
CD8b (PE)
31.3
22.9
25.4
11.4
23.0
16.0
17.4
5.62

FIGURE2

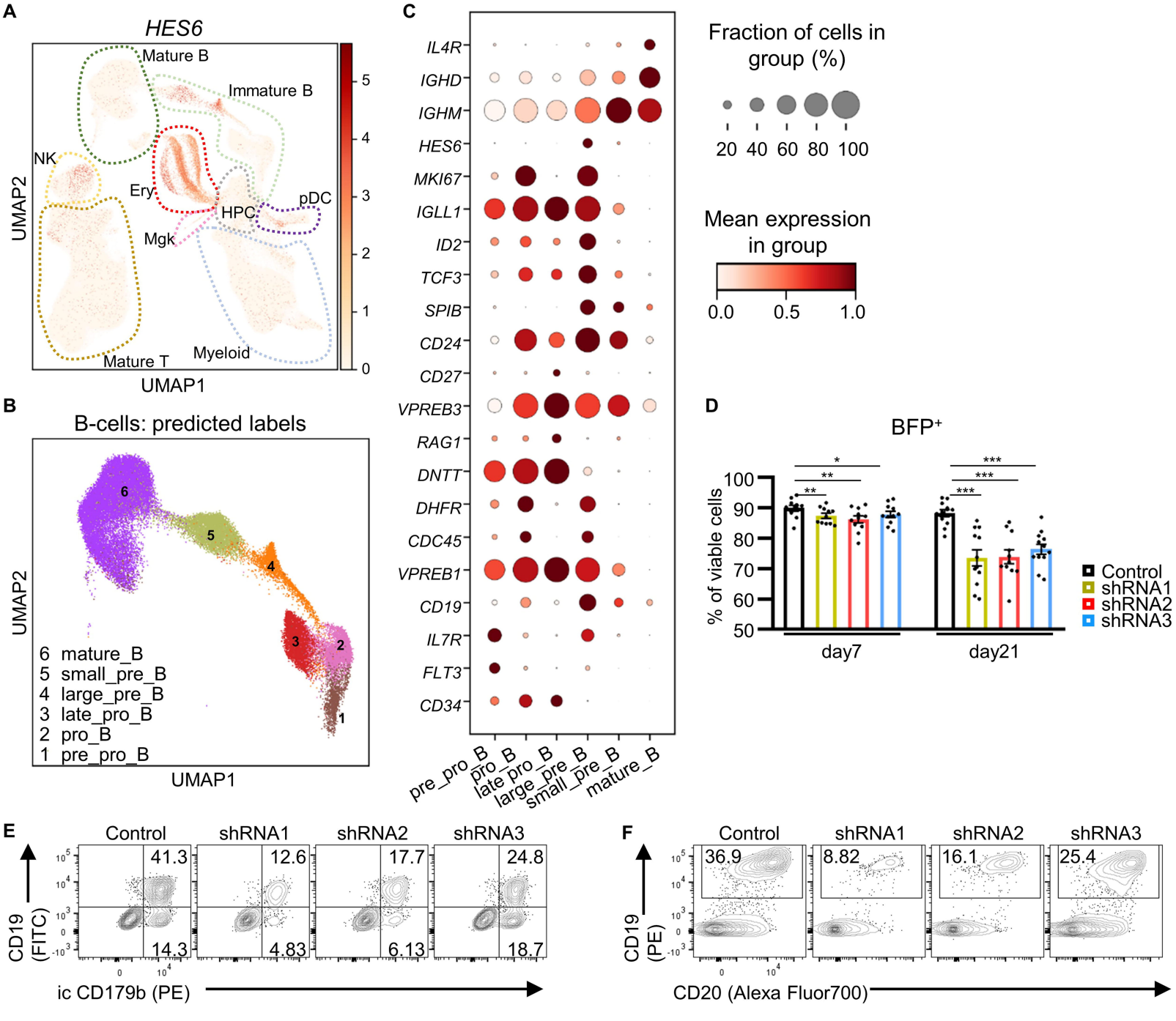
A
HES6
Mature B
Immature B
NK
Ery
HPC
pDC
Mgk
Mature T
Myeloid
UMAP2
UMAP1
B
B-cells: predicted labels
6 mature_B
5 small_pre_B
4 large_pre_B
3 late_pro_B
2 pro_B
1 pre_pro_B
C
IL4R
IGHD
IGHM
HES6
MKI67
IGLL1
ID2
TCF3
SPIB
CD24
CD27
VPREB3
RAG1
DNTT
DHFR
CDC45
VPREB1
CD19
IL7R
FLT3
CD34
pre_pro_B
pro_B
late_pro_B
large_pre_B
small_pre_B
mature_B
Fraction of cells in group (%)
Mean expression in group
D
BFP+
% of viable cells
day7
day21
Control
shRNA1
shRNA2
shRNA3
E
Control
shRNA1
shRNA2
shRNA3
41.3
14.3
12.6
4.83
17.7
6.13
24.8
18.7
CD19 (FITC)
ic CD179b (PE)
F
36.9
8.82
16.1
25.4
CD19 (PE)
CD20 (Alexa Fluor700)

FIGURE3

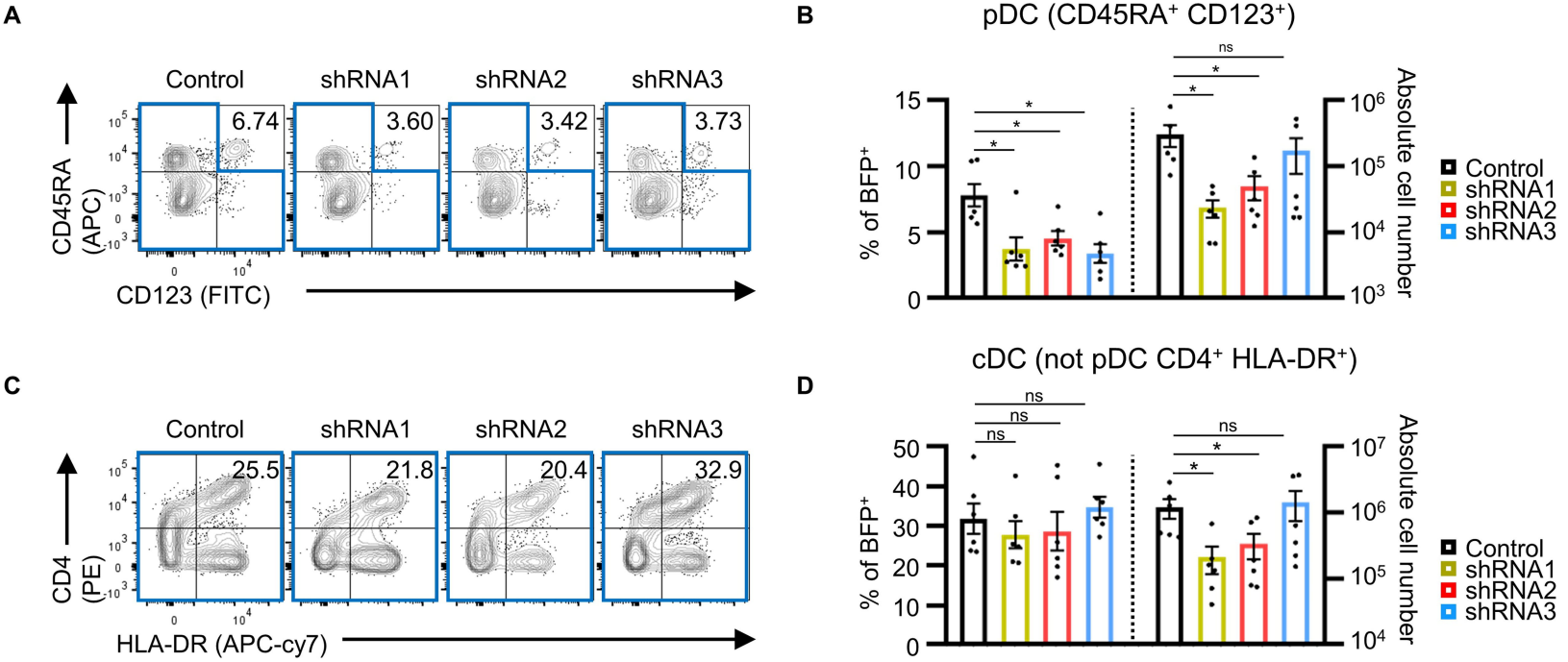
A
Control
shRNA1
shRNA2
shRNA3
6.74
3.60
3.42
3.73
CD45RA (APC)
CD123 (FITC)
B
pDC (CD45RA+ CD123+)
% of BFP+
Absolute cell number
Control
shRNA1
shRNA2
shRNA3
ns
C
25.5
21.8
20.4
32.9
CD4 (PE)
HLA-DR (APC-cy7)
D
cDC (not pDC CD4+ HLA-DR+)

FIGURE4

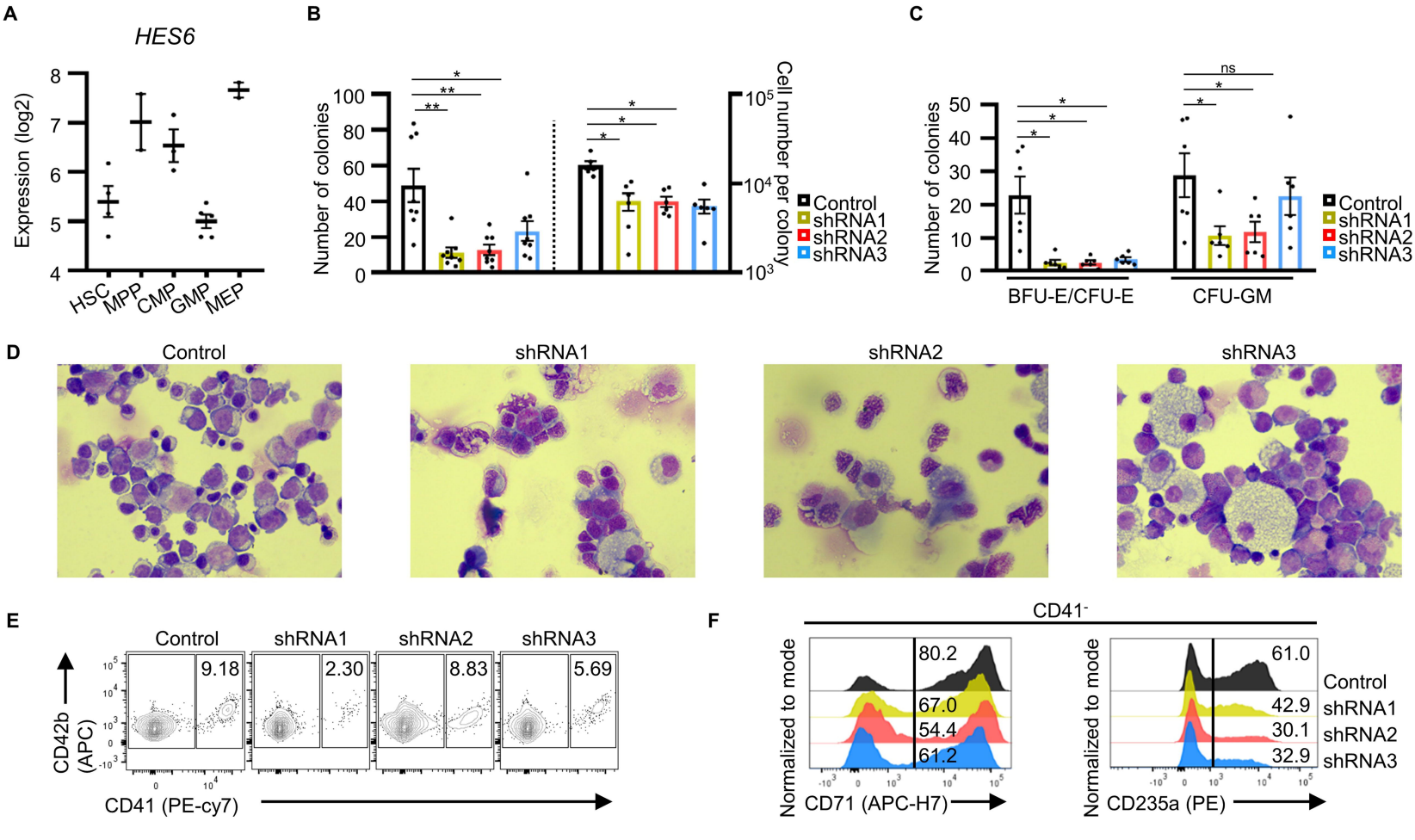
A
HES6
Expression (log2)
HSC
MPP
CMP
GMP
MEP
B
Number of colonies
Cell number per colony
Control
shRNA1
shRNA2
shRNA3
C
Number of colonies
ns
BFU-E/CFU-E
CFU-GM
Control
shRNA1
shRNA2
shRNA3
D
Control
shRNA1
shRNA2
shRNA3
E
Control
shRNA1
shRNA2
shRNA3
9.18
2.30
8.83
5.69
CD42b (APC)
CD41 (PE-cy7)
F
CD41-
Normalized to mode
80.2
67.0
54.4
61.2
CD71 (APC-H7)
61.0
42.9
30.1
32.9
CD235a (PE)
Control
shRNA1
shRNA2
shRNA3

FIGURE5

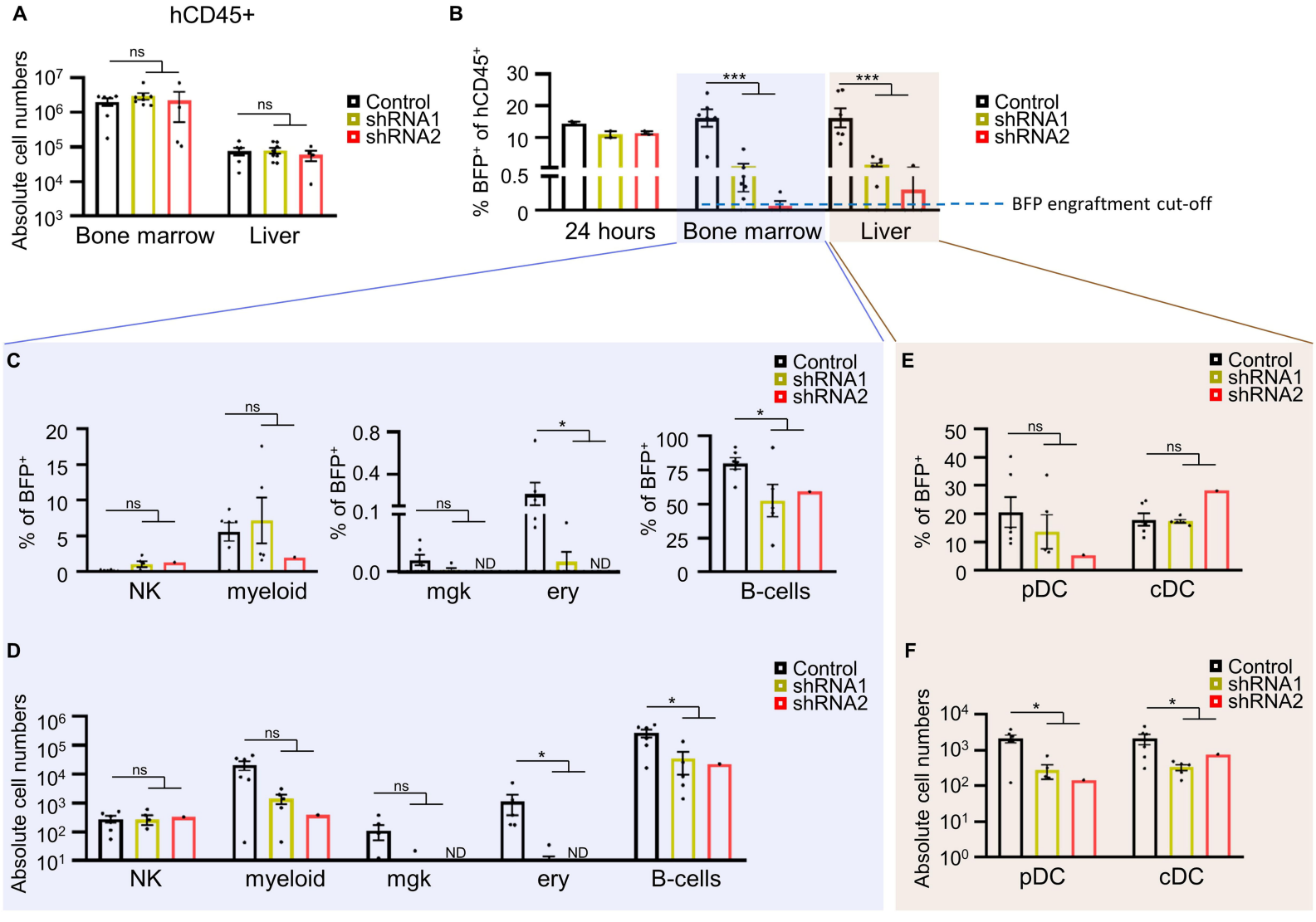
A
hCD45+
Absolute cell numbers
Bone marrow
Liver
ns
Control
shRNA1
shRNA2
B
% BFP+ of hCD45+
24 hours
Bone marrow
Liver
***
BFP engraftment cut-off
C
% of BFP+
NK
myeloid
mgk
ery
B-cells
ND
*
D
Absolute cell numbers
E
pDC
cDC
F

FIGURE6

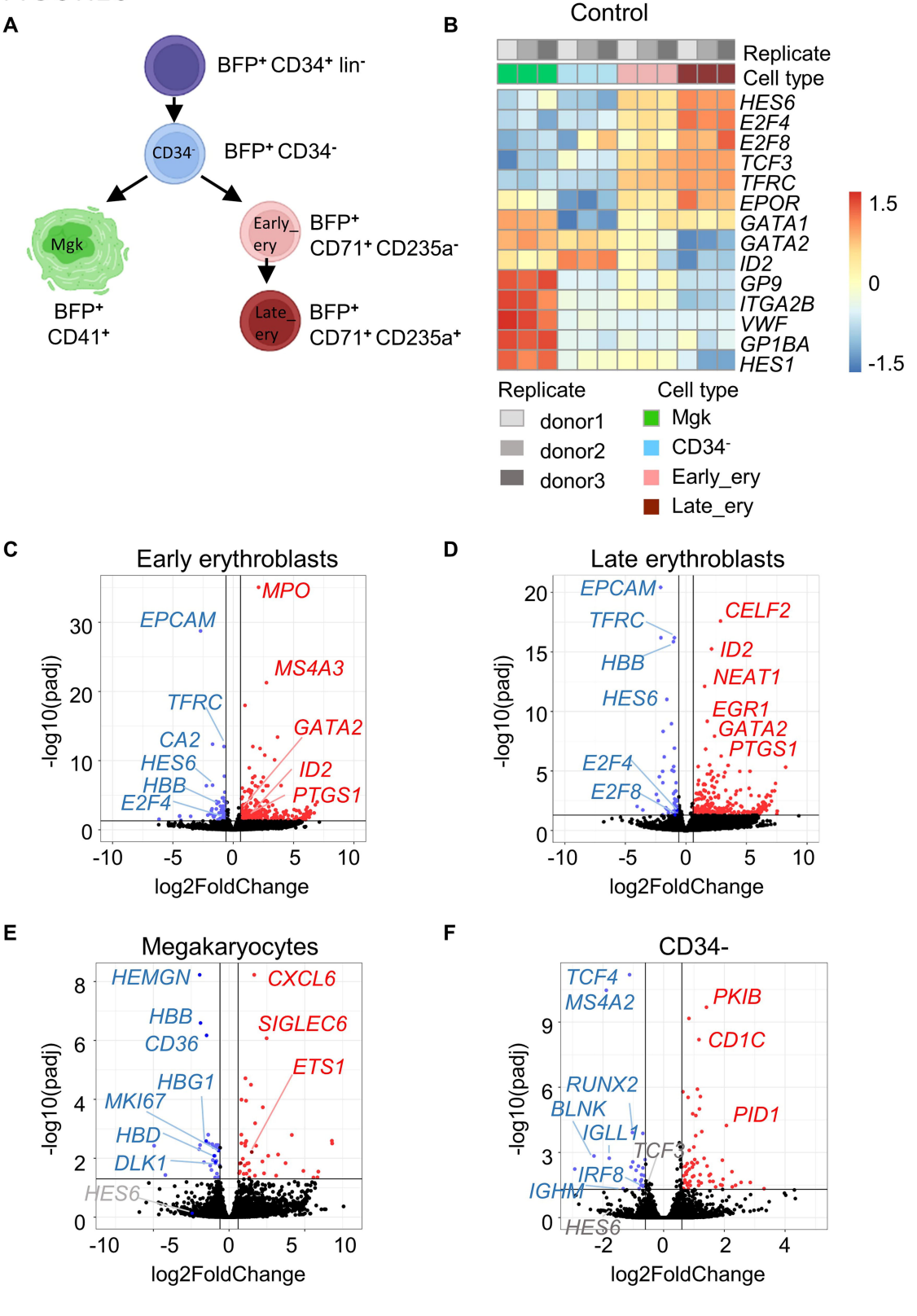
A
BFP+ CD34+ lin-
CD34-
BFP+ CD34-
Mgk
Early_ery
BFP+ CD71+ CD235a-
BFP+ CD41+
Late_ery
BFP+ CD71+ CD235a+
B
Control
Replicate
Cell type
HES6
E2F4
E2F8
TCF3
TFRC
EPOR
GATA1
GATA2
ID2
GP9
ITGA2B
VWF
GP1BA
HES1
1.5
0
-1.5
Replicate
donor1
donor2
donor3
Cell type
Mgk
CD34-
Early_ery
Late_ery
C
Early erythroblasts
MPO
EPCAM
MS4A3
TFRC
GATA2
CA2
HES6
ID2
HBB
PTGS1
E2F4
-log10(padj)
log2FoldChange
D
Late erythroblasts
EPCAM
CELF2
TFRC
ID2
HBB
NEAT1
HES6
EGR1
GATA2
PTGS1
E2F4
E2F8
-log10(padj)
log2FoldChange
E
Megakaryocytes
HEMGN
CXCL6
HBB
SIGLEC6
CD36
ETS1
HBG1
MKI67
HBD
DLK1
HES6
-log10(padj)
log2FoldChange
F
CD34-
TCF4
MS4A2
PKIB
CD1C
RUNX2
BLNK
PID1
IGLL1
TCF3
IRF8
IGHM
HES6
-log10(padj)
log2FoldChange

FIGURE7

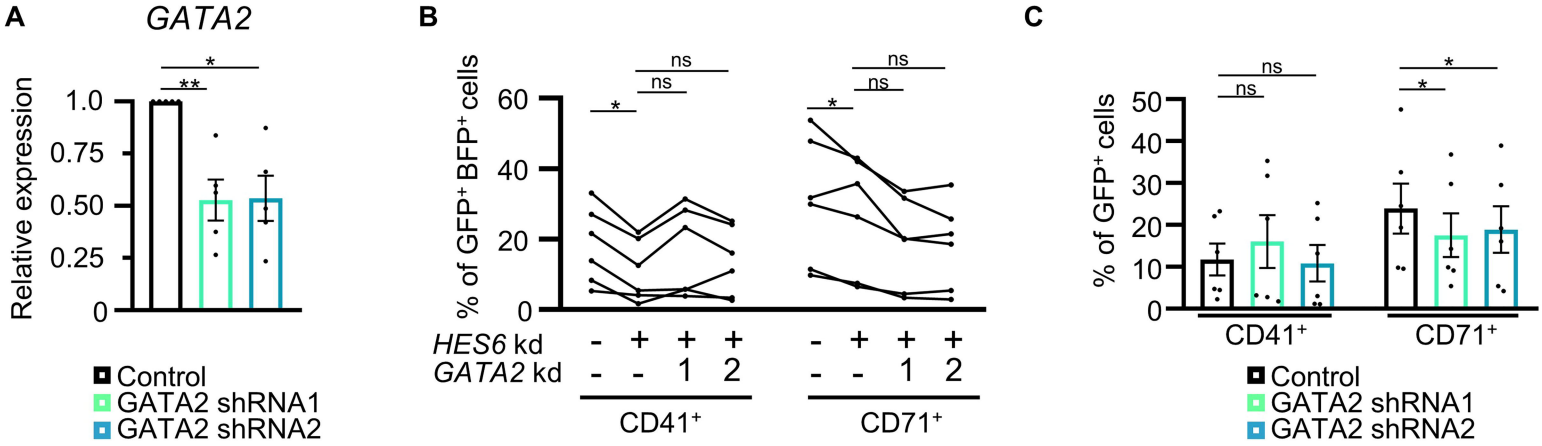
A
GATA2
Relative expression
1.0
0.75
0.50
0.25
0
*
**
Control
GATA2 shRNA1
GATA2 shRNA2
B
% of GFP+ BFP+ cells
60
40
20
0
ns
ns
*
HES6 kd - + + +
GATA2 kd - - 1 2
CD41+
CD71+
C
% of GFP+ cells
50
40
30
20
10
0
ns
*
CD41+
CD71+
Control
GATA2 shRNA1
GATA2 shRNA2

FIGURE8

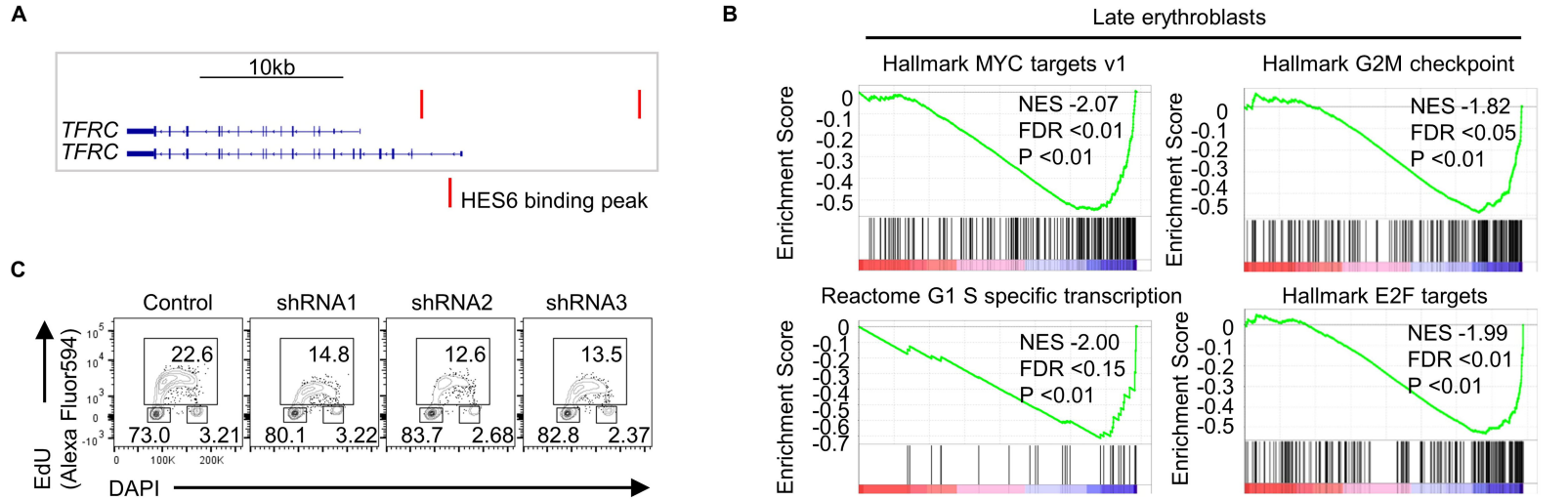
A
10kb
TFRC
TFRC
HES6 binding peak
B
Late erythroblasts
Hallmark MYC targets v1
NES -2.07
FDR <0.01
P <0.01
Hallmark G2M checkpoint
NES -1.82
FDR <0.05
P <0.01
Reactome G1 S specific transcription
NES -2.00
FDR <0.15
P <0.01
Hallmark E2F targets
NES -1.99
FDR <0.01
P <0.01
Enrichment Score
C
Control
shRNA1
shRNA2
shRNA3
22.6
14.8
12.6
13.5
73.0
3.21
80.1
3.22
83.7
2.68
82.8
2.37
EdU (Alexa Fluor594)
DAPI

Supplemental Information for: '*HES6* knockdown in human hematopoietic precursor cells reduces their *in vivo* engraftment potential and their capacity to differentiate into erythroid cells, B cells, T cells and plasmacytoid dendritic cells.'

Methods

HES6 and *GATA2* knockdown using lentiviral constructs

In the control SHC002 vector (MISSION pLKO.1, Sigma), the puromycin resistance gene was replaced by eBFP or eGFP as described[1,2] for *HES6* or *GATA2* knockdown, respectively. Three different shRNA sequences targeting *HES6*, of which two were previously validated[3] and two shRNA sequences targeting *GATA2* were selected (Table S2), were cloned in the pLKO.1 backbone and constructs were validated by sequencing. Lentivirus was produced by transfecting HEKT-cells with the transfer plasmid, envelope plasmid VSV-G and packaging plasmid P8.91 using the TransIT lenti Transfection reagent (Sopachem, #MIR6600).

In vitro HES6 knockdown (co)culture experiments

After transduction, $CD34^+lineage^-$ (lin^-: $CD3^-CD14^-CD19^-CD56^-$) BFP^+HSPCs were sorted (BD Biosciences, FACSAriaIII or FacsAria Fusion) with a purity of >95%. (Co)cultures were initiated with $2*10^4$ cells/ml in differentiation specific conditions (Table S1). For the Methocult™ (StemCell, #04445) colony-forming assays, 250 $CD34^+BFP^+$ HSPCs were plated per 35mm dish in duplicates.

RNA isolation, cDNA conversion and knockdown efficiency using qRT-PCR

Part of the $CD34^+lin^-BFP^+$ sorted cells, that were used in single *HES6* knockdown (co)cultures, was used for determining the knockdown efficiency of shRNAs targeting *HES6*. Part of the $CD34^+lin^-BFP^-GFP^+$ sorted cells, that were used in single *GATA2* knockdown cultures, was used for determining the knockdown efficiency of shRNAs targeting *GATA2*. After RNA extraction (Qiagen, #217084) and cDNA conversion (Bio-Rad, #1725038), qPCR was performed using SYBR Green (Bio-Rad, #172-5274) with primers for housekeeping genes[4] and genes of interest (Table S3).

Analysis of colony forming assay

After 10 days, three different colony types were counted based on their morphology (BFU-E/CFU-E: burst-forming unit-erythroid/colony-forming unit-erythroid, CFU-GM: colony-forming unit-granulocyte, macrophage, CFU-GEMM: colony-forming unit-granulocyte, erythrocyte, macrophage, megakaryocyte). After microscopic evaluation of the colonies, the complete culture was collected in a 15 ml tube for subsequent manual cell counting, flow cytometry and cytospin. For the analysis of colony counts, total cell counts and flow cytometry, we calculated the mean of duplicate samples. After counting of the various colonies up to $5*10^4$ cells of each duplicate culture condition were collected and pooled per condition. After washing with PBS, cells were resuspended in 300µl RPMI 1640 (Gibco, #11530586). Of this cell suspension, 5 drops were loaded in the cytospin chamber and spun down for 5 minutes (Tharmac, CellSpin

I). After air-drying, the cytospin slides were automatically stained in May-Grunwald-Giemsa solution and evaluated using the Leica DM 3000 LED microscope (original magnification 500x).

Analysis of previously published single cell RNA-seq

The thymic single cell data used in this study has previously been published and the analysis has been described in detail[5–8]. Markov affinity-based graph imputation of cells (MAGIC)[9] was used to denoise the data and impute dropout values. Cell cycle scoring was conducted using the G2/M and S phase marker genes provided in the Seurat package[10]. Two public bone marrow data sets (Setty et al.[11], https://data.humancellatlas.org/explore/projects/cc95ff89-2e68-4a08-a234-480eca21ce79, only adult peripheral blood and adult bone marrow data) were combined and preprocessed using Pegasus to remove cells will less than 500 or more than 6000 genes and cells with more than 10% mitochondrial reads. Data was batch corrected with bbknn and the UMAP visualization constructed with scanpy. An additional published bone marrow scRNA-seq data set[12] was used to extract developing B cells and annotations were transferred to the bone marrow data using celltypist[13]. Cell cycle scoring for bone marrow data was carried out using scanpy. Box plots, violin plots and dot plots for single cell data were generated with ggplot/Seurat or scanpy.

In vivo reconstitution

All animal experiments were performed with approval and in accordance with the guidelines of the Ethical Committee for Experimental Animals at the Faculty of Medicine and Health Sciences of Ghent University (ECD20-20). CB $CD34^+$ HSPC were isolated and pre-cultured for 1 to 3 days prior to transduction with lentivirus. Four hours after transduction, bulk HSPCs were intrahepatically injected in sublethally irradiated (100cGy) NOD SCID gamma (NSG) mice, aged one to three days old. 8-9 weeks post-injection, the mice were sacrificed by cervical dislocation and single-cell suspensions of liver, bone marrow and thymus were generated as previously described[14].

Flow cytometry

10^4-10^5 cells per sample were used for surface staining. Cells were blocked with anti-human and anti-mouse FcR (Miltenyi, #130-059-901 and #130-092-575) to avoid non-specific binding of antibodies. Subsequently, cells were stained with anti-human monoclonal antibodies, in different panels dependent on how many days cells were cultured and on culture conditions (Table S4). For intracellular staining of CD179b (clone HSL11, PE), up to 10^5 cells were fixated and permeabilized after surface staining using the Foxp3/Transcription Factor Staining Buffer Set according to manufacturer's instructions (eBioscience, #00-5523-00). Cell survival was investigated using the PE Annexin V apoptosis Detection kit I according to manufacturer's instructions (BD Pharmingen, #559763). Analysis of flow cytometric data was done using FlowJo (version 10.6.2).

RNA sequencing

RNA sequencing was performed on sorted control and *HES6* (shRNA1 and shRNA2) shRNA-transduced subpopulations for three donors after four days of culturing CB $CD34^+$ cells in the megakaryocyte-erythroid differentiation assay. Cells were stained with CD34-PerCP-cy5.5, CD71-APC-H7, CD235a-PE, CD41-PE-cy7, CD45-BV510. Within the BFP^+ population we sorted megakaryocytes ($CD41^+$ cells), early and late erythroblasts ($CD71^+$ $CD235^-$ $CD41^-$ and $CD71^+$ $CD235^+$ $CD41^-$). The fourth subset within the BFP^+

population was CD71$^-$ CD235$^-$ CD41$^-$ CD34$^-$. RNA from sorted cells was extracted as described above. The RNA sequencing libraries were prepared using the QuantSeq 3' mRNA-Seq Library Prep FWD kit (Lexogen) using different quantities of input RNA (Table S5) as described previously[15]. Differential gene expression was determined by R package DESeq2, adjusted p-values below 0.05 were considered significant. Heatmaps were generated with the R package "pheatmap". Volcano plots were made using the R package "ggplot2", adjusted p-values below 0.05 and absolute values of log2(foldchange) above 0.6 were considered significant. Enrichment analyses were performed with GSEA.

In vitro HES6-GATA2 double knockdown culture experiments

After transduction with a GFP lentivirus (control or *GATA2* knockdown) and BFP (control or *HES6* knockdown) lentivirus (33% cells in medium supplemented with 3x pre-culture cytokines, 33% GFP lentivirus and 33% BFP lentivirus), two sorting strategies were used (BD Biosciences, FACSAriaIII or FacsAria Fusion). For the control GFP – control BFP condition only CD34$^+$lin$^-$ BFP$^+$GFP$^+$ cells were sorted while for the *HES6* shRNA2 transduced conditions (with either control GFP, *GATA2* shRNA1 or *GATA2* shRNA2) both CD34$^+$lin$^-$ BFP$^+$GFP$^+$ as CD34$^+$lin$^-$ BFP$^-$GFP$^+$ cells were sorted, all with a purity of >95%. Cultures in megakaryocyte/erythroid-lineage supporting conditions (see Table S1) were initiated with maximum 2*10^4 cells/ml.

Cell cycle analysis

Cell cycle analysis was done using the Click-iT™ Plus EdU kit (Invitrogen, #C10646). EdU was added to the cultures for 45 minutes at 10µM (incubation at 37°), afterwards cells were collected and washed in PBS. Part of the cells was taken for intracellular cell cycle analysis according to the manufacturer's protocol, while part of the cells was used to determine BFP expression, without fixation or staining.

Statistical analysis

All statistical analysis was performed using Graphpad Prism (version 8.0.1). Bar graphs represent the mean and the error bar the standard error of the mean (SEM). For analysis of the *in vitro* co-cultures, comparison of percentages, colony numbers or absolute cell counts between control and a knockdown condition was done using non-parametric Wilcoxon signed-rank test, with a two-tailed p-value set at 0,05. For analysis of the *in vivo* experiment, comparison of control and *HES6* knockdown samples (combined shRNA1 and shRNA2) was done using non-parametric Mann Whitney U test, with a two-tailed p-value set at 0,05. Analysis of knockdown efficiencies using qPCR was done using non-parametric paired students t-test, with a two-tailed p-value set at 0,05.

Tables

Table S1. Pre-culture and (co)culture media according to application

(co)culture	Feeder	Pre-culture (before transduction)			(Co)culture		
		Cell culture medium*	**Cytokines****	**CO2 conditions**	**Cell culture medium***	**Cytokines****	**CO2 conditions**
B coculture	MS5	IMDM (Gibco, #12440053) with 10% FCS	SCF and Flt3-L (100ng/ml) TPO (20 ng/ml)	7%	IMDM (Gibco, #12440053) with 5% FCS, 10% hABserum	SCF and IL-7 (20ng/ml)	5%
NK coculture	MS5					IL-15 (10ng/ml) SCF, Flt3-L and IL-7 (5ng/ml)	
Myeloid coculture	MS5					SCF, Flt3-L and TPO (20ng/ml) GM-CSF and GCSF (10ng/ml)	
DC coculture	OP9-lie				Homemade MEMα (ThermoFisher, #12000-014) with 20% FCS	SCF and GM-CSF (20 ng/ml) Flt3-L (100 ng/ml) (Kirkling et al, 2018 [16])	7%
Mgk/ery culture	Feeder-free					TPO (50ng/ml) EPO and SCF (5ng/ml)	
T coculture	OP9-DLL4					SCF, Flt3-L and IL-7 (5ng/ml)	
Semi-solid colony-forming assay	Feeder-free	SFEM II (Stemcell, #09605)		5%	MethoCult™ H4435 Enriched (StemCell, # # 04445)	Supplemented in MethoCult™ medium	5%

** SCF (Peprotech, #300-07), Flt3L (Miltenyi, #130-096-479), TPO (Peprotech, #300-18), GMCSF (#), GCSF (#), EPO (#), IL-15 (#), IL-7 (#)

* supplemented with 100IU/ml penicillin, 100µg/ml streptomycin and 2mM L-glutamine

Table S2. shRNA constructs*

Target for knockdown	**Construct**	**Target sequence**	**Target region of *HES6***
HES6	shRNA1	AGCTTGAACTTGCCACTTCAG	3’ UTR
	shRNA2**	CAGCCTGACCACAGCCCAAAT	Exon 4
	shRNA3**	CGAGCTCCTGAACCATCTGCT	Exon 4
GATA2	shRNA1	CCGGCACCTGTTGTGCAAATT	Exon5
	shRNA2	GTGCAAATTGTCAGACGACAA	Exon5

*sequence for ligation into pLKO vector: 5’ CCGG—21bp sense—CTCGAG—21bp antisense—TTTTTG 3’

**validated by western blot by Xu et al[3]

Table S3. qPCR primers for housekeeping genes

	forward	**Reverse**
SDHA	CTGGAACGGTGAAGGTGACA	AAGGGACTTCCTGTAACAATGCAA
B2M	TGCTGTCTCCATGTTTGATGTATCT	TCTCTGCTCCCCACCTCTAAGT
ACTB	TGGGAACAAGAGGGCATCTG	CCACCACTGCATCAATTCATG
HES6	Ordered primer set from Bio-Rad, #10025636	
GATA2	CAGCAAGGCTCGTTCCTGTTCA	ATGAGTGGTCGGTTCTGCCCAT

Table S4. Flow cytometry staining panels per (co)culture condition

Staining panel	**Used antibodies ***
T	CD45 Percp-cy5.5 (clone HI30), CD34 FITC (clone 581), CD7 Alexa Fluor700 (clone MT701), CD5 PE-cy7 (clone UCHT2), CD4 BV510 (clone RPAT4), CD8β PE (clone 2ST8.5H7), HLA-DR APC-eFluor780 (clone LN3)
B - only surface	CD45 PerCP-cy5.5 (clone HI30), CD19 PE (cone HIB19), CD20 Alexa Fluor 700 (clone 2H7)
B – surface and intracellular	CD45 PerCP-cy5.5 (clone HI30), CD19 FITC (clone HIB19), CD34 APC (clone 581), intracellular CD179b PE (clone HSL11)
DC	CD45 Percp-cy5.5 (clone HI30), HLA-DR APC-eFluor780 (clone LN3), CD45RA APC (clone HI100), CD4 PE (clone RPAT4), CD123 FITC (clone AC145)
NK	CD45 FITC (clone 5B1), CD94 Percp-cy5.5 (clone DX22), CD56 PE (clone 5.1H11)
Methocult	CD45 BV510 (clone HI30), CD235a PE (clone KC16), CD15 PE (clone HI98)
Myeloid	CD45 PerCP-cy5.5 (clone HI30), CD14 FITC (clone 63D3), CD15 PE (clone HI98)
Mgk/ery	CD45 Percp-cy5.5 (clone HI30), CD42b APC (clone HIP1), CD71 APC-H7 (clone MA712), CD235a PE (clone KC16), CD41 PE-Cy7 (clone P2)
Myeloid**	hCD45 Percp-cy5.5 (clone HI30), CD33 APC (clone P67.6)
NK**	hCD45 Percp-cy5.5 (clone HI30), CD3 APC-cy7 (clone UCHT1), CD56 PE (clone 5.1H11)
Mgk/ery**	hCD45 Percp-cy5.5 (clone HI30), CD41 PE-Cy7 (clone P2), CD71 APC-H7 (clone MA712)
B (surface)**	hCD45 Percp-cy5.5 (clone HI30), CD19 PE (cloneHIB19), CD20 Alexa Fluor 700 (clone 2H7)
DC***	hCD45 Percp-cy5.5 (clone HI30), CD123 PE-cy7 (clone 6H6), CD45RA FITC (clone HI100), CD4 PE (clone RPAT4), HLA-DR APC-eFluor780 (clone LN3)

* in all panels Zombie Red™ Fixable Viability Kit (Biolegend, #423109) was used (1/1000 dilution) as a live/dead marker

** analysis of bone marrow samples of *in vivo* experiment

*** analysis of liver samples of *in vivo* experiment

Table S5. RNA input for RNA-seq per cell type

Cell type	**Input RNA (ng)**	**Exceptions (ng)**
$CD41^+$ (megakaryocytes)	9,35	
$CD34^-$ precursors	109,2	
$CD71^+CD235^-$ (early erythroblasts)	12,75	
$CD71^+CD235^+$ (late erythroblasts)	11,55	Donor 2 shRNA2: 4,4

Table S6. RNA-seq results: up-regulated genes (HES6 knockdown vs control) in $CD34^-$ precursors

log2FoldChange	pvalue	padj	symbol	Ensembl ID
1.409407	4.78E-14	2.07E-10	*PKIB*	ENSG00000135549
0.83337	2.09E-13	6.79E-10	*MS4A6A*	ENSG00000110077
1.163096	2.47E-12	6.41E-09	*CD1C*	ENSG00000158481
1.111889	5.67E-10	1.22E-06	*SLC7A11*	ENSG00000151012
0.634699	8.71E-10	1.61E-06	*ARPC3*	ENSG00000111229
1.209556	1.65E-09	2.68E-06	*CLEC5A*	ENSG00000258227
0.805721	2.02E-09	2.92E-06	*PLIN2*	ENSG00000147872
1.178945	7.67E-09	9.94E-06	*MRC1*	ENSG00000260314
0.957715	1.41E-08	1.66E-05	*SESN3*	ENSG00000149212
1.061511	1.85E-08	2E-05	*CLEC10A*	ENSG00000132514
2.067484	5.77E-08	5.75E-05	*PID1*	ENSG00000153823
1.256474	1.19E-07	0.00011	*IFI6*	ENSG00000126709
1.056071	2.23E-07	0.00017	*NCF2*	ENSG00000116701
0.994963	8.52E-07	0.000563	*RCBTB2*	ENSG00000136161
0.842862	1.3E-06	0.000803	*DSC2*	ENSG00000134755
1.332647	3.61E-06	0.00187	*HIC1*	ENSG00000177374
1.02294	4.28E-06	0.002131	*SVIL*	ENSG00000197321
1.934807	5.09E-06	0.002275	*TGM5*	ENSG00000104055
0.925298	7.02E-06	0.002937	*NDRG2*	ENSG00000165795
1.10785	7.31E-06	0.00296	*PDK4*	ENSG00000004799
0.775585	8.26E-06	0.003245	*LY86*	ENSG00000112799
0.986369	9.77E-06	0.003517	*SPRED1*	ENSG00000166068
1.430419	1.21E-05	0.004229	*PLA2G7*	ENSG00000146070
0.717067	1.31E-05	0.004353	*ASGR2*	ENSG00000161944
0.606664	1.47E-05	0.00465	*PPCS*	ENSG00000127125
0.946659	1.58E-05	0.00477	*MS4A7*	ENSG00000166927
0.845829	2.11E-05	0.005823	*SLC36A1*	ENSG00000123643
0.772088	2.79E-05	0.007368	*CTSD*	ENSG00000117984
2.249965	2.97E-05	0.007711	*TSHZ3*	ENSG00000121297
0.732279	3.34E-05	0.008492	*CPVL*	ENSG00000106066
1.54136	4.04E-05	0.010067	*SCN4B*	ENSG00000177098
0.746368	4.16E-05	0.010163	*IL6ST*	ENSG00000134352
1.202772	4.37E-05	0.010482	*RTN1*	ENSG00000139970
1.496493	5.09E-05	0.011586	*BCL2A1*	ENSG00000140379
0.661458	5.25E-05	0.011734	*THEMIS2*	ENSG00000130775
0.992436	5.51E-05	0.012111	*HERC5*	ENSG00000138646
0.950048	6.11E-05	0.013194	*SYT11*	ENSG00000132718
1.957835	8.03E-05	0.017073	*PROCR*	ENSG00000101000
0.697179	9.03E-05	0.01857	*TMEM170B*	ENSG00000205269
1.150539	0.000114	0.02144	*RGS1*	ENSG00000090104
1.521639	0.00012	0.02145	*PARM1*	ENSG00000169116
0.866426	0.000121	0.02145	*GPR82*	ENSG00000171657
1.628033	0.000118	0.02145	*PTGIR*	ENSG00000160013

2.550807	0.000136	0.023907	*VSIG4*	ENSG00000155659
2.854097	0.000139	0.024092	*MGAM*	ENSG00000257335
0.753344	0.00015	0.025345	*PTAFR*	ENSG00000169403
0.650268	0.000153	0.025345	*SLC30A1*	ENSG00000170385
1.238152	0.000151	0.025345	*CCL2*	ENSG00000108691
0.79658	0.000165	0.026371	*AFDN*	ENSG00000130396
1.875664	0.000205	0.030835	*FPR3*	ENSG00000187474
0.780869	0.000222	0.032291	*CPQ*	ENSG00000104324
2.369418	0.000232	0.03266	*IL31RA*	ENSG00000164509
1.926882	0.000232	0.03266	*GPNMB*	ENSG00000136235
1.153811	0.000234	0.03266	*CCNA1*	ENSG00000133101
0.878577	0.000239	0.032913	*MSMO1*	ENSG00000052802
5.16217	0.000293	0.037627	*C1QA*	ENSG00000173372
2.259803	0.000306	0.038526	*FAM171B*	ENSG00000144369
1.712009	0.000312	0.038878	*CMKLR1*	ENSG00000174600
0.636889	0.00037	0.045237	*TSEN34*	ENSG00000170892
0.658788	0.000396	0.0467	*CYRIA*	ENSG00000197872
3.307525	0.000396	0.0467	*OLFM1*	ENSG00000130558
0.814199	0.000409	0.047293	*ZMAT3*	ENSG00000172667

Table S7. RNA-seq results: down-regulated genes (HES6 knockdown vs control) in $CD34^-$ precursors

log2FoldChange	pvalue	padj	symbol	Ensembl ID
-1.12252	5.08E-16	6.59E-12	*TCF4*	ENSG00000196628
-1.88926	5.29E-15	3.43E-11	*MS4A2*	ENSG00000149534
-1.02793	1.4E-07	0.000121	*RUNX2*	ENSG00000124813
-0.68467	1.64E-07	0.000133	*CCDC50*	ENSG00000152492
-2.29414	2.48E-06	0.001458	*BLNK*	ENSG00000095585
-1.79242	3.42E-06	0.001849	*IGLL1*	ENSG00000128322
-0.61076	4.45E-06	0.002139	*TMEM109*	ENSG00000110108
-1.01678	6.31E-06	0.002728	*SLAMF7*	ENSG00000026751
-0.8301	1.25E-05	0.004254	*PRTN3*	ENSG00000196415
-1.07648	1.52E-05	0.004692	*KCNE5*	ENSG00000176076
-0.68315	1.76E-05	0.005174	*EIF4EBP2*	ENSG00000148730
-2.9281	2.07E-05	0.005823	*RUBCNL*	ENSG00000102445
-0.90605	2.46E-05	0.006645	*MYBL2*	ENSG00000101057
-0.72763	4.55E-05	0.010734	*CTSG*	ENSG00000100448
-0.64	5.06E-05	0.011586	*FADS1*	ENSG00000149485
-0.72988	8.66E-05	0.018112	*GUCD1*	ENSG00000138867
-0.93891	9.31E-05	0.018675	*COL24A1*	ENSG00000171502
-0.75543	0.000118	0.02145	*S100A10*	ENSG00000197747
-0.74822	0.000215	0.032094	*HMGN5*	ENSG00000198157
-0.68606	0.000242	0.033087	*PSME2*	ENSG00000100911
-0.65537	0.000263	0.035463	*IRF8*	ENSG00000140968
-0.67468	0.000272	0.036394	*PDLIM1*	ENSG00000107438
-1.33233	0.000395	0.0467	*IGHM*	ENSG00000211899
-0.80743	0.000401	0.046832		ENSG00000279602

Table S8. RNA-seq results: up-regulated genes (HES6 knockdown vs control) in megakaryocytes

log2FoldChange	pvalue	padj	symbol	Ensembl ID
1.663191	6.65E-13	5.93E-09	*CXCL8*	ENSG00000169429
2.48243	3.03E-10	8.44E-07	*SIGLEC6*	ENSG00000105492
1.08181	8.29E-09	1.92E-05	*CYP1B1*	ENSG00000138061
1.448119	1.61E-08	3.19E-05	*CCND2*	ENSG00000118971
0.8203	5.88E-08	0.000102	*COX7C*	ENSG00000127184
1.124102	7.18E-08	0.000111	*SLC22A17*	ENSG00000092096
2.232325	1.33E-07	0.000186	*SNHG19*	ENSG00000260260
1.722667	5.12E-07	0.000648	*C12orf76*	ENSG00000174456
0.811627	1.36E-06	0.001581	*ARPC3*	ENSG00000111229
4.148061	1.63E-06	0.001617	*INHBA*	ENSG00000122641
6.793755	2.75E-06	0.002558	*CRHBP*	ENSG00000145708
1.135222	3.18E-06	0.002606	*SYT11*	ENSG00000132718
1.068378	4.07E-06	0.003092	*KCNQ1OT1*	ENSG00000269821
0.814891	4.22E-06	0.003092	*MALAT1*	ENSG00000251562
6.812312	4.62E-06	0.003131	*HDC*	ENSG00000140287
1.787982	7.77E-06	0.003763	*SH2D2A*	ENSG00000027869
1.070072	7.81E-06	0.003763	*TUBA1A*	ENSG00000167552
1.499381	1.54E-05	0.006141	*ETS1*	ENSG00000134954
3.240239	1.93E-05	0.007482	*TRIM22*	ENSG00000132274
2.586995	2.29E-05	0.008248	*FOSL2*	ENSG00000075426
0.912391	3.01E-05	0.010468	*IRF2BPL*	ENSG00000119669
2.204223	3.98E-05	0.012885		ENSG00000234425
1.292893	4.89E-05	0.014637	*BTG2*	ENSG00000159388
0.771797	5.06E-05	0.014637	*CDK6*	ENSG00000105810
3.734066	5.07E-05	0.014637	*TNFRSF10B*	ENSG00000120889
1.203739	5.52E-05	0.015071	*KLHDC8B*	ENSG00000185909
0.697803	5.49E-05	0.015071	*NEAT1*	ENSG00000245532
1.029351	6.69E-05	0.017593	*IL1B*	ENSG00000125538
1.344376	0.000106	0.025961	*PAPPA*	ENSG00000182752
4.912364	0.000112	0.026865	*SLC7A8*	ENSG00000092068
0.718614	0.00012	0.02835	*SNHG3*	ENSG00000242125
5.898249	0.000123	0.028455	*NEB*	ENSG00000183091
0.662547	0.00014	0.03197	*HGD*	ENSG00000113924
2.311061	0.000145	0.032494	*ANXA1*	ENSG00000135046
1.150767	0.000153	0.03328	*VIM*	ENSG00000026025
0.970715	0.000158	0.033819	*CSF2RB*	ENSG00000100368
3.111682	0.000187	0.038909	*SGK1*	ENSG00000118515
1.711638	0.00019	0.038923	*LSR*	ENSG00000105699
5.841119	0.000225	0.044705	*ANKDD1B*	ENSG00000189045
1.336293	0.000237	0.045248	*BAZ2B*	ENSG00000123636
5.576799	0.000235	0.045248		ENSG00000225173

Table S9. RNA-seq results: down regulated genes (HES6 knockdown vs control) in megakaryocytes

log2FoldChange	pvalue	padj	symbol	Ensembl ID
-1.94036	8.51E-13	5.93E-09	*HEMGN*	ENSG00000136929
-1.88442	5.5E-11	2.56E-07	*HBB*	ENSG00000244734
-1.48478	1.94E-10	6.74E-07	*CD36*	ENSG00000135218
-1.37684	1.48E-06	0.001589	*CTNNAL1*	ENSG00000119326
-1.51214	3.16E-06	0.002606	*HBG1*	ENSG00000213934
-1.34752	4.72E-06	0.003131	*DGKI*	ENSG00000157680
-1.37067	4.96E-06	0.003141	*DYNLT5*	ENSG00000152760
-1.108	5.48E-06	0.00332	*DUSP7*	ENSG00000164086
-0.84544	6.67E-06	0.003572	*HMMR*	ENSG00000072571
-1.91464	6.62E-06	0.003572	*PAPSS2*	ENSG00000198682
-0.73172	6.28E-06	0.003572	*UBE2C*	ENSG00000175063
-4.95073	7.83E-06	0.003763	*FAM178B*	ENSG00000168754
-1.03695	8.9E-06	0.004134	*STK40*	ENSG00000196182
-0.83697	1.06E-05	0.004615	*ACER3*	ENSG00000078124
-1.97517	1.16E-05	0.004908	*LIPH*	ENSG00000163898
-0.69292	1.34E-05	0.005485	*MKI67*	ENSG00000148773
-0.98409	2.31E-05	0.008248	*HBD*	ENSG00000223609
-0.942	2.25E-05	0.008248	*SERPINH1*	ENSG00000149257
-1.07112	3.4E-05	0.011555	*EIF4EBP2*	ENSG00000148730
-0.83445	3.72E-05	0.012323	*CYB5R3*	ENSG00000100243
-0.89808	4.22E-05	0.013362	*DLK1*	ENSG00000185559
-1.65961	4.41E-05	0.013663	*ALKAL2*	ENSG00000189292
-0.89405	5.15E-05	0.014637	*CLEC1B*	ENSG00000165682
-0.61954	6.59E-05	0.017593	*UBE2J1*	ENSG00000198833
-1.24515	6.83E-05	0.017626	*RBPMS2*	ENSG00000166831
-1.16346	0.000101	0.025026	*CCN1*	ENSG00000142871
-0.8008	0.000152	0.03328	*RHAG*	ENSG00000112077
-4.20605	0.000176	0.037131	*LRRC17*	ENSG00000128606
-0.68183	0.000218	0.044055	*ARPC5*	ENSG00000162704
-0.91719	0.000232	0.045248	*PDE5A*	ENSG00000138735

Table S10. RNA-seq results: up-regulated genes (HES6 knockdown vs control) in early erythroblasts

log2FoldChange	pvalue	padj	symbol	Ensembl ID
2.097469	6.41E-40	8.71E-36	*MPO*	ENSG00000005381
2.751566	1.18E-25	5.37E-22	*MS4A3*	ENSG00000149516
0.975316	3.04E-22	1.03E-18	*CELF2*	ENSG00000048740
3.670641	1.45E-17	3.95E-14	*LINC00926*	ENSG00000247982
1.623884	5.22E-16	9.22E-13	*HDC*	ENSG00000140287
2.22121	1.16E-15	1.75E-12	*RNASE2*	ENSG00000169385
2.611048	1.2E-14	1.64E-11	*TSPOAP1*	ENSG00000005379
3.426254	6.31E-14	7.8E-11	*CSTA*	ENSG00000121552
1.329091	9.82E-13	1.11E-09	*HLA-DRA*	ENSG00000204287
1.783753	1.84E-11	1.78E-08	*HLA-DPB1*	ENSG00000223865
2.490429	2.79E-11	2.53E-08	*ATP8B4*	ENSG00000104043
1.617116	3.53E-11	3E-08	*TNFSF13B*	ENSG00000102524
2.316011	1.58E-10	1.26E-07	*ELANE*	ENSG00000197561
1.568268	2.04E-10	1.54E-07	*RFLNB*	ENSG00000183688
3.962926	5.94E-10	4.04E-07	*CD48*	ENSG00000117091
1.83306	7.09E-10	4.25E-07	*SORL1*	ENSG00000137642
2.864895	6.94E-10	4.25E-07	*CLEC12A*	ENSG00000172322
2.728413	7.59E-10	4.29E-07	*SERPINB10*	ENSG00000242550
2.059958	1.19E-09	6.45E-07	*KBTBD11*	ENSG00000176595
0.743683	1.78E-09	9.3E-07	*ACTG1*	ENSG00000184009
1.307296	3.07E-09	1.55E-06	*BASP1*	ENSG00000176788
1.358283	3.59E-09	1.74E-06	*HLA-DPA1*	ENSG00000231389
2.446985	4.86E-09	2.28E-06	*RAB32*	ENSG00000118508
1.527866	5.1E-09	2.31E-06	*PRKCB*	ENSG00000166501
1.220345	5.57E-09	2.44E-06	*HLA-A*	ENSG00000206503
0.943554	7.1E-09	3.01E-06	*LAPTM5*	ENSG00000162511
1.40235	7.89E-09	3.25E-06	*PKM*	ENSG00000067225
1.463545	1.27E-08	4.93E-06	*ATF7IP2*	ENSG00000166669
1.472023	4.43E-08	1.67E-05	*TENT5A*	ENSG00000112773
0.756416	5.01E-08	1.84E-05	*MLC1*	ENSG00000100427
1.412371	7.16E-08	2.46E-05	*SESN3*	ENSG00000149212
1.4018	8.13E-08	2.69E-05	*TUBA1A*	ENSG00000167552
0.688813	9.8E-08	3.17E-05	*ARPC2*	ENSG00000163466
1.841392	1.54E-07	4.87E-05	*MNDA*	ENSG00000163563
2.733461	1.97E-07	6.09E-05	*PRTN3*	ENSG00000196415
2.524546	2.37E-07	7E-05	*SYNE1*	ENSG00000131018
1.939355	2.75E-07	7.63E-05	*SRGN*	ENSG00000122862
2.829713	3.34E-07	8.9E-05	*CLEC5A*	ENSG00000258227
6.954929	3.62E-07	9.45E-05	*CD200*	ENSG00000091972
1.457034	5.54E-07	0.000134	*CAMK1D*	ENSG00000183049
2.09033	5.7E-07	0.000136	*CXCL8*	ENSG00000169429
1.442522	6.15E-07	0.000144	*FUT4*	ENSG00000196371
1.915807	7.01E-07	0.00016	*GFI1*	ENSG00000162676

1.072712	7.37E-07	0.000164	*COTL1*	ENSG00000103187
0.843122	1.01E-06	0.000221	*SERPINE2*	ENSG00000135919
6.801138	1.14E-06	0.000246	*PSMB9*	ENSG00000240065
3.263983	1.26E-06	0.000267	*BMERB1*	ENSG00000166780
0.827916	1.37E-06	0.000282	*GIHCG*	ENSG00000257698
0.768889	1.36E-06	0.000282		ENSG00000244879
1.802476	1.72E-06	0.000348	*SMYD3*	ENSG00000185420
0.994363	1.84E-06	0.000362	*APP*	ENSG00000142192
2.174151	2.04E-06	0.000386	*CYFIP2*	ENSG00000055163
1.153253	2.45E-06	0.000456	*FAM189B*	ENSG00000160767
2.943386	2.51E-06	0.000461	*TIMP2*	ENSG00000035862
6.124717	3.05E-06	0.000553	*ADA2*	ENSG00000093072
2.318926	3.26E-06	0.000582	*CLC*	ENSG00000105205
0.752138	3.59E-06	0.000633	*SNHG8*	ENSG00000269893
1.062842	6.23E-06	0.001019	*PNKD*	ENSG00000127838
2.101905	7.46E-06	0.001179	*TRIM22*	ENSG00000132274
2.416579	7.32E-06	0.001179	*SMIM24*	ENSG00000095932
5.039138	7.41E-06	0.001179	*GDF15*	ENSG00000130513
6.025457	8.15E-06	0.001258	*FAM171B*	ENSG00000144369
2.553982	8.46E-06	0.001276	*IL6R*	ENSG00000160712
0.723074	8.55E-06	0.001276	*HLA-B*	ENSG00000234745
3.496076	8.84E-06	0.001306	*SLC22A17*	ENSG00000092096
3.528654	9.15E-06	0.001322	*IL1RL1*	ENSG00000115602
0.738119	1.07E-05	0.001531	*GATA2*	ENSG00000179348
1.988767	1.1E-05	0.001558	*BEND4*	ENSG00000188848
1.346569	1.12E-05	0.001563	*NDRG1*	ENSG00000104419
1.04302	1.19E-05	0.00161	*DPYSL2*	ENSG00000092964
5.221764	1.22E-05	0.001646	*IL21R*	ENSG00000103522
5.444926	1.33E-05	0.001775	*IQCG*	ENSG00000114473
6.389607	1.38E-05	0.001815	*CEP83-DT*	ENSG00000278916
0.81915	1.4E-05	0.001823	*VAMP8*	ENSG00000118640
4.387756	1.41E-05	0.001823	*SCAT2*	ENSG00000257596
1.509764	1.46E-05	0.001871	*KCNAB2*	ENSG00000069424
2.996023	1.49E-05	0.001888	*SELL*	ENSG00000188404
0.949831	1.52E-05	0.001894	*CD74*	ENSG00000019582
0.769584	1.52E-05	0.001894	*SAMSN1*	ENSG00000155307
2.69743	1.62E-05	0.001985	*ANPEP*	ENSG00000166825
2.117503	1.96E-05	0.002294	*CREBRF*	ENSG00000164463
2.641709	1.92E-05	0.002294	*GSN*	ENSG00000148180
6.297301	1.99E-05	0.002311		ENSG00000270062
1.004938	2.05E-05	0.002355	*ID2*	ENSG00000115738
1.869451	2.07E-05	0.002358	*KCNQ1OT1*	ENSG00000269821
1.613004	2.12E-05	0.002383	*BGLT3*	ENSG00000260629
1.420124	2.2E-05	0.002452	*TPM4*	ENSG00000167460
1.076349	2.49E-05	0.002733	*EMB*	ENSG00000170571
1.326641	2.49E-05	0.002733	*PTGS1*	ENSG00000095303

2.71058	2.55E-05	0.00275	*KIF21B*	ENSG00000116852
4.159856	2.54E-05	0.00275	*FBXL15*	ENSG00000107872
2.294747	2.58E-05	0.002765	*CDC42SE1*	ENSG00000197622
2.830438	2.76E-05	0.002907	*NAP1L3*	ENSG00000186310
2.632759	2.75E-05	0.002907	*FAS*	ENSG00000026103
0.932314	3.19E-05	0.003256	*ARHGAP15*	ENSG00000075884
1.259231	3.15E-05	0.003256	*ANGPT1*	ENSG00000154188
6.148808	3.18E-05	0.003256		ENSG00000274922
0.70153	3.36E-05	0.00341	*APMAP*	ENSG00000101474
6.078896	3.55E-05	0.003563	*ARHGAP11B*	ENSG00000285077
5.555889	3.75E-05	0.003623	*CRYGD*	ENSG00000118231
0.809196	3.77E-05	0.003623	*CYTL1*	ENSG00000170891
2.069424	3.79E-05	0.003623	*NUDT11*	ENSG00000196368
3.623353	3.83E-05	0.003625	*HCST*	ENSG00000126264
6.704152	3.89E-05	0.003641	*CDC37L1-DT*	ENSG00000273061
0.896798	4.21E-05	0.003918	*ITPR1*	ENSG00000150995
6.407183	4.35E-05	0.00402		ENSG00000278376
1.842221	4.43E-05	0.004068	*MSRB3*	ENSG00000174099
1.242584	4.61E-05	0.004171	*FAM107B*	ENSG00000065809
4.357243	4.86E-05	0.004313	*KLHL13*	ENSG00000003096
1.270702	5.18E-05	0.004565	*RASGRP2*	ENSG00000068831
2.675919	5.28E-05	0.00463		ENSG00000271869
6.371641	5.89E-05	0.005064	*AKAP12*	ENSG00000131016
6.00349	6.76E-05	0.005634	*RAB7B*	ENSG00000276600
1.90678	6.7E-05	0.005634	*TFEC*	ENSG00000105967
2.187723	6.71E-05	0.005634	*PTPRE*	ENSG00000132334
5.832236	7.17E-05	0.005936	*SLC28A3*	ENSG00000197506
6.13082	7.47E-05	0.006076	*FBN2*	ENSG00000138829
6.117857	7.47E-05	0.006076		ENSG00000260588
0.750419	7.43E-05	0.006076	*RAC2*	ENSG00000128340
4.248149	7.63E-05	0.00617	*SH3BGRL3*	ENSG00000142669
3.452218	7.92E-05	0.006365	*VAV1*	ENSG00000141968
1.677858	8.22E-05	0.006528	*EIF3J-DT*	ENSG00000179523
3.40572	8.62E-05	0.006811	*MIR34AHG*	ENSG00000228526
6.279426	8.78E-05	0.006896	*S100P*	ENSG00000163993
1.427201	8.98E-05	0.007006	*PRAF2*	ENSG00000243279
0.806979	9.02E-05	0.007006	*GRAMD4*	ENSG00000075240
5.973596	9.19E-05	0.007092		ENSG00000267279
2.437881	9.39E-05	0.007168	*DCUN1D3*	ENSG00000188215
5.944113	9.55E-05	0.007244	*PARD3B*	ENSG00000116117
2.646527	0.000101	0.007517	*SYT11*	ENSG00000132718
5.995478	0.000103	0.00761	*CC2D2A*	ENSG00000048342
1.570489	0.000113	0.008329	*CTSG*	ENSG00000100448
2.377746	0.000118	0.008434	*FOSL2*	ENSG00000075426
1.095891	0.000118	0.008434	*IRAK3*	ENSG00000090376
1.009988	0.000116	0.008434	*MT2A*	ENSG00000125148

6.174995	0.000117	0.008434		ENSG00000274213
0.816303	0.000119	0.008454	*B4GALT5*	ENSG00000158470
1.465766	0.00012	0.008485	*ANKRD33B*	ENSG00000164236
4.550605	0.000122	0.008553	*ABCB1*	ENSG00000085563
0.799334	0.000122	0.008553	*DTD1*	ENSG00000125821
1.432472	0.000128	0.008929	*SPRED1*	ENSG00000166068
6.1109	0.000137	0.009399	*PSPN*	ENSG00000125650
4.893368	0.000143	0.009676	*SLC2A5*	ENSG00000142583
3.411536	0.000148	0.009963	*MRC2*	ENSG00000011028
1.189551	0.00015	0.009971	*WWC3*	ENSG00000047644
3.915008	0.000157	0.010337	*LDOC1*	ENSG00000182195
0.830028	0.00016	0.01051	*ST8SIA6*	ENSG00000148488
5.91576	0.000167	0.01074		ENSG00000285669
1.203523	0.000166	0.01074	*ASCC1*	ENSG00000138303
1.345524	0.000166	0.01074	*FRY*	ENSG00000073910
1.926857	0.000167	0.01074	*LYSMD2*	ENSG00000140280
1.643967	0.000168	0.01074	*SNHG20*	ENSG00000234912
2.809153	0.000178	0.011277	*FGL2*	ENSG00000127951
2.62229	0.000186	0.011673	*UBTD2*	ENSG00000168246
0.829506	0.000187	0.011679	*CBX6*	ENSG00000183741
6.118828	0.000191	0.011777	*NR5A2*	ENSG00000116833
2.752127	0.000192	0.011777	*ANXA6*	ENSG00000197043
3.598322	0.000191	0.011777	*PIMREG*	ENSG00000129195
1.397	0.000204	0.012379	*KCNK5*	ENSG00000164626
5.839532	0.000209	0.012606	*ADGRL1-AS1*	ENSG00000267169
2.315871	0.000213	0.012733	*ZNF462*	ENSG00000148143
1.286024	0.000214	0.012733	*PRXL2A*	ENSG00000122378
1.878279	0.000221	0.012989	*BST1*	ENSG00000109743
6.198964	0.000222	0.012989		ENSG00000277218
5.218952	0.000224	0.012989	*PTAFR*	ENSG00000169403
1.312936	0.000237	0.013588	*TUBB2B*	ENSG00000137285
0.7155	0.000235	0.013588	*VMP1*	ENSG00000062716
5.812117	0.000251	0.014287	*KCTD17*	ENSG00000100379
2.17904	0.000256	0.01448	*SHTN1*	ENSG00000187164
1.016408	0.000264	0.014835	*TPP1*	ENSG00000166340
5.99536	0.000274	0.01525		ENSG00000262089
6.29222	0.000277	0.015374	*RNVU1-6*	ENSG00000201558
5.834291	0.000294	0.016161	*SMOX*	ENSG00000088826
4.131385	0.000299	0.016324	*PTGER4*	ENSG00000171522
6.014024	0.000304	0.016541	*PPP1R3F*	ENSG00000049769
1.012591	0.000308	0.01666	*DRAM2*	ENSG00000156171
3.301227	0.00032	0.017253	*FGGY*	ENSG00000172456
2.188189	0.000322	0.017294	*ARHGAP30*	ENSG00000186517
3.540235	0.00033	0.017633	*TMEM259*	ENSG00000182087
5.710736	0.000331	0.017654		ENSG00000229666
0.719089	0.000349	0.018543	*ACTN1*	ENSG00000072110

3.936135	0.000355	0.018765	*MAP10*	ENSG00000212916
5.237301	0.000362	0.018996	*FAM43A*	ENSG00000185112
3.452211	0.000364	0.019003	*LOC554206*	ENSG00000262587
1.762562	0.000372	0.01936	*ERG*	ENSG00000157554
1.37313	0.000397	0.02056	*SMIM3*	ENSG00000256235
5.659547	0.000398	0.02056	*EDA2R*	ENSG00000131080
0.667954	0.000404	0.020699	*DAD1*	ENSG00000129562
5.673854	0.000403	0.020699	*FAM219B*	ENSG00000178761
5.249372	0.000409	0.020869	*CROCC*	ENSG00000058453
2.808229	0.000421	0.021406	*PXDN*	ENSG00000130508
3.889872	0.000429	0.02175	*HGF*	ENSG00000019991
3.183905	0.000433	0.021808	*GIMAP6*	ENSG00000133561
5.659714	0.000433	0.021808	*SPTAN1*	ENSG00000197694
0.622593	0.000439	0.022013	*AIF1*	ENSG00000204472
0.609775	0.000453	0.02248	*RNF168*	ENSG00000163961
2.045568	0.000453	0.02248	*FGFBP3*	ENSG00000174721
2.153347	0.000459	0.022612		ENSG00000275202
0.668579	0.000463	0.022686	*RGS10*	ENSG00000148908
0.828141	0.000471	0.022925	*TCEAL4*	ENSG00000133142
1.031466	0.000473	0.022925	*NEAT1*	ENSG00000245532
1.051138	0.000472	0.022925	*FAM30A*	ENSG00000226777
1.155501	0.00048	0.023207	*TRAPPC1*	ENSG00000170043
1.56524	0.000489	0.023527	*SLC22A15*	ENSG00000163393
5.960711	0.000492	0.023527	*LPAR4*	ENSG00000147145
5.548064	0.000492	0.023527		ENSG00000280129
1.26851	0.000506	0.023951	*UBE2W*	ENSG00000104343
5.599088	0.000529	0.024789	*BAALC*	ENSG00000164929
1.743959	0.000535	0.02495	*CXCR4*	ENSG00000121966
5.515986	0.000536	0.02495		ENSG00000285730
5.87233	0.000542	0.025117	*MS4A7*	ENSG00000166927
5.700245	0.000552	0.025436	*ZNF311*	ENSG00000197935
2.087712	0.000557	0.025578	*ETV5*	ENSG00000244405
3.287692	0.000561	0.025659	*PABIR3*	ENSG00000156500
1.828566	0.000571	0.026014	*MYO1F*	ENSG00000142347
5.698	0.000573	0.026043	*B3GNT7*	ENSG00000156966
1.343616	0.000576	0.026094	*RPS6KA1*	ENSG00000117676
0.636702	0.00059	0.026583	*ARHGDIB*	ENSG00000111348
5.601263	0.000595	0.026673		ENSG00000272663
2.060155	0.0006	0.026737	*TOX*	ENSG00000198846
4.109803	0.000608	0.027006	*INKA2*	ENSG00000197852
0.633279	0.000623	0.027412	*CCNY*	ENSG00000108100
3.711534	0.000624	0.027412		ENSG00000276900
1.442334	0.00065	0.028224	*RCSD1*	ENSG00000198771
4.559205	0.000666	0.02883		ENSG00000270871
5.55852	0.000673	0.029015	*PRUNE2*	ENSG00000106772
5.959459	0.00068	0.029224	*PLK2*	ENSG00000145632

5.052378	0.000686	0.029288		ENSG00000273837
1.150492	0.000697	0.029703	*NAP1L5*	ENSG00000177432
1.361988	0.000701	0.029732	*PSMB8*	ENSG00000204264
1.367787	0.000703	0.029732	*PI4KA*	ENSG00000241973
1.146168	0.000706	0.029797	*STK39*	ENSG00000198648
5.439349	0.000712	0.029848	*PRELID3A*	ENSG00000141391
5.644287	0.000711	0.029848	*C5AR1*	ENSG00000197405
1.161904	0.000724	0.030183	*DBNL*	ENSG00000136279
1.037603	0.00076	0.031178	*HLA-DRB1*	ENSG00000196126
3.796575	0.000766	0.031178	*GPM6B*	ENSG00000046653
0.949513	0.000757	0.031178	*C1GALT1C1*	ENSG00000171155
0.715562	0.000754	0.031178	*PDLIM1*	ENSG00000107438
2.040896	0.000772	0.03129	*CHMP4A*	ENSG00000254505
1.619419	0.000786	0.031671	*BEX1*	ENSG00000133169
1.529829	0.000791	0.03178	*CA5B*	ENSG00000169239
1.101381	0.000802	0.032146	*FCER1A*	ENSG00000179639
0.951539	0.000812	0.032428	*MARCKS*	ENSG00000277443
1.039366	0.000815	0.032488	*NQO2*	ENSG00000124588
2.645667	0.000822	0.032543	*DPF3*	ENSG00000205683
5.613345	0.000822	0.032543		ENSG00000277511
1.02485	0.000825	0.032588	*UTRN*	ENSG00000152818
2.097977	0.000858	0.033643	*TRERF1*	ENSG00000124496
1.892987	0.000859	0.033643	*DMXL2*	ENSG00000104093
4.620909	0.000873	0.033983	*HPSE*	ENSG00000173083
5.468499	0.000871	0.033983	*ZNF709*	ENSG00000242852
5.998278	0.000903	0.034857	*PHLDA3*	ENSG00000174307
0.75773	0.000943	0.036144	*ABI2*	ENSG00000138443
5.432641	0.000951	0.036201	*FRMD3*	ENSG00000172159
3.367231	0.000969	0.036577	*CXCL2*	ENSG00000081041
1.356049	0.00097	0.036577	*ZFP90*	ENSG00000184939
0.772262	0.000975	0.036594	*PXK*	ENSG00000168297
5.516707	0.001011	0.037732		ENSG00000277170
1.324954	0.001041	0.038635	*FXYD5*	ENSG00000089327
2.348588	0.00106	0.039251	*RASAL3*	ENSG00000105122
1.605766	0.001075	0.039686	*RNASE3*	ENSG00000169397
1.149921	0.001093	0.040064	*RHOQ*	ENSG00000119729
5.322563	0.001094	0.040064	*ANKRD18A*	ENSG00000180071
3.629447	0.001097	0.040067	*PPP1R16B*	ENSG00000101445
5.515987	0.001115	0.040297	*GABBR1*	ENSG00000204681
3.983901	0.001116	0.040297	*RBM26-AS1*	ENSG00000227354
3.356026	0.001108	0.040297	*PLXNB2*	ENSG00000196576
2.554845	0.001182	0.042035	*IRF5*	ENSG00000128604
1.205736	0.001191	0.042247	*LAMTOR4*	ENSG00000188186
5.734556	0.001195	0.042267	*LIN7A*	ENSG00000111052
4.426144	0.001202	0.042297	*STOX1*	ENSG00000165730
1.746907	0.0012	0.042297	*ATP2A3*	ENSG00000074370

2.070155	0.001216	0.042687	*MAP1A*	ENSG00000166963
1.338254	0.001249	0.043603	*XYLT1*	ENSG00000103489
3.171254	0.001287	0.044701	*RNVU1-19*	ENSG00000275538
0.826009	0.001293	0.044798	*TP53INP1*	ENSG00000164938
0.634542	0.001308	0.0452	*CCDC90B*	ENSG00000137500
5.612773	0.001337	0.045739		ENSG00000272432
5.319437	0.001334	0.045739	*HOMER3*	ENSG00000051128
1.791205	0.001333	0.045739		ENSG00000269688
3.870456	0.001367	0.046294	*CLDN10*	ENSG00000134873
0.659257	0.001361	0.046294	*PMP22*	ENSG00000109099
1.357256	0.001366	0.046294	*LAIR1*	ENSG00000167613
4.615352	0.00139	0.046844		ENSG00000224934
5.160194	0.0014	0.047079	*SIGLEC6*	ENSG00000105492
1.885338	0.001408	0.047106		ENSG00000273117
1.648771	0.001425	0.047463	*PAG1*	ENSG00000076641
5.698999	0.001425	0.047463		ENSG00000272186
1.930854	0.001437	0.047621	*GCNT2*	ENSG00000111846
1.903078	0.001436	0.047621	*C12orf57*	ENSG00000111678
1.085051	0.001444	0.04774	*SAC3D1*	ENSG00000168061
0.632958	0.001452	0.047863	*SNX12*	ENSG00000147164
2.408652	0.001477	0.048578	*ARL11*	ENSG00000152213
5.602542	0.001489	0.048873	*ARMH1*	ENSG00000198520
2.820799	0.001539	0.049882	*TRH*	ENSG00000170893
0.662158	0.001535	0.049882	*PRSS57*	ENSG00000185198
5.312195	0.001539	0.049882	*ADGRE5*	ENSG00000123146
2.975624	0.001549	0.04999	*GPR65*	ENSG00000140030

Table S11. RNA-seq results: down-regulated genes (HES6 knockdown vs control) in early erythroblasts

log2FoldChange	pvalue	padj	symbol	Ensembl ID
-2.70912	2.64E-33	1.79E-29	*EPCAM*	ENSG00000119888
-1.71198	1.84E-16	4.17E-13	*CA2*	ENSG00000104267
-0.76399	5.43E-16	9.22E-13	*TFRC*	ENSG00000072274
-0.73185	1.75E-11	1.78E-08	*FECH*	ENSG00000066926
-1.71152	4.99E-10	3.57E-07	*HES6*	ENSG00000144485
-2.22391	7.2E-10	4.25E-07	*HOOK1*	ENSG00000134709
-0.69878	9.09E-09	3.63E-06	*RHAG*	ENSG00000112077
-0.80274	6.46E-08	2.31E-05	*ZBTB7A*	ENSG00000178951
-0.90141	7.24E-08	2.46E-05	*UGCG*	ENSG00000148154
-0.74288	2.21E-07	6.68E-05	*NADK2*	ENSG00000152620
-0.72183	2.52E-07	7.22E-05	*MCM10*	ENSG00000065328
-0.74425	2.55E-07	7.22E-05	*OAT*	ENSG00000065154
-1.40369	2.91E-07	7.9E-05	*TLCD4*	ENSG00000152078
-1.20704	3.85E-07	9.88E-05	*CDH1*	ENSG00000039068
-0.6049	5.06E-07	0.000125	*RPL22L1*	ENSG00000163584
-1.34558	7.07E-07	0.00016	*HBB*	ENSG00000244734
-0.70158	1.78E-06	0.000355	*FAM210B*	ENSG00000124098
-1.06392	1.92E-06	0.000372	*SLC29A1*	ENSG00000112759
-0.85293	1.95E-06	0.000373	*HMGN5*	ENSG00000198157
-0.84831	5.18E-06	0.00089	*METTL13*	ENSG00000010165
-0.91649	5.3E-06	0.0009	*TGM2*	ENSG00000198959
-1.75659	5.49E-06	0.000921	*FAM178B*	ENSG00000168754
-1.40211	5.84E-06	0.000967	*GAL*	ENSG00000069482
-0.60252	8.1E-06	0.001258	*NUP210*	ENSG00000132182
-0.98365	9E-06	0.001314	*XK*	ENSG00000047597
-1.80935	1.18E-05	0.00161	*COCH*	ENSG00000100473
-0.77328	1.53E-05	0.001894	*EIF4EBP2*	ENSG00000148730
-0.88294	1.94E-05	0.002294	*STRADB*	ENSG00000082146
-0.65998	1.94E-05	0.002294	*PM20D2*	ENSG00000146281
-1.03803	3.08E-05	0.003221	*B3GALNT1*	ENSG00000169255
-1.8015	3.61E-05	0.003563	*SPTB*	ENSG00000070182
-0.77764	3.58E-05	0.003563	*TUBB6*	ENSG00000176014
-1.17577	3.84E-05	0.003625	*PI4K2B*	ENSG00000038210
-0.76976	4.78E-05	0.004274	*RIDA*	ENSG00000132541
-1.89594	5.5E-05	0.00479	*LINC01133*	ENSG00000224259
-0.6596	5.61E-05	0.004857	*E2F4*	ENSG00000205250
-0.79287	6.51E-05	0.005565	*CCDC71L*	ENSG00000253276
-0.66026	6.72E-05	0.005634	*APOC1*	ENSG00000130208
-1.50813	9.77E-05	0.007373	*DNAJA4*	ENSG00000140403
-2.11	9.93E-05	0.007456	*LGALS3*	ENSG00000131981
-0.6106	0.000117	0.008434	*TRIB2*	ENSG00000071575
-0.8128	0.000115	0.008434	*GUCD1*	ENSG00000138867
-0.80379	0.000131	0.009111	*HLTF*	ENSG00000071794

-4.43441	0.000141	0.009651	*CTSE*	ENSG00000196188
-1.6623	0.000149	0.009963	*IL15RA*	ENSG00000134470
-0.71041	0.000152	0.01005	*CA8*	ENSG00000178538
-4.45084	0.000169	0.010773	*HBA2*	ENSG00000188536
-3.52608	0.000178	0.011277	*EMP2*	ENSG00000213853
-0.71923	0.000188	0.011689	*JAK2*	ENSG00000096968
-0.65898	0.000192	0.011777	*ALDH5A1*	ENSG00000112294
-0.61876	0.000195	0.011908	*CPNE3*	ENSG00000085719
-0.63566	0.000214	0.012733	*KRR1*	ENSG00000111615
-0.87732	0.000224	0.012989	*LEPR*	ENSG00000116678
-0.67462	0.000237	0.013588	*ALAD*	ENSG00000148218
-1.60605	0.000262	0.014762	*SLC2A14*	ENSG00000173262
-0.60969	0.000285	0.015754	*LRRCC1*	ENSG00000133739
-0.67964	0.000356	0.018765	*NME4*	ENSG00000103202
-1.09089	0.000443	0.022128	*DUSP2*	ENSG00000158050
-1.00857	0.000457	0.022595	*MEX3D*	ENSG00000181588
-0.74091	0.000494	0.023566	*RFESD*	ENSG00000175449
-0.7148	0.000497	0.023611	*RAD17*	ENSG00000152942
-0.6939	0.000526	0.024775	*PIK3R4*	ENSG00000196455
-0.67712	0.000591	0.026583	*BLVRB*	ENSG00000090013
-0.67616	0.000597	0.026691	*JMJD1C*	ENSG00000171988
-0.7057	0.000612	0.027065	*MXD1*	ENSG00000059728
-6.15031	0.000685	0.029288	*ESYT3*	ENSG00000158220
-0.65472	0.000744	0.030914	*BAG2*	ENSG00000112208
-0.72152	0.000763	0.031178	*ZFP36L1*	ENSG00000185650
-0.77256	0.000774	0.031292	*FOXJ2*	ENSG00000065970
-0.82454	0.000848	0.033407	*TRMT11*	ENSG00000066651
-1.27746	0.000947	0.036145	*SLC39A4*	ENSG00000147804
-0.62617	0.000978	0.036613	*ADD2*	ENSG00000075340
-4.33378	0.001118	0.040297	*SLC6A8*	ENSG00000130821
-0.66747	0.001163	0.041685	*CD44*	ENSG00000026508
-0.8938	0.00118	0.042035	*CAPRIN2*	ENSG00000110888
-0.69477	0.00132	0.045506	*HBG1*	ENSG00000213934
-0.91225	0.001386	0.046837	*TOB1*	ENSG00000141232
-0.86797	0.001542	0.049882	*LIN9*	ENSG00000183814

Table S12. RNA-seq results: up-regulated genes (HES6 knockdown vs control) in late erythroblasts

log2FoldChange	pvalue	padj	symbol	Ensembl ID
2.856788	4.11E-22	2.6E-18	*CELF2*	ENSG00000048740
2.116957	2.71E-19	5.71E-16	*ID2*	ENSG00000115738
1.54921	4.35E-16	7.86E-13	*NEAT1*	ENSG00000245532
1.76249	4.8E-13	6.76E-10	*EGR1*	ENSG00000120738
2.362142	1.14E-11	1.2E-08	*GATA2*	ENSG00000179348
1.630967	1.61E-10	1.46E-07	*ATF7IP2*	ENSG00000166669
2.907682	6.69E-10	5.65E-07	*PTGS1*	ENSG00000095303
1.959083	4.2E-09	3.13E-06	*PRAF2*	ENSG00000243279
3.486418	4.86E-09	3.42E-06	*HLA-DRB1*	ENSG00000196126
1.014799	6.38E-09	4.23E-06	*ACTG1*	ENSG00000184009
8.237323	7.9E-09	4.76E-06	*MIR34AHG*	ENSG00000228526
2.121954	1.91E-08	1.05E-05	*TP53INP1*	ENSG00000164938
5.29072	2.04E-08	1.05E-05	*GDF15*	ENSG00000130513
4.451133	2.29E-08	1.07E-05	*ITGA2B*	ENSG00000005961
3.219238	2.93E-08	1.32E-05	*ZNF462*	ENSG00000148143
1.762966	4.34E-08	1.83E-05	*LAPTM5*	ENSG00000162511
1.989766	4.26E-08	1.83E-05	*FYN*	ENSG00000010810
2.665699	5.79E-08	2.36E-05	*TIMP1*	ENSG00000102265
3.126627	8.04E-08	3.08E-05	*CFAP210*	ENSG00000154479
2.274598	9.63E-08	3.59E-05	*EIF3J-DT*	ENSG00000179523
2.134195	1.65E-07	5.98E-05	*HLA-DPA1*	ENSG00000231389
1.061558	1.76E-07	6.18E-05	*STAT3*	ENSG00000168610
2.549163	2.37E-07	8.12E-05	*GCSAML*	ENSG00000169224
7.398936	3.52E-07	0.000111	*TMEM233*	ENSG00000224982
1.493107	3.88E-07	0.00012	*FLNA*	ENSG00000196924
0.999584	4.4E-07	0.000133	*CBX6*	ENSG00000183741
1.444342	4.93E-07	0.000142	*FAM189B*	ENSG00000160767
1.585084	4.84E-07	0.000142	*MAGEF1*	ENSG00000177383
2.162977	6.64E-07	0.000187	*HLA-DRA*	ENSG00000204287
2.353936	8.84E-07	0.000243	*SESN3*	ENSG00000149212
5.222117	1.06E-06	0.000286	*CYFIP2*	ENSG00000055163
4.508767	1.47E-06	0.000387	*PINLYP*	ENSG00000234465
1.483148	1.55E-06	0.0004	*CYTOR*	ENSG00000222041
3.287503	1.65E-06	0.000417	*PRKCB*	ENSG00000166501
1.487929	1.75E-06	0.000434	*H1-10*	ENSG00000184897
7.315048	1.93E-06	0.000471	*PLXNB2*	ENSG00000196576
1.60183	2.01E-06	0.000478	*PDLIM1*	ENSG00000107438
7.127615	2.15E-06	0.000486		ENSG00000272843
4.186563	2.15E-06	0.000486	*SND1-IT1*	ENSG00000279078
1.157974	2.91E-06	0.000635	*ULK3*	ENSG00000140474
1.188546	3.06E-06	0.000656	*ABI2*	ENSG00000138443
2.29248	3.16E-06	0.000667	*GDF11*	ENSG00000135414
1.874801	3.28E-06	0.00068	*KAZALD1*	ENSG00000107821

0.860729	3.71E-06	0.000758	*RPS18*	ENSG00000231500
0.926889	3.88E-06	0.00078		ENSG00000244879
1.067011	4.42E-06	0.000861	*ST3GAL2*	ENSG00000157350
4.103259	4.84E-06	0.000917	*DYNLT2*	ENSG00000184786
6.732813	5.56E-06	0.001035	*AKAP12*	ENSG00000131016
1.299791	5.75E-06	0.001055	*ZNF271P*	ENSG00000257267
5.377805	6.16E-06	0.001114	*LINC02987*	ENSG00000267575
2.686271	6.4E-06	0.001141	*NT5M*	ENSG00000205309
6.040577	7.08E-06	0.001245	*FIZ1*	ENSG00000179943
6.977438	7.18E-06	0.001245	*CPB2-AS1*	ENSG00000235903
6.613806	9.33E-06	0.001541	*AMHR2*	ENSG00000135409
1.54518	9.37E-06	0.001541	*CBFA2T3*	ENSG00000129993
2.430026	9.15E-06	0.001541		ENSG00000267002
2.024891	1.09E-05	0.001751	*HLA-A*	ENSG00000206503
2.693389	1.09E-05	0.001751	*CSKMT*	ENSG00000214756
1.488943	1.24E-05	0.001936	*ATP6V1F*	ENSG00000128524
3.687718	1.23E-05	0.001936	*MPO*	ENSG00000005381
2.075687	1.38E-05	0.002125	*ZSCAN16-AS1*	ENSG00000269293
1.084766	1.42E-05	0.00217	*MLC1*	ENSG00000100427
1.300774	1.49E-05	0.002225	*ACTN1*	ENSG00000072110
0.975996	1.56E-05	0.002292	*PIM2*	ENSG00000102096
0.791035	1.93E-05	0.00278	*TRIAP1*	ENSG00000170855
1.788161	2.29E-05	0.003187	*CD74*	ENSG00000019582
7.061471	2.46E-05	0.003346		ENSG00000272795
3.45034	2.86E-05	0.003858	*PIK3R3*	ENSG00000117461
6.437087	3.1E-05	0.004133	*TRERF1*	ENSG00000124496
6.345263	3.23E-05	0.004254	*LINC00562*	ENSG00000260388
6.33226	3.33E-05	0.004349	*DOCK2*	ENSG00000134516
4.13847	3.9E-05	0.004993	*H2BC8*	ENSG00000273802
0.606298	4.02E-05	0.005087	*CD63*	ENSG00000135404
2.11049	4.12E-05	0.00517	*KCTD10*	ENSG00000110906
6.552066	4.45E-05	0.005425	*NRM*	ENSG00000137404
2.218904	4.39E-05	0.005425	*MS4A6A*	ENSG00000110077
1.790575	4.46E-05	0.005425	*ARRB2*	ENSG00000141480
3.641854	4.57E-05	0.005512	*MARCHF2*	ENSG00000099785
2.203473	5.12E-05	0.006008	*FDXR*	ENSG00000161513
1.700942	5.33E-05	0.006191	*WWC3*	ENSG00000047644
6.880276	6.14E-05	0.007073		ENSG00000283341
5.974731	6.23E-05	0.007103	*ARL10*	ENSG00000175414
3.874786	6.62E-05	0.007483	*PTENP1*	ENSG00000237984
6.542763	6.88E-05	0.007705	*PGM1*	ENSG00000079739
1.576905	7.25E-05	0.008056	*DPYSL2*	ENSG00000092964
1.875023	7.49E-05	0.008184	*TUBB2B*	ENSG00000137285
0.971904	8.14E-05	0.008658	*HDGFL3*	ENSG00000166503
2.115118	8.08E-05	0.008658	*SELENOW*	ENSG00000178980
6.33289	8.32E-05	0.008777	*ARHGAP30*	ENSG00000186517

4.531312	8.43E-05	0.008824	*CERK*	ENSG00000100422
3.451001	8.56E-05	0.008879		ENSG00000260793
6.635021	8.78E-05	0.009034		ENSG00000286138
1.334002	0.000103	0.010121	*CCND3*	ENSG00000112576
1.338286	0.000103	0.010121	*AKR1B1*	ENSG00000085662
6.077029	0.000105	0.010171		ENSG00000230177
4.6194	0.000107	0.010303	*CD1C*	ENSG00000158481
6.566592	0.000111	0.010534	*PHLDA3*	ENSG00000174307
2.406939	0.000127	0.011836	*SPEN-AS1*	ENSG00000179743
0.906373	0.000127	0.011836	*CPEB4*	ENSG00000113742
6.29021	0.000129	0.011906		ENSG00000226853
1.990765	0.00013	0.011906	*HLA-DPB1*	ENSG00000223865
3.344786	0.000132	0.011983	*PSMB8*	ENSG00000204264
0.64902	0.000143	0.012804	*CAPZB*	ENSG00000077549
2.758007	0.000145	0.012929		ENSG00000278774
3.116223	0.000154	0.013493	*ATXN1*	ENSG00000124788
6.139386	0.000153	0.013493	*XAGE2*	ENSG00000155622
0.922376	0.000163	0.013956	*TIMP3*	ENSG00000100234
2.980254	0.000167	0.014228	*KCNK6*	ENSG00000099337
5.569186	0.000173	0.014572		ENSG00000205464
1.384977	0.000177	0.014718	*IMPA1*	ENSG00000133731
6.140039	0.000176	0.014718		ENSG00000232470
3.707969	0.000178	0.014736	*ATP6V0E2*	ENSG00000171130
1.641017	0.000182	0.014962	*TUBA1A*	ENSG00000167552
1.213687	0.000183	0.014962	*TST*	ENSG00000128311
1.537467	0.000189	0.015253	*MOSMO*	ENSG00000185716
6.413102	0.000191	0.015326		ENSG00000272186
6.001609	0.000199	0.015526	*CDKN1A*	ENSG00000124762
1.105393	0.0002	0.015526	*BRI3*	ENSG00000164713
2.559531	0.000195	0.015526	*DAPK1*	ENSG00000196730
3.063004	0.000198	0.015526	*PKM*	ENSG00000067225
6.079845	0.000211	0.016269	*PDK4*	ENSG00000004799
0.692278	0.000213	0.016274	*ARPC2*	ENSG00000163466
6.380642	0.000213	0.016274	*TTI2*	ENSG00000129696
1.407132	0.000216	0.016277	*KLHDC8B*	ENSG00000185909
1.717993	0.000215	0.016277	*GTF3C5*	ENSG00000148308
1.633014	0.000219	0.016288	*SSR4*	ENSG00000180879
6.297715	0.000218	0.016288		ENSG00000225511
0.851441	0.000221	0.016366	*BTG1*	ENSG00000133639
1.70452	0.000222	0.016366	*CALM3*	ENSG00000160014
1.733382	0.000227	0.016628		ENSG00000260708
1.35076	0.00023	0.016759	*GNA15*	ENSG00000060558
1.035924	0.000236	0.017069	*IRF2BPL*	ENSG00000119669
2.914084	0.000238	0.017109	*LEF1*	ENSG00000138795
1.449417	0.000241	0.017225	*PEA15*	ENSG00000162734
1.322418	0.000245	0.017439	*SERF2*	ENSG00000140264

0.926422	0.000247	0.017439	*AGPAT3*	ENSG00000160216
1.759741	0.000251	0.017666	*TYMSOS*	ENSG00000176912
3.571767	0.000253	0.01768	*CXCL3*	ENSG00000163734
1.889473	0.000264	0.018362		ENSG00000272716
6.654569	0.000289	0.019464		ENSG00000272662
5.934963	0.000288	0.019464	*PRDM1*	ENSG00000057657
1.013295	0.000289	0.019464	*RAC2*	ENSG00000128340
2.662637	0.000295	0.019735	*HLA-E*	ENSG00000204592
3.134382	0.000319	0.021011	*DMAP1*	ENSG00000178028
3.632636	0.000326	0.021398	*SYNE1*	ENSG00000131018
1.187807	0.000337	0.021973	*SERPINE2*	ENSG00000135919
1.076273	0.00034	0.022054	*PMP22*	ENSG00000109099
1.677428	0.000343	0.022144	*ITPR1*	ENSG00000150995
2.849946	0.000354	0.022774	*PTK2B*	ENSG00000120899
0.699995	0.000364	0.023257	*MTHFR*	ENSG00000177000
6.113946	0.000371	0.023269	*CD244*	ENSG00000122223
3.442952	0.000367	0.023269	*NEURL1B*	ENSG00000214357
1.355781	0.000371	0.023269	*HSD17B10*	ENSG00000072506
7.537513	0.00037	0.023269	*EDA2R*	ENSG00000131080
4.808107	0.000376	0.023371	*TRMT61A*	ENSG00000166166
2.206183	0.000385	0.023784	*SHTN1*	ENSG00000187164
3.171261	0.00041	0.025173	*OAS3*	ENSG00000111331
0.839137	0.000412	0.025222	*MTSS1*	ENSG00000170873
3.020208	0.000424	0.025814		ENSG00000272086
5.109329	0.000429	0.02587	*CD70*	ENSG00000125726
6.195852	0.000433	0.02587	*MTMR11*	ENSG00000014914
1.518515	0.000431	0.02587	*LAMTOR4*	ENSG00000188186
2.095145	0.000441	0.025891	*IFI6*	ENSG00000126709
5.876827	0.000445	0.025891	*RNVU1-19*	ENSG00000275538
6.227324	0.000447	0.025891	*TBCE*	ENSG00000285053
2.647214	0.000448	0.025891	*CBLL1-AS1*	ENSG00000241764
0.669552	0.000437	0.025891	*STOM*	ENSG00000148175
3.262193	0.00044	0.025891	*SMPD1*	ENSG00000166311
1.638861	0.000458	0.026264	*MANF*	ENSG00000145050
2.341182	0.000469	0.026623		ENSG00000201674
5.989042	0.000467	0.026623		ENSG00000273619
4.343128	0.000476	0.026881	*JAKMIP2*	ENSG00000176049
2.994618	0.000492	0.027434	*ILRUN-AS1*	ENSG00000272288
5.431713	0.000491	0.027434	*TRO*	ENSG00000067445
3.984692	0.000501	0.027739		ENSG00000248124
5.715525	0.000502	0.027739	*LOC105371414*	ENSG00000260279
5.042785	0.000505	0.027801		ENSG00000273148
1.14386	0.000508	0.027872	*ACSM3*	ENSG00000005187
5.235046	0.000532	0.028339	*TMEM158*	ENSG00000249992
5.82877	0.000528	0.028339	*ZDHHC11*	ENSG00000188818
1.802991	0.000532	0.028339	*SRA1*	ENSG00000213523

5.902059	0.000523	0.028339		ENSG00000271888
4.846929	0.000528	0.028339	*SNHG11*	ENSG00000174365
5.402242	0.000548	0.028989	*STAG3*	ENSG00000066923
5.629016	0.000567	0.029655	*BEND4*	ENSG00000188848
4.359445	0.000571	0.02974	*CLDND2*	ENSG00000160318
1.330824	0.000586	0.03038	*AGO1*	ENSG00000092847
1.227258	0.000588	0.03038	*VPS4A*	ENSG00000132612
1.899023	0.000598	0.030801	*PIEZO1*	ENSG00000103335
2.00697	0.000618	0.031435	*WAS*	ENSG00000015285
5.176286	0.000633	0.031819		ENSG00000243193
0.671543	0.000647	0.03224	*EID1*	ENSG00000255302
3.788006	0.00071	0.033947		ENSG00000273437
5.575865	0.00071	0.033947	*CLU*	ENSG00000120885
4.670718	0.000695	0.033947	*PYGB*	ENSG00000100994
0.695155	0.000749	0.035265	*MAN1A2*	ENSG00000198162
6.112771	0.000747	0.035265	*FRMD6-AS1*	ENSG00000273888
1.53441	0.000759	0.035532	*ANXA4*	ENSG00000196975
1.339947	0.00076	0.035532	*REC8*	ENSG00000100918
2.582403	0.000765	0.035626	*HLA-F-AS1*	ENSG00000214922
5.892826	0.000769	0.035649	*RTN1*	ENSG00000139970
1.429017	0.000778	0.035952	*KCNK5*	ENSG00000164626
2.212922	0.000818	0.037134	*AIF1*	ENSG00000204472
3.104509	0.000812	0.037134	*ABLIM1*	ENSG00000099204
0.764653	0.000813	0.037134	*TM7SF3*	ENSG00000064115
0.667198	0.000817	0.037134	*RDH11*	ENSG00000072042
3.114948	0.000824	0.037283	*MLLT11*	ENSG00000213190
1.728171	0.000839	0.037798	*MEX3A*	ENSG00000254726
1.281183	0.000873	0.039218	*STK39*	ENSG00000198648
7.508341	0.000889	0.039632	*NUDT11*	ENSG00000196368
5.629854	0.000937	0.041343	*RHOC*	ENSG00000155366
0.697894	0.000965	0.04198	*EIF4E2*	ENSG00000135930
0.622706	0.00096	0.04198	*JPT1*	ENSG00000189159
5.962074	0.000996	0.042287		ENSG00000270742
2.840021	0.000982	0.042287	*FAXDC2*	ENSG00000170271
0.709682	0.000998	0.042287	*TMEM258*	ENSG00000134825
2.336821	0.000999	0.042287	*ST8SIA1*	ENSG00000111728
3.76995	0.000986	0.042287	*TFIP11-DT*	ENSG00000261188
0.791471	0.001005	0.042406	*NPM3*	ENSG00000107833
2.86848	0.001021	0.042796	*MAP1A*	ENSG00000166963
6.04887	0.001018	0.042796	*RAI1*	ENSG00000108557
3.906269	0.001026	0.042864	*CAVIN1*	ENSG00000177469
5.226404	0.001032	0.04298		ENSG00000274428
4.22161	0.00104	0.043194	*SPINDOC*	ENSG00000168005
5.699726	0.00105	0.043458	*SLCO2B1*	ENSG00000137491
1.873032	0.001058	0.043623	*IRAK3*	ENSG00000090376
3.074392	0.001064	0.043626	*KCNQ1OT1*	ENSG00000269821

5.127526	0.001078	0.043873	*DMTF1-AS1*	ENSG00000224046
1.060246	0.001093	0.044347	*SEC14L1*	ENSG00000129657
4.248693	0.00111	0.04482		ENSG00000263934
6.042369	0.00115	0.046081	*MIR762HG*	ENSG00000260083
0.60944	0.001161	0.046388	*NDUFS6*	ENSG00000145494
4.718078	0.001182	0.046787	*CCNG2*	ENSG00000138764
1.564262	0.001177	0.046787	*TENT5A*	ENSG00000112773
1.321602	0.00118	0.046787	*MAGEH1*	ENSG00000187601
5.757167	0.001194	0.047102	*LIPE-AS1*	ENSG00000213904
4.263923	0.001203	0.047262		ENSG00000273382
1.845635	0.001206	0.047262	*STON2*	ENSG00000140022
5.728386	0.00122	0.04752	*LINC00173*	ENSG00000196668
0.788269	0.001239	0.048135	*SOCS7*	ENSG00000274211
2.742942	0.001273	0.048838	*MRC1*	ENSG00000260314
1.916529	0.001285	0.049174		ENSG00000271869
5.126631	0.00131	0.049227	*HHLA3*	ENSG00000197568
2.124147	0.001297	0.049227	*CST3*	ENSG00000101439
3.554307	0.001301	0.049227	*ZNF554*	ENSG00000172006
3.778147	0.001338	0.049969	*GDI1*	ENSG00000203879

Table S13. RNA-seq results: down-regulated genes (HES6 knockdown vs control) in late erythroblasts

log2FoldChange	pvalue	padj	symbol	Ensembl ID
-2.08861	3.03E-25	3.83E-21	*EPCAM*	ENSG00000119888
-0.9478	2.07E-20	6.54E-17	*TFRC*	ENSG00000072274
-2.06663	1.83E-20	6.54E-17	*COCH*	ENSG00000100473
-1.03261	5.53E-20	1.4E-16	*HBB*	ENSG00000244734
-1.57737	6.23E-15	9.86E-12	*HES6*	ENSG00000144485
-1.19767	8.63E-13	1.09E-09	*RPL22L1*	ENSG00000163584
-1.8797	4.11E-12	4.74E-09	*LGALS3*	ENSG00000131981
-0.94644	1.26E-10	1.23E-07	*NME4*	ENSG00000103202
-1.79417	8.33E-10	6.59E-07	*HOOK1*	ENSG00000134709
-1.00777	6.68E-09	4.23E-06	*CD44*	ENSG00000026508
-1.14908	1.51E-08	8.7E-06	*PM20D2*	ENSG00000146281
-1.00226	2.08E-08	1.05E-05	*CA2*	ENSG00000104267
-1.92134	2.23E-08	1.07E-05	*CPVL*	ENSG00000106066
-2.19529	8.02E-08	3.08E-05	*SQOR*	ENSG00000137767
-1.9092	3.01E-07	9.79E-05	*PTGR1*	ENSG00000106853
-0.81286	2.99E-07	9.79E-05	*DLGAP5*	ENSG00000126787
-0.82502	2.04E-06	0.000478	*CAPRIN2*	ENSG00000110888
-0.89996	2.44E-06	0.000541	*ATAD5*	ENSG00000176208
-1.01804	4.01E-06	0.000793	*RHNO1*	ENSG00000171792
-2.43469	4.85E-06	0.000917	*HBM*	ENSG00000206177
-0.92909	1.48E-05	0.002225	*STYX*	ENSG00000198252
-0.70204	1.86E-05	0.002702	*ZFP36L1*	ENSG00000185650
-0.72307	2.01E-05	0.002866	*HMGN5*	ENSG00000198157
-2.28525	2.23E-05	0.003134	*GLIPR2*	ENSG00000122694
-0.7603	2.44E-05	0.003346	*NMI*	ENSG00000123609
-0.95144	3.67E-05	0.004736	*SLC31A1*	ENSG00000136868
-0.94954	4.71E-05	0.005621	*GABPB2*	ENSG00000143458
-0.84127	8E-05	0.008655	*EIF4EBP2*	ENSG00000148730
-0.73325	9.3E-05	0.009417	*SMARCAD1*	ENSG00000163104
-4.02644	9.27E-05	0.009417	*DSG2*	ENSG00000046604
-0.89204	9.44E-05	0.009487	*B3GALNT1*	ENSG00000169255
-0.7245	0.000103	0.010121	*NUP210*	ENSG00000132182
-1.66262	0.000135	0.012212	*SEC14L4*	ENSG00000133488
-0.69639	0.000156	0.013502	*KIF23*	ENSG00000137807
-0.85458	0.00016	0.013796	*STRADB*	ENSG00000082146
-0.68232	0.000185	0.015013	*IPO11*	ENSG00000086200
-1.59052	0.000197	0.015526	*FSBP*	ENSG00000265817
-3.55975	0.000274	0.018965	*WIPF3*	ENSG00000122574
-1.47081	0.000286	0.019464	*CTSZ*	ENSG00000101160
-0.73338	0.000296	0.019735	*E2F4*	ENSG00000205250
-1.02243	0.000377	0.023371	*VANGL1*	ENSG00000173218
-0.87567	0.000429	0.02587	*ICA1*	ENSG00000003147
-0.6835	0.000444	0.025891	*BAG2*	ENSG00000112208

-0.60567	0.000489	0.027434	*TUBB6*	ENSG00000176014
-0.65062	0.000549	0.028989	*ALAD*	ENSG00000148218
-1.09519	0.000564	0.029621	*ADI1*	ENSG00000182551
-0.71909	0.000607	0.031104	*METTL13*	ENSG00000010165
-0.91825	0.000674	0.033451	*RGCC*	ENSG00000102760
-0.74214	0.000679	0.033583	*CYBRD1*	ENSG00000071967
-0.60999	0.000709	0.033947	*ATP1A1*	ENSG00000163399
-1.43704	0.000693	0.033947	*CMAHP*	ENSG00000168405
-0.83017	0.000698	0.033947	*CA8*	ENSG00000178538
-0.77524	0.00072	0.034257	*KLF13*	ENSG00000169926
-0.99073	0.000737	0.034932	*LIN9*	ENSG00000183814
-0.75437	0.000894	0.039736	*WASHC5*	ENSG00000164961
-0.79023	0.000902	0.039918	*PSAT1*	ENSG00000135069
-0.91801	0.000998	0.042287	*METTL9*	ENSG00000197006
-0.82103	0.000978	0.042287	*ENOSF1*	ENSG00000132199
-0.90647	0.001065	0.043626	*FBXO34*	ENSG00000178974
-1.9091	0.001248	0.048324	*SLC22A16*	ENSG00000004809
-0.89517	0.001254	0.048428	*TBC1D24*	ENSG00000162065
-0.63655	0.001265	0.04868	*XK*	ENSG00000047597
-0.90135	0.0013	0.049227	*E2F8*	ENSG00000129173
-0.81084	0.001329	0.049768	*DNAJA4*	ENSG00000140403

Supplemental figures

SUPPLEMENTAL FIGURE1

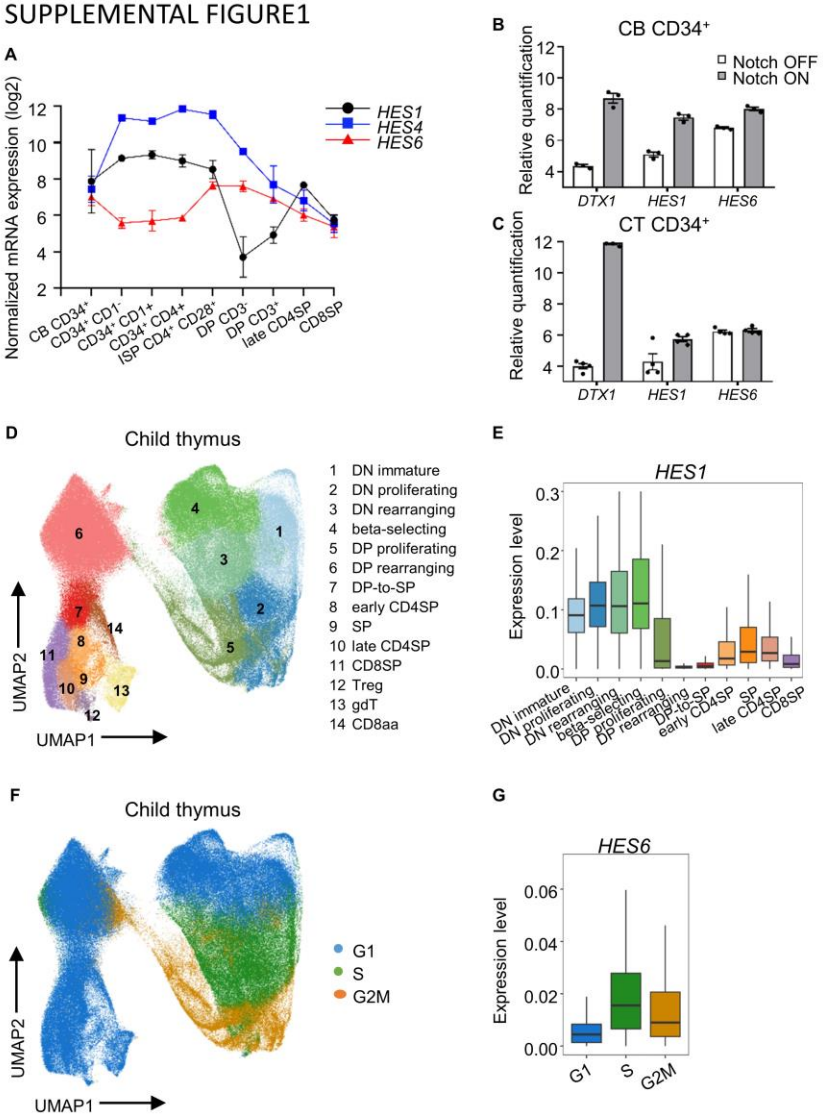

Supplemental Figure 1. *HES6* expression in human post-natal thymocytes. (A) Line plots showing log_2 normalized mRNA expression of *HES1* (black), *HES4* (blue) and *HES6* (red) based on bulk RNA-seq on sorted subsets of human post-natal thymocytes[17]. Data is presented as the average expression of two independent experiments from two donors and error bars indicate the standard error of the mean (SEM). CB: cord blood; ISP: immature single positive ($CD4^+$); DP: double positive ($CD4^+CD8^+$); SP: single positive. (B-C) Bar graphs derived from micro-array data show log_2 normalized probe intensities for *DTX1*, *HES1* and *HES6* after culture of cord blood (CB) $CD34^+$ HSPCs for 72 hours (B) or $CD34^+$ thymocytes (CT) for 48 hours (C) on OP9-GFP (Notch OFF) or OP9-DLL1 (Notch ON) feeder [18,19]. Data is presented as the average expression of three (B) and four (C) replicates and error bars indicate SEM. (D-G) Results derived from scRNA-seq data of human post-natal thymocytes [20]. UMAP visualization with annotation of differentiation stadia (D) and cell-cycle stages (F) and boxplots (E,G) showing pseudo-bulk log-normalized imputed mRNA expression level of *HES1* across differentiation stadia (E) and showing pseudo-bulk log-normalized imputed mRNA expression level of *HES6* across cell-cycle stadia (G). DN:

double negative ($CD4^-CD8^-$); DP: double positive ($CD4^+CD8^+$); SP: single positive. Boxplots show median and first and third quartile.

SUPPLEMENTAL FIGURE2

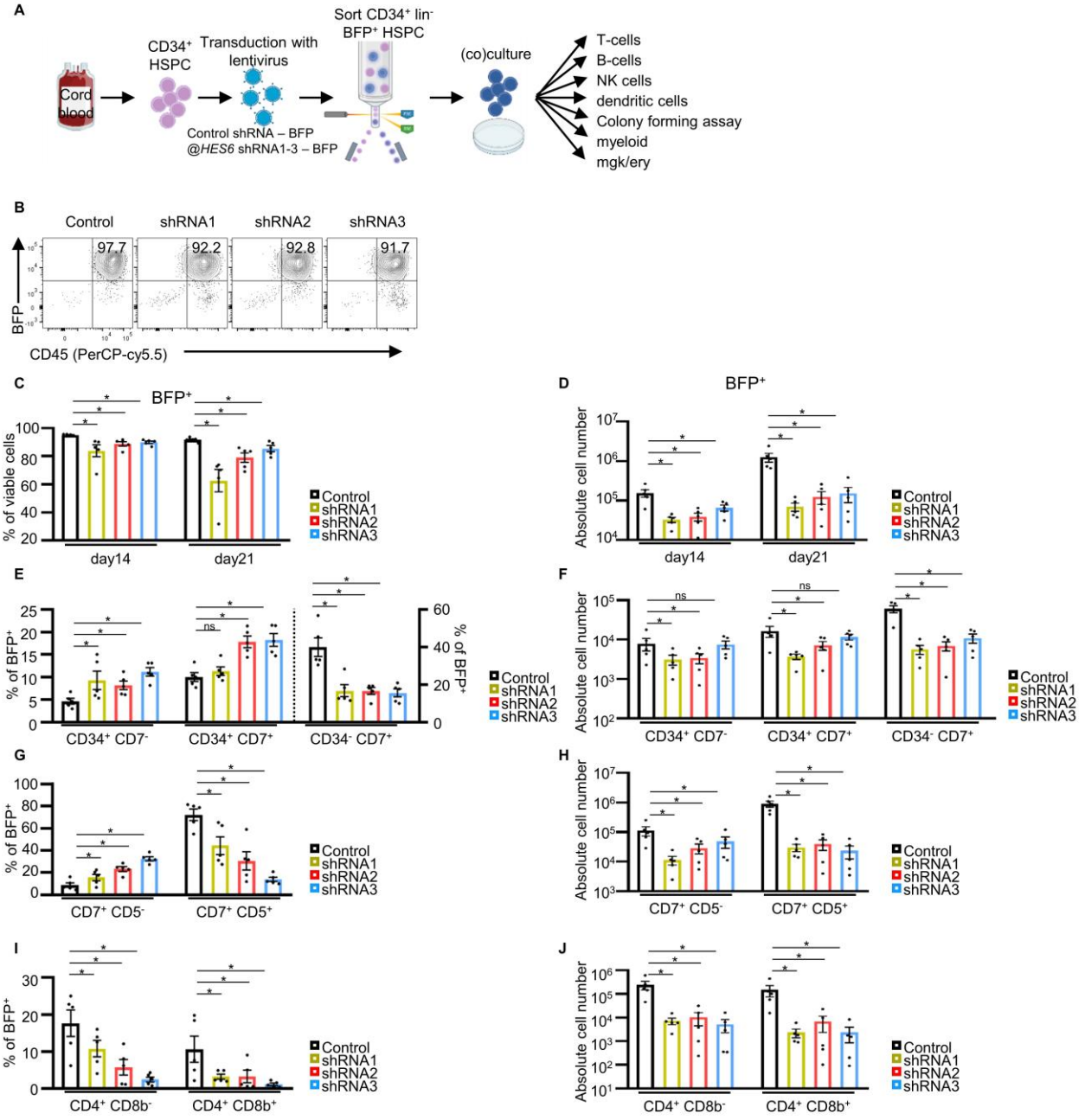

Supplemental Figure 2. *HES6* is important for early *in vitro* T-cell development. (A) Schematic overview illustrating the experimental workflow used to study the impact of *HES6* knockdown on human hematopoiesis. (B-J) Flow cytometric analysis (B) and bar graphs (C-J) of control shRNA and *HES6* shRNA-transduced CD34^{+}Lin^{-}BFP^{+} HSPC cultured *in vitro* in T-lineage supporting conditions for a total of three weeks (N=5). Flow cytometric analysis of CD45 and BFP after 14 days (B) and bar graphs showing CD45^{+}BFP^{+} frequencies within live cells (C) and absolute cell numbers of CD45^{+}BFP^{+} cells (D) at different time points. Bar graphs showing frequencies (E) and absolute cell numbers (F) of populations based on CD34 and CD7 expression within BFP^{+} population at day 14. Bar graphs showing frequencies (G) and absolute cell numbers (H) of populations based on CD7 and CD5 expression within BFP^{+} population at

day 21. Bar graphs showing frequencies (I) and absolute cell numbers (J) of populations based on CD4 and CD8b expression within BFP^+ population at day 21. (C-J) Data are presented as average of five replicates ± standard error of the mean (Wilcoxon matched-pairs signed-rank test, *P<0.05; ns: not significant). Contour plots shown are representative for five replicates.

SUPPLEMENTAL FIGURE3

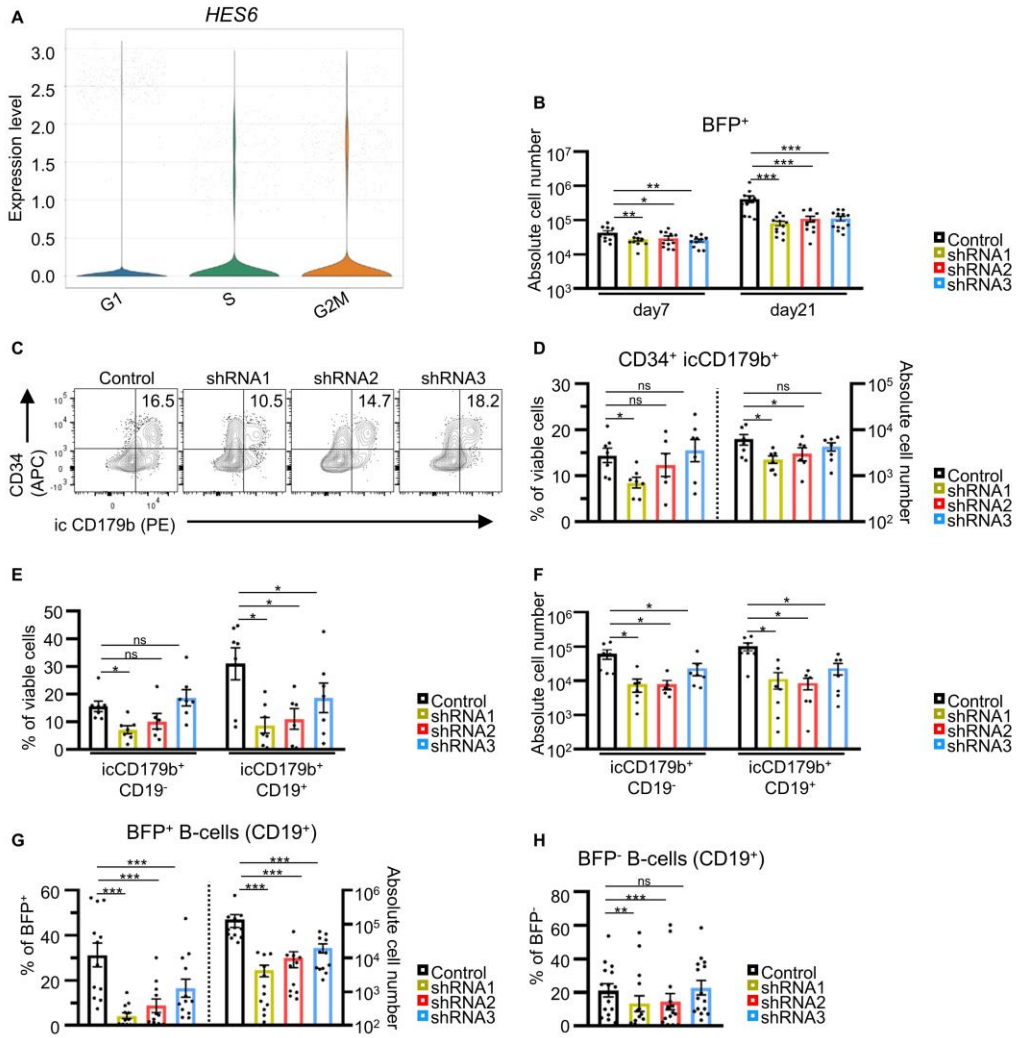

Supplemental Figure 3. *HES6* is important for early *in vitro* B-cell development. (A) Violin plot showing pseudo-bulk log-normalized expression level of *HES6* in different cell-cycle stages within B cells from human bone marrow (Figure 2B). (B-H) Flow cytometric analysis (C) and bar graphs (B, D-H) of control shRNA and *HES6* shRNA-transduced $CD34^{+}Lin^{-}BFP^{+}$ HSPC cultured *in vitro* in B-lineage supporting conditions for a total of three weeks. (B) Bar graphs showing absolute cell numbers of $CD45^{+}BFP^{+}$ cells at day 7 (N=11) and day 21 (N=12; shRNA2: N=11). Flow cytometric analysis (C) showing gating and bar graphs (D) showing frequencies and absolute cell numbers of $CD34^{+}$ and intracellular (ic) $CD179b^{+}$ population within live cells at day 7 (N=7; shRNA2: N=6). Contour plots (C) with frequencies shown are from a representative replicate. Bar graphs showing frequencies (E) and absolute cell numbers (F) of $CD19^{+}$ $icCD179b^{+}$ population within live cells at day 21 (N=7; shRNA2: N=6), and frequencies and absolute cell numbers of B-cells ($CD19^{+}$) within $CD45^{+}BFP^{+}$ cells (G) or frequencies of B-cells ($CD19^{+}$) within $CD45^{+}BFP^{-}$ cells (H) at day 21 (N=12; shRNA2: N=11). Data are presented as average of all replicates ± standard error of the mean (Wilcoxon matched-pairs signed-rank test, *P<0.05, **P<0.01; ***P<0.001; ns: not significant).

SUPPLEMENTAL FIGURE4

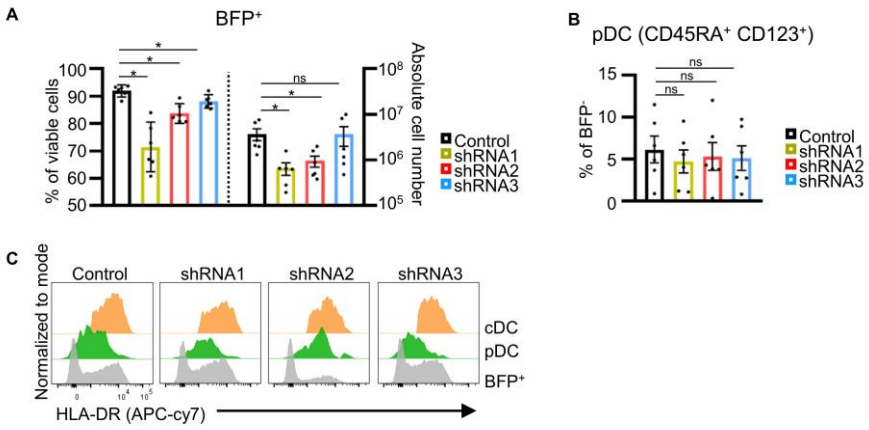

Supplemental Figure 4. *HES6* knockdown impairs *in vitro* pDC development. Bar graphs (A-B) and flow cytometric analysis (C) of control shRNA and *HES6* shRNA-transduced $CD34^+Lin^-BFP^+$ HSPC cultured in DC-lineage supporting conditions for a total of two weeks (N=6), showing frequencies and absolute cell numbers of $CD45^+$ BFP^+ cells, gated on live cells (A) and frequencies of pDCs ($CD45RA^+CD123^+$) within the BFP^- population (B) at day 14. (C) Histogram showing HLA-DR expression in all BFP^+ cells (grey), pDCs (green) and cDCs ($CD4^+HLA\text{-}DR^+$ non-pDCs) (orange) at day 14 for control or *HES6* knockdown. (A-B) Data are presented as average of six replicates ± standard error of the mean (Wilcoxon matched-pairs signed-rank test, *P<0.05; ns: not significant).

SUPPLEMENTAL FIGURE5

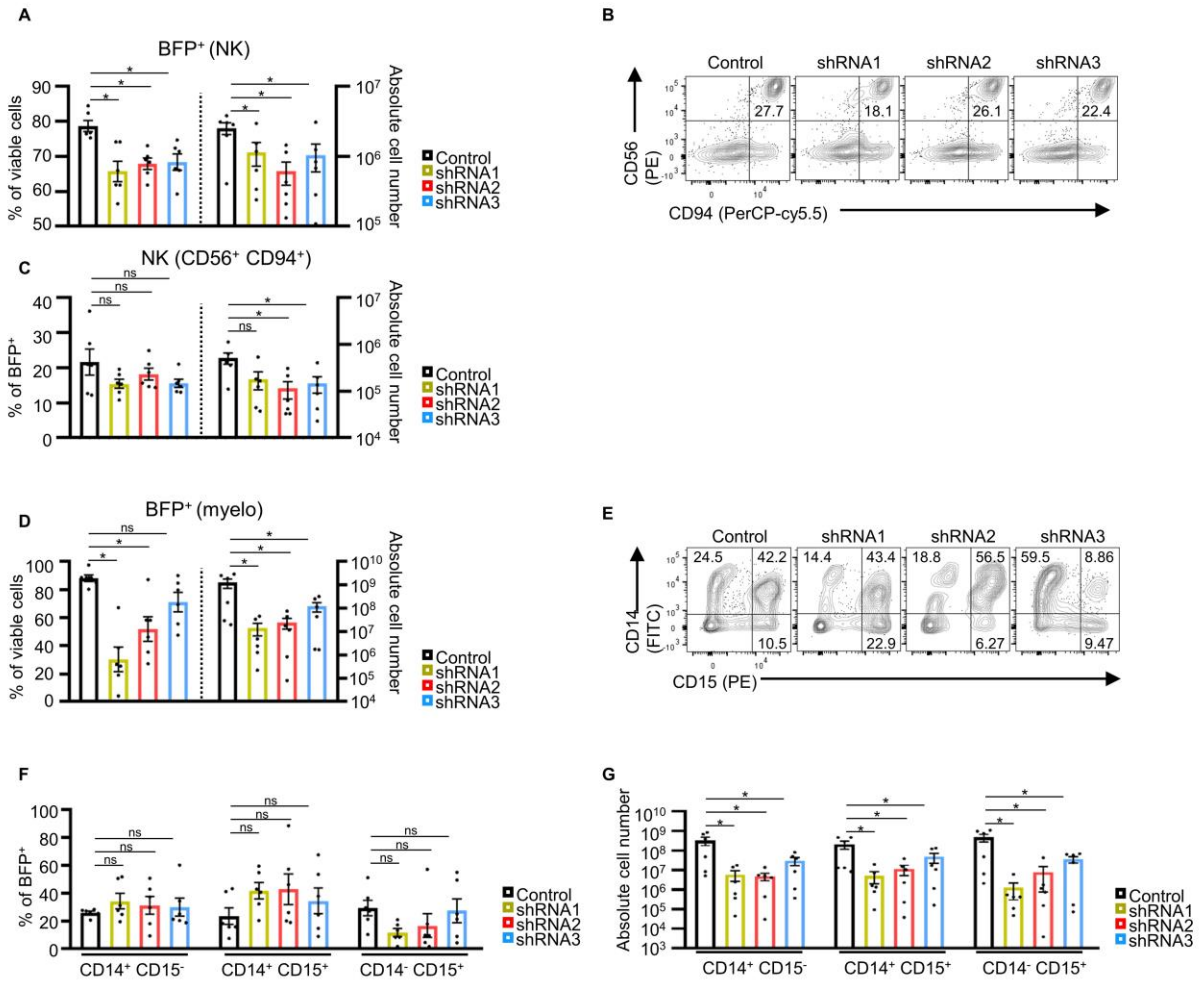

Supplemental Figure 5. *HES6* knockdown doesn't affect *in vitro* NK and myeloid development. (A-C) Flow cytometric analysis (B) and bar graphs (A, C) of control shRNA and *HES6* shRNA-transduced $CD34^+Lin^-BFP^+$ HSPC cultured in NK-lineage supporting conditions for a total of three weeks (N=6), showing frequencies and absolute cell numbers of $CD45^+BFP^+$ cells (A) and gating (B), frequencies and absolute cell numbers (C) of NK cells ($CD56^+CD94^+$) within BFP^+ population at day 21. (D-G) Bar graphs (D, F-G) and flow cytometric analysis (E) of control shRNA and *HES6* shRNA-transduced $CD34^+Lin^-BFP^+$ HSPC cultured in myeloid-lineage supporting conditions for a total of four weeks (N=6), showing frequencies and absolute cell numbers of $CD45^+BFP^+$ cells (D) and frequencies and absolute cell numbers of cell populations based on CD14 and CD15 expression within BFP^+ cells (E-G) at day 28. (B,E) Contour plots shown are representative for six replicates. (A-G) Data are presented as average of six replicates ± standard error of the mean (Wilcoxon matched-pairs signed-rank test, *P<0.05; ns: not significant).

SUPPLEMENTAL FIGURE6

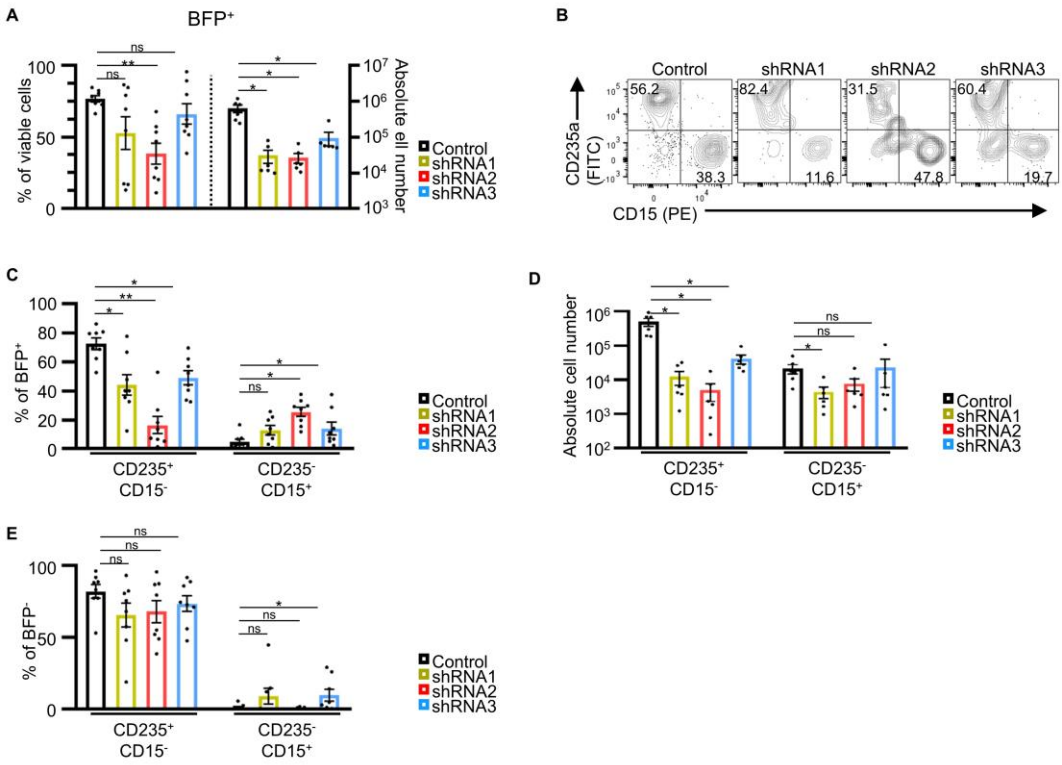

Supplemental Figure 6. *HES6* knockdown impairs colony forming capacity of HSPCs. (A-E) Flow cytometric analysis (B) and bar graphs (A, C-E) of control shRNA and *HES6* shRNA-transduced $CD34^{+}Lin^{-}BFP^{+}$ HSPC cultured in semi-solid colony-forming assay, Methocult, for a total of 10 days. (A) Bar graphs showing frequencies (N=8) and absolute cell numbers (N=6) of $CD45^{+}BFP^{+}$ cells, gated on live cells. (B-D) Contour plots (B) showing CD235a and CD15 expression within $CD45^{+}BFP^{+}$ cells and bar graphs showing frequencies (C) and absolute cell numbers (D) of erythroid ($CD235a^{+}CD15^{-}$) and myeloid ($CD235a^{-}CD15^{+}$) cells within BFP^{+} cells (N=6). Contour plots shown are representative for eight replicates. (E) Bar graphs showing frequencies of erythroid ($CD235a^{+}CD15^{-}$) and myeloid ($CD235a^{-}CD15^{+}$) cells within BFP^{-} cells (N=8). Data are presented as average of all replicates ± standard error of the mean (Wilcoxon matched-pairs signed-rank test, *P<0.05, **P<0.01; ns: not significant).

SUPPLEMENTAL FIGURE7

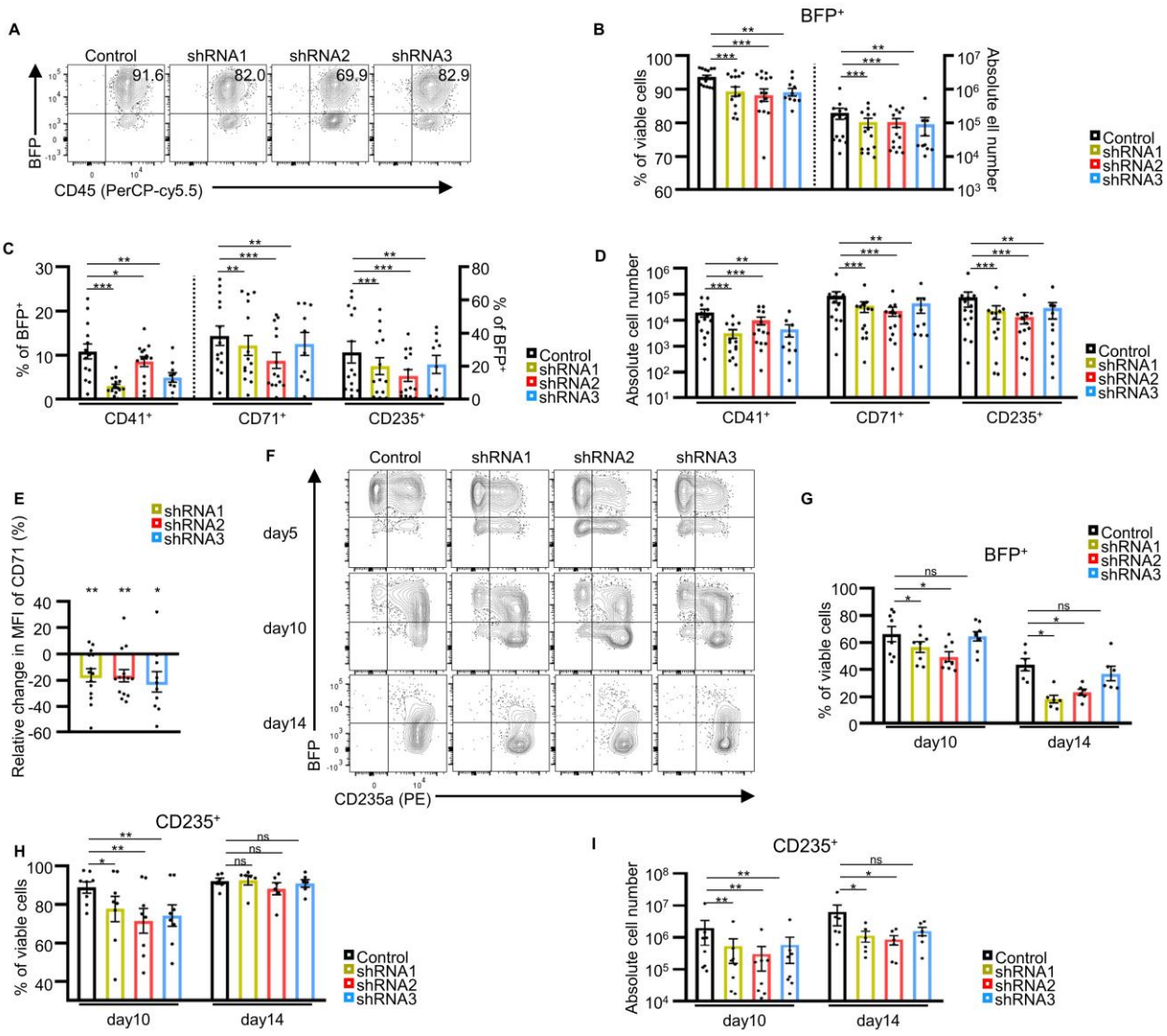

Supplemental Figure 7. *HES6* knockdown reduces *in vitro* megakaryocyte and erythroid development. Flow cytometric analysis (A, F) and bar graph (B-E, G-I) of control shRNA and *HES6* shRNA-transduced CD34$^+$Lin$^-$BFP$^+$ HSPC cultured in megakaryocyte/erythroid-lineage supporting conditions for a total of two weeks. (A-B) Contour plots (A) showing gating of CD45$^+$BFP$^+$ population and the frequencies and total cell numbers (B) of this population within live cells at day five (N=14, shRNA3: N=11). (B-D) Bar graphs showing frequencies (C) and absolute cell numbers (D) of megakaryocytes (CD41$^+$) and CD71$^+$ or CD235a$^+$ erythroblasts, gated as shown in Figure 4E-F), within CD45$^+$BFP$^+$ population at day five (N=14, shRNA3: N=11). (E) Relative change in MFI of CD71 expression within the BFP$^+$ CD71$^+$ erythroblasts (gating as shown in Figure 4E-F) at day five for the three *HES6* shRNA conditions compared to the control (N=14, shRNA3: N=11). Data are presented as average of the replicates ± standard error of the mean (SEM) (one sample Wilcoxon test). (F-G) Contour plots (F) and bar graphs (G) showing BFP downregulation during erythroid (CD235a upregulation) development in all conditions, which explains

extensive BFP downregulation over time (day10: N=8, day14: N=6). (H-I) Bar graphs showing frequencies (H) and absolute cell numbers (I) of $CD235^{+}$ erythroblasts (gating as shown in Figure 4E-F) within viable cell population at day 10 (N=8) and day 14 (N=6). (A, F) Contour plots shown are representative for one of the replicates. (B-D, G-I) Data are presented as average of the replicates ± (Wilcoxon matched-pairs signed-rank test, *P<0.05, **P<0.01; ***P<0.001; ns: not significant).

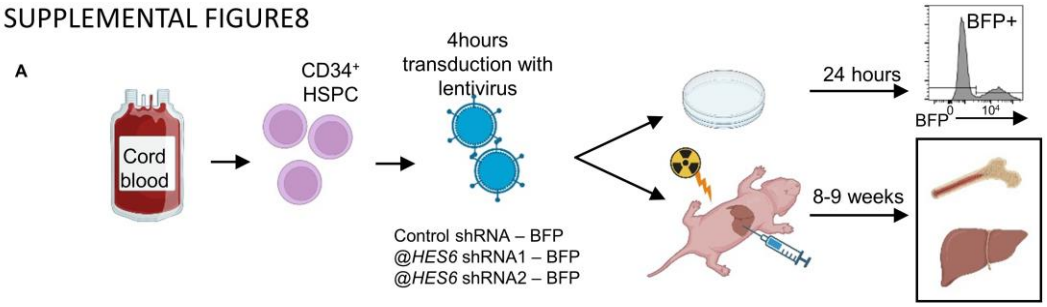

Supplemental Figure 8. *HES6* knockdown *in vivo* experimental set-up. (A) Schematic overview showing preculture, transduction and intrahepatic injection of cord blood $CD34^+$ enriched HSPC (BFP^+ and BFP^-) in NSG mice, which were sublethally irradiated and analyzed after 8-9 weeks (results are shown in Figure 5).

SUPPLEMENTAL FIGURE9

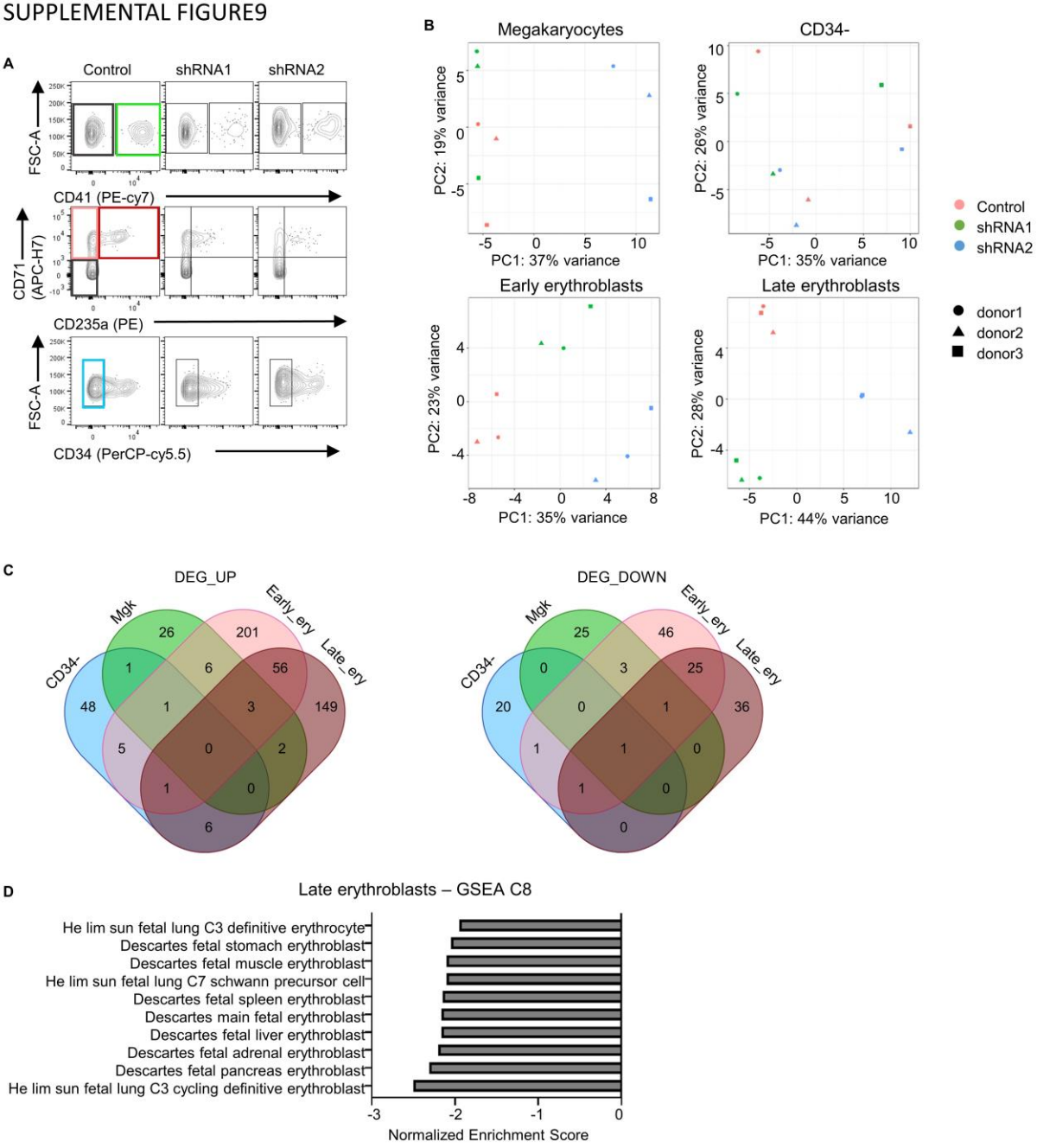

Supplemental Figure 9. RNA-seq analysis reveals molecular pathways downstream of *HES6* knockdown during erythroid development. (A) Flow cytometry data of sorted subpopulations of control shRNA and *HES6* shRNA-transduced (shRNA1 and shRNA2 were used) $CD34^{+}Lin^{-}BFP^{+}$ HSPC cultured for four days in megakaryocyte/erythroid-lineage supporting conditions. Bulk RNA-seq was performed on these four subpopulations. Sorted megakaryocytes ($CD41^{+}$, green) within BFP^{+} population, erythroblasts (early erythroblasts, pink, $CD71^{+}CD235^{-}$ and late erythroblasts, red, $CD71^{+}CD235^{+}$) are gated within $BFP^{+}CD41^{-}$ population and $CD34^{-}$ precursors are gated within $BFP^{+}CD41^{-}CD71^{-}CD235^{-}$ population (light blue, $CD34^{-}$). Contour plots shown are representative for three independent donors. (B-D) Results from data analysis of bulk RNA-seq of cell populations as discussed in Figure 6. (B) PCA plots from three

independent donors with two *HES6* knockdown conditions and control condition for megakaryocytes ($CD41^+$), $CD34^-$ precursor cells and early ($CD71^+CD235^-$) and late ($CD71^+CD235^+$) erythroblasts. (C) Venn diagram showing overlap between differentially up- and downregulated genes (DEG_UP and DEG_down respectively) in different cell populations between control and HES6 knockdown (Table S6-13). (D) GSEA results showing normalized enrichment score for top 10 of gene sets (FDR <25% and p<0.01) enriched in control sample within late erythroblasts.

SUPPLEMENTAL FIGURE10

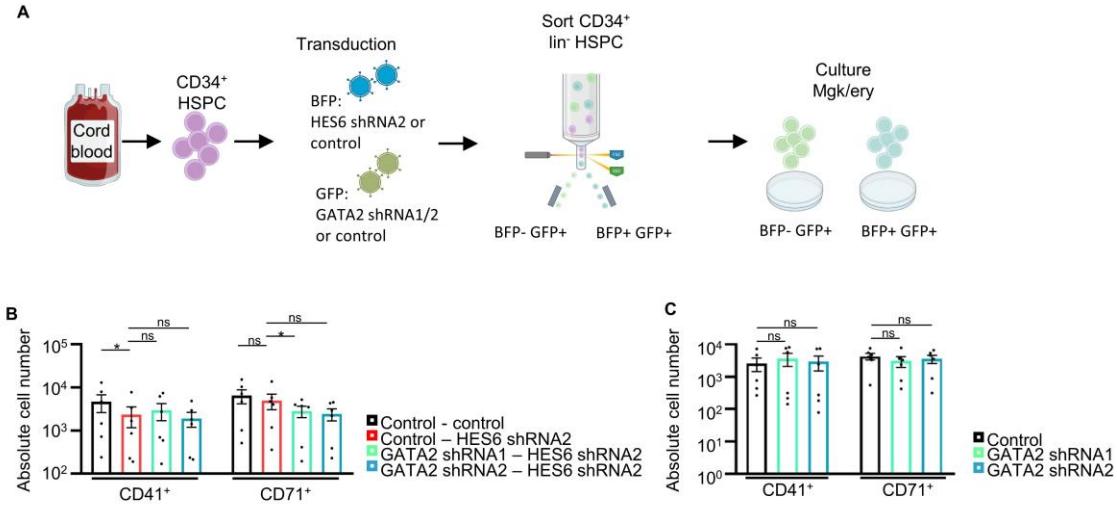

Supplemental Figure 10. *GATA2* knockdown fails to rescue impaired *in vitro* megakaryo-erythroid development upon *HES6* knockdown. (A) Schematic overview illustrating the experimental workflow used to study the impact of double *GATA2-HES6* knockdown (GFP^+BFP^+) or single *GATA2* knockdown (GFP^+BFP^-) on human megakaryo-erythropoiesis. (B-C) Bar graphs showing results of *in vitro* experiments to study the impact of double *GATA2-HES6* knockdown (GFP^+BFP^+) (B) or single *GATA2* knockdown (GFP^+BFP^-) (C) on human megakaryo-erythropoiesis (N=6) as described in Figure 7. Bar graphs showing absolute cell numbers of indicated subpopulations within GFP^+BFP^+ population (B) or GFP^+BFP^- population (C) in the different knockdown conditions. Data are presented as average of six replicates ± standard error of the mean (Wilcoxon matched-pairs signed-rank test, *P<0.05; ns: not significant).

SUPPLEMENTAL FIGURE11

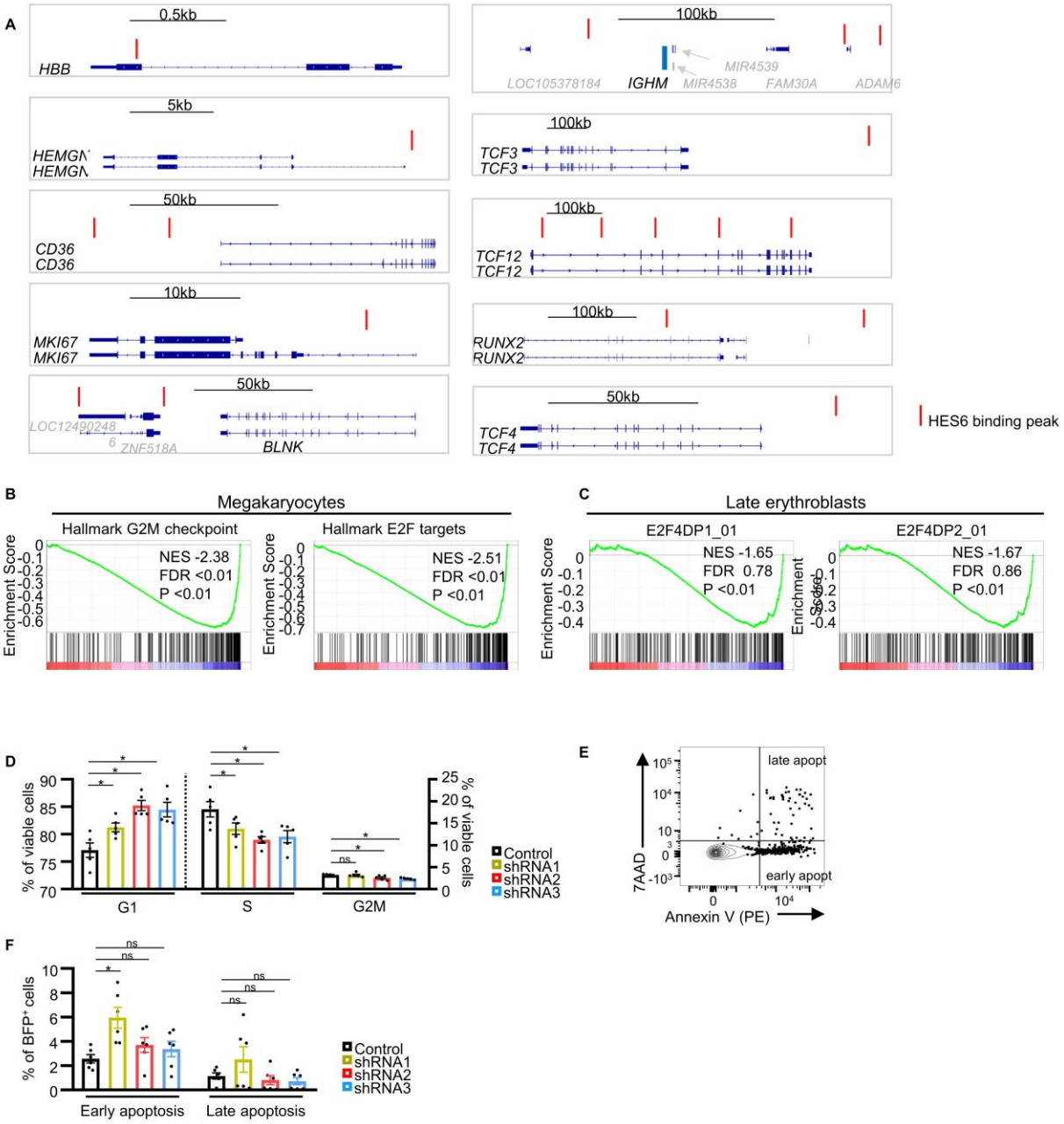

Supplemental Figure 11. *HES6* knockdown impacts cell cycle progression. (A) Analysis of recently published ChIP-seq data of *HES6* in erythroid cells[21] and significant *HES6* binding peaks are indicated in red. Genes shown are important for erythroid (*HBB*), megakaryocyte (*HEMGN*, *CD36*, *MKI67*), T- and B-cell (*BLNK*, *IGHM*, *TCF3*, *TCF12*) and pDC (*RUNX2*, *TCF4*) development. (B-C) Results from data analysis of bulk RNA-seq of sorted cell populations as discussed in Figure 6. Preranked GSEA results showing enrichment of cell-cycle related gene sets in control sample within megakaryocytes (B) and showing enrichment, though with a high FDR, of genes with *E2F4* motif regions within region around transcription start site in control sample within late erythroblasts (C). NES: Normalized enrichment score; FDR: false detection rate. (D-F) Flow cytometry analysis (E) and bar graphs (D, F) of control shRNA

and *HES6* shRNA-transduced $CD34^{+}Lin^{-}BFP^{+}$ HSPC cultured in megakaryocyte/erythroid-lineage supporting conditions for three days. (D) Bar graphs showing frequencies of different cell cycle stages, gating as shown in Figure 8C, within live population, at day3 (N=5). (E-F) Contour plot showing gating (E) and bar graphs showing frequencies (F) of early and late apoptosis within BFP^{+} population at day3 (N=6). Contour plot shown is representative for six replicates. Data are presented as average of all replicates ± standard error of the mean (Wilcoxon matched-pairs signed-rank test, *P<0.05, ns: not significant).

References

1. Van De Walle I, Dolens AC, Durinck K, et al. GATA3 induces human T-cell commitment by restraining Notch activity and repressing NK-cell fate. Nat Commun. 2016;7.

2. Dolens A, Durinck K, Lavaert M, et al. Distinct Notch1 and BCL11B requirements mediate human γδ/αβ T cell development. EMBO Rep. 2020;21(5).

3. Xu Y, Liu X, Zhang H, et al. Overexpression of HES6 has prognostic value and promotes metastasis via the Wnt/ß-catenin signaling pathway in colorectal cancer. Oncol Rep. 2018;40(3):1261-1274.

4. Vandesompele J, De Preter K, Pattyn F, et al. Accurate normalization of real-time quantitative RT-PCR data by geometric averaging of multiple internal control genes. Genome Biol. 2002;3(7):research0034.1. doi:10.1186/gb-2002-3-7-research0034

5. Roels J, Van Hulle J, Lavaert M, et al. Transcriptional dynamics and epigenetic regulation of E and ID protein encoding genes during human T cell development. Front Immunol. 2022;13(July):1-24.

6. Lavaert M, Liang KL, Vandamme N, et al. Integrated scRNA-Seq Identifies Human Postnatal Thymus Seeding Progenitors and Regulatory Dynamics of Differentiating Immature Thymocytes. Immunity. 2020;52(6):1088-1104.e6. doi:10.1016/j.immuni.2020.03.019

7. Park JE, Botting RA, Domínguez Conde C, et al. A cell atlas of human thymic development defines T cell repertoire formation. Science (1979). 2020;367(6480):eaay3224.

8. Le J, Park JE, Ha VL, et al. Single-Cell RNA-Seq Mapping of Human Thymopoiesis Reveals Lineage Specification Trajectories and a Commitment Spectrum in T Cell Development. Immunity. 2020;52(6):1105-1118.e9.

9. van Dijk D, Sharma R, Nainys J, et al. Recovering Gene Interactions from Single-Cell Data Using Data Diffusion. Cell. 2018;174(3):716-729.e27.

10. Stuart T, Butler A, Hoffman P, et al. Comprehensive Integration of Single-Cell Data. Cell. 2019;177(7):1888-1902.e21.

11. Setty M, Kiseliovas V, Levine J, Gayoso A, Mazutis L, Pe'er D. Characterization of cell fate probabilities in single-cell data with Palantir. Nat Biotechnol. 2019;37(4):451-460.

12. Suo C, Dann E, Goh I, et al. Mapping the developing human immune system across organs. Science (1979). 2022;376(6597).

13. Domínguez Conde C, Xu C, Jarvis LB, et al. Cross-tissue immune cell analysis reveals tissue-specific features in humans. Science (1979). 2023;376(6594):eabl5197.

14. Filtjens J, Taveirne S, Van Acker A, et al. Abundant stage-dependent Ly49E expression by liver NK cells is not essential for their differentiation and function. J Leukoc Biol. 2013;93(5):699-711.

15. De Decker M, Lavaert M, Roels J, et al. HES1 and HES4 have non-redundant roles downstream of Notch during early human T-cell development. Haematologica. 2020;106(1):130-141.

16. Kirkling ME, Cytlak U, Lau CM, et al. Notch Signaling Facilitates In Vitro Generation of Cross-Presenting Classical Dendritic Cells. Cell Rep. 2018;23(12):3658-3672.e6.

17. Roels J, Kuchmiy A, De Decker M, et al. Distinct and temporary-restricted epigenetic mechanisms regulate human αβ and γδ T cell development. Nat Immunol. 2020;21(10):1280-1292.

18. Durinck K, Wallaert A, Van de Walle I, et al. The notch driven long non-coding RNA repertoire in T-cell acute lymphoblastic leukemia. Haematologica. 2014;99(12):1808-1816.

19. Loontiens S, Dolens AC, Strubbe S, et al. PHF6 Expression Levels Impact Human Hematopoietic Stem Cell Differentiation. Front Cell Dev Biol. 2020;8.

20. Roels J, Van Hulle J, Lavaert M, et al. Transcriptional dynamics and epigenetic regulation of E and ID protein encoding genes during human T cell development. Front Immunol. 2022;13(July):1-24.

21. Wang Z, Wang P, Zhang J, et al. The novel GATA1-interacting protein HES6 is an essential transcriptional cofactor for human erythropoiesis. Nucleic Acids Res. Published online March 17, 2023.